EFFECT OF SULFUR ON THE ELEMENTARY REACTIONS OF FISCHER-TROPSCH SYNTHESIS ON COBALT SURFACES

A Thesis Submitted to the
Graduate School of Engineering and Science of
İzmir Institute of Technology
in Partial Fulfillment of the Requirements for the Degree of

MASTER OF SCIENCE

in Chemical Engineering

by
Yağmur DAĞA

May, 2020
IZMİR

ACKNOWLEDGEMENTS

ABSTRACT

EFFECT OF SULFUR ON THE ELEMENTARY REACTIONS OF FISCHER-TROPSCH SYNTHESIS ON COBALT SURFACES

Industrial observations indicate that sulfur acts a poison for Fischer-Tropsch Synthesis (FTS) and surface science studies show that sulfur blocks the adsorption sites for reactants on cobalt surfaces. However, various experimental studies have indicated conflicting results about the effect of sulfur on cobalt FTS catalyst activity and selectivity. This study aims to clarify the effect of sulfur on cobalt FTS catalysts by molecular modelling of the elementary reactions of FTS on surfaces that are present on sulfur covered cobalt surfaces that are present in fcc-Co nanoparticles, using Density Functional Theory (DFT).

For 0.25 ML sulfur coverage, it is found that on bare, C and O covered surfaces, S is the main dissociation product, while HS can be present on low coverages. Atomic sulfur decreases the adsorption energies of all species investigated, while the decrease is more pronounced for CO compared to H_2. The effect of S on the elementary FTS reactions direct and H-assisted CO dissociation, carbon hydrogenation, carbon coupling and oxygen removal are also investigated. The results indicate that S inhibits mainly the oxygen removal reaction, in terms of both H_2O and CO_2. CO dissociation is not inhibited but rather slowed down, due to increasing activation barriers. It is also found that carbon hydrogenation barriers are significantly decreased, while carbon coupling barriers are unaffected. These results indicate that the intrinsic effect of sulfur poisoning would be to increase methane selectivity, while decreasing the selectivity to long chain hydrocarbons.

ÖZET

KOBALT YÜZEYLERİNDEKİ KÜKÜRTÜN FISCHER TROPSCH SENTEZİNİN TEMEL REAKSİYONLARINA ETKİSİ

Endüstriyel gözlemlerin sonucunda, sülfürün Fischer-Tropsch Sentezi (FTS) için zehirleyici bir etkiye sahip olduğu ve yüzey bilimi çalışmaları, sülfürün kobalt yüzeyindeki reaktantların adsorpsiyon bölgelerini blokladığını göstermektedir. Öte yandan, çeşitli deneysel çalışmalar sülfürün kobalt FTS katalizörlerinin aktivite ve ürün seçilimi üzerinde çelişen sonuçlar göstermektedir. Bu çalışma, sülfürün kobalt bazlı FTS katalizörleri üzerindeki etkisini anlamak için, fcc-Co nanoparçacığı üzerindeki temel reaksiyonları, moleküler modelleme yöntemi ile yoğunluk fonksiyoneli teorisi kullanarak incelemeyi amaçlamaktadır.

0.25 ML sülfür kaplı yüzey için, sülfür yalın, C ve O kaplı yüzeylerde ana parçalanma ürünü iken düşük kaplı yüzeylerde HS de olabilmektedir. Atomik sülfürün tüm türlerin adsorpsiyon enerjilerini düşürdüğü gözlemlenirken, CO adsorpsiyon enerjisindeki düşüş H_2'ye kıyasla daha fazladır. Sülfürün etkisi FTS ana reaksiyonları, direkt ve h-destekli CO parçanlaması, karbon hidrojenleşmesi, karbon eşleşmesi ve oksijen giderme reaksiyonları üzerinde incelenmiştir. Bu sonuçlara göre, oksijen giderme reaksiyonu hem H_2O hem de CO_2 formunda, sülfür tarafından engellemektedir. CO parçalanması ise engellenmemiş, ancak aktivasyon bariyerleri yükseldiği için yavaşlamıştır. Karbon hidrojenleşme bariyerleri ciddi miktarda düşerken, karbon eşleşme bariyerlerinde bir değişim gözlemlenmemiştir. Bu çalışma sülfür zehirlenmesinin eseas nedeni olarak, sülfürün metan seçilimini artırırken uzun zincirli hidrokarbon seçilimini azaltması olarak göstermektedir.

TABLE OF CONTENTS

LIST OF TABLES

LIST OF FIGURES

Dedicated to Eser KANA,

CHAPTER 1

INTRODUCTION

Currently, approximately 15 million barrels of crude oil is demanded per day and 69% of this amount is required to produce liquid transport fuels [1]. Crude oil does not have sustainable property and in the same manner it was estimated that world will face scarcity in the production of crude oil contrarily to demand of the transportation energy within the next half of century [1]. As a result, alternative sustainable energy production become very essential. Many researchers are in progress to convert agricultural products (such as lignocellulose biomass) into liquid fuels without exploiting existing agricultural resources for human food chain. Countries' energy requirement cannot be solved with this option but could reduce dependency of crude oil [2].

Fisher-Tropsch Synthesis (FTS) consists of the exothermic reaction between a mixture of predominantly H_2 and CO (syngas) which produces long chain hydrocarbons (which can be converted to synthetic fuels) as the main product and water as the main by-product. Cobalt-based catalysts are widely used in industrial FTS due to their high activity, high selectivity to linear paraffin and low water gas shift activity.

Industrial observations indicated that sulfur, one of the impurities in the syngas feed, acts a poison for FTS[3] and surface science studies showed that sulfur blocks the adsorption sites for CO and H_2 on cobalt surfaces [4]. However, various experimental studies have shown contradictory results, i.e. that ppm amounts of sulfur result in the increase/decrease of catalytic activity or selectivity increases towards olefins or CH_4 [5].

This study aims to clarify the effect of sulfur on cobalt FTS catalysts by molecular (computational) modelling of the adsorption of the reactants CO and H, and the elementary reactions of FTS on surfaces that are present on fcc-cobalt nanoparticles, using periodic plane-wave Density Functional Theory (DFT) calculations utilizing Vienna ab-Initio Simulation Package (VASP). In this study:

- Chapter 1 is summarized the fundamental of catalysts, importance of Fischer Tropsch Synthesis (FTS) reaction, reactors and catalysts of FTS, information about Density Functional Theory and the aim of the study.

- Chapter 2 is summarized of literature survey related to effect of sulfur impurities on activity and selectivity of FTS.

- Chapter 3 gives the information about computational methodology and shows calculation steps of the study.

- Chapter 4 contains results of the study.

- Chapter 5 is related to discussion of the results combined with the literature.

- Chapter 6 is the summary of the study and it contains conclusions of the study.

1.1. Fundamentals of Catalysis

Catalyst utilization in the reaction does not follow the stoichiometric relations of the reaction equation. Catalyst effect for specified reaction increases the rate of the reaction at operating temperature or decreases the temperature at given rate. Simple reactions have no unstable intermediate product in thermodynamic approach and catalyst activity is to increase forward and reverse reaction rate (forward *kf* and reverse *kb*) as the ratio of the reverse and forward reaction rate (*kf/kb*) does not change in equilibrium conditions. At this manner a conflict is arisen that catalyst cannot start a reaction pathway that is not thermodynamically feasible [6]. Catalyst action is obeyed the laws of thermodynamics without any exceptions.

Catalyst increases the rate of the reaction by reducing the required activation energy (E) of any specific reaction (see in Figure 1.1). As an example for solid catalyst; "Transition State Theory" refers that a higher reaction rate indicates a higher reaction rate constants [6]:

$$k_v = \frac{kT}{H} e^{-\Delta G^{\#}/RT} \qquad \qquad \textbf{Equation 1}$$

k: Boltzmann constant

h: Plank constant

T: Temperature

R: gas constant

$\Delta G^{\#}$: Free energy for activated state

The higher k_v means a lower free energy $\Delta G^\#$ in catalytic reaction at a constant temperature.

$$\Delta G^\# = \Delta H^\# - T\Delta S^\#$$ **Equation 2**

In addition, $\Delta S^\#$ is lower than the same amount for non-catalytic reaction, the reason for that the particle attached on the surface of the catalyst loses a degree of freedom which means that ΔH^* must have lower value in order to have lover $\Delta G^\#$ dwelling on the non-catalyzed reaction.

Transition state theory refers that $\Delta H^\# = E_a$, which indicates that no change is obtained in the number of molecules in the reaction, and it explains reduction in the activation energy reduction (see Figure 1.1). Different catalyst types, which depends on the phase of the catalyst and reactants, can be specified [7]. In homogeneous catalysis, catalyst is in the same phase with reactants and there is no phase boundary occurs. But in heterogeneous catalysis, there exists a phase boundary which separates catalyst and reactants. Lastly, enzymatic catalysis is not included neither homogeneous nor heterogeneous catalyst class.

Homogeneous catalysis is a process where the catalyst is in the same phase with reactants (i.e. all molecules in the gas or liquid phase). Atmospheric chemistry can be given as example in general. Ozone in the atmosphere decomposes with the chlorine atoms as follows:

$$Cl + O_3 \rightarrow ClO_3$$

$$ClO_3 \rightarrow ClO + O_2$$

$$ClO + O \rightarrow Cl + O_2$$
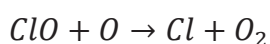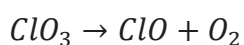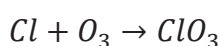
In heterogeneous catalysis, solids catalyze the reaction of gas molecules or solutions. Since solids are impenetrable if they do not have porous characteristics, resulting of that catalytic reactions are occurred at surface of the catalyst. Active metals of the catalysts are reduced to nanometric sizes to maximize their surface areas and reduce the cost of greater priced materials (e.g. Platinum) and are supported on an inert material as porous structure. Heterogeneous catalysis is the "benchmark" as it is the most important catalysis class in petrochemical and chemical industry [8].
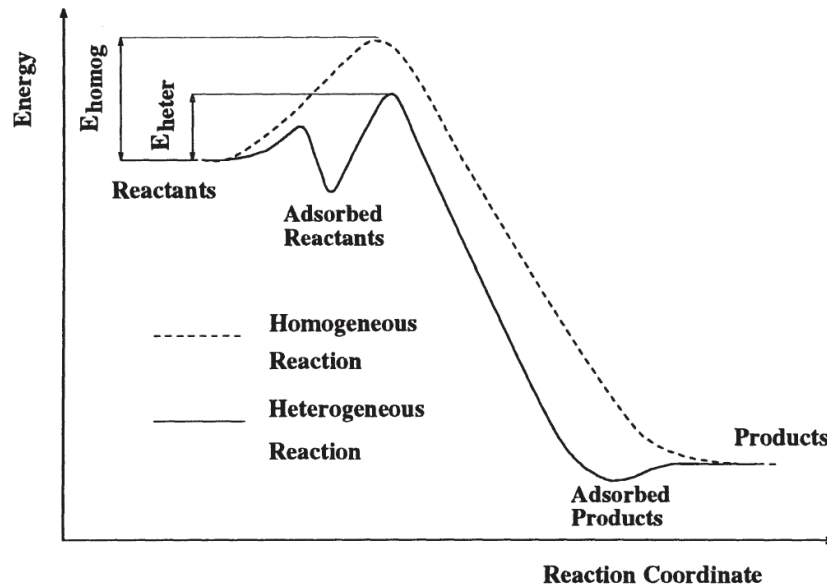
Figure 1.1 Energy pathways of the heterogeneous and homogeneous reactions [8]

1.1.1. Modelling of Heterogeneous Catalysis

Schematic which refers the main steps included in heterogeneous catalysis can be summarized as follows [9].

1. Reactants are diffused to the surface
2. Adsorption of the reactants is occurred at the surface
3. Chemical reactions take place on the surface
4. Products are desorbed from the surface
5. Products are diffused away from the surface

Each of these steps differs in rate and the slowest step determines the process rate (process- determining rate). The faster steps are Step 1 and 5 in general, it can be exception as the catalyst has greater efficiency. Limitations of the catalytic reaction rate is that the quantity of reactants which goes to the wall and kinetic properties of the surface do not affect the surface reaction [9]. This is the progress of "the diffusion controlled" catalysis.

Adsorption

The molecule or atom and the solid surface interaction creates bonding between them and it results the adsorption formation [8]. Physical adsorption that is physisorption is

formed when the solid surface and gas molecules interact and create bonds with van der Waals forces which forces occur between inert atoms and molecules. Other forces which can be involved are electrostatic forces with constant dipole moment for molecules, induced polar interactions for polarized molecules, dispersion forces for nonpolar atoms and molecules which forces obtained depending on the fluctuation of the density of the electrons. Besides, boiling point (condensation) of the gas is directly related to the strength of these forces which is depended on the physical properties of the adsorbed gas. The chemical structure of the solid does not affect directly the physisorption [8]. Bond is important only at low temperatures (~100-300 K) and the bond energy between the particle and the surface is low (10-50 kJ/mole). When the temperature increases, the gas molecules moves away more or less from the surface [8]. The importance of the physisorption in heterogeneous catalysis is extended that it can be pioneer step of chemisorption. Chemisorption is associated to the properties of the solid surface. Properties of the solid surface can differ from the bulk solid reason for that unsaturated bonds are not observed on the surface. Actually, conditions of the atom on the surface and the bulk atom are not the same, because atom on the surface does not have its full complement neighborhood [8].

Reaction

In heterogeneous catalysis, one of the reacting particles must be first chemisorbed at least in order to obtain a reaction catalytically on a solid surface [8]. As a result, if physisorption cannot play a major role directly, chemisorption is accepted as fundamental step to "make ready" the atoms and molecules which are reacted. This mechanism equips a reaction pathways with lower activation energy than the one related to the homogenous reaction (see Figure 1.1). The first mechanism of the reaction, the recombination between gas atom and adsorbed atom is considered as the free atom hits the adatom and reacts with it. Recombined molecule is resulted and it is called Eley-Rideal Mechanism (E-R) and schematic of this is indicated basically [10] as follows.

$$A + B* \rightarrow AB*$$

A, B symbols refer atoms. AB* is continued to absorb after the recombination of atoms. The partial pressure of the gas phase atoms and surface coverage directly affects the rate of the reaction. Step rate bases can be written as follows [8].

$$V_{ER} = k [A] [B*]$$

The second mechanism is the new order between two adatoms and called the Langmuir- Hinshelwood Mechanism (L-H) and represented as follows [10].

$$A * + B * \rightarrow AB * + *$$
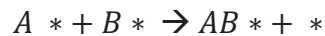
It is clearly seen that this type of reaction can be possible if adatoms are diffused over the solid surface. Moving way of the adatoms is to jump from one reaction potential to other one [10] surpassing a barrier potential (Em) which is lower than the desorption energy (Ed). While this action takes place, particles do not leave the surface totally, indeed. Potential barrier (Em) can be obtained as ~0.1-0.2 Ed depending on the literature survey and this value is directly related to the extensions of the surface coverage, which it decreases when (θ) increases, defects of the surface and crystallographic orientation of the surface. The existing of the energy barrier Em indicates that the L-H mechanism is efficient at higher temperature depending upon an E-R mechanism as an activated process.

Desorption

The next step after the E-R or L-H recombination, surface and molecule do not create a chemical bond, thus they are free to move away from the wall. This is called Desorption as phenomenon. It shows that desorption is not a "sudden" reaction and the molecules may drop down in physisorption well before leaving the wall (see Figure 1.1). Desorption is quite fast process and reaction and desorption are accepted as single step by many authors for all cases. The significance of this phenomenon settled in that recombination energy can be left totally or partially on the wall when the molecules move away from the wall. The amount of the energy left on the wall is directly affect the time characteristic of the desorption by the relaxation process of the internal molecular energy [10]. This indicates that molecules can move away from the surface within an excited state and "quench" after in the gas next to the wall. Any other option for leaving the surface is that they can leave the surface in thermal equilibrium with it.

1.1.2. Catalyst Deactivation

Catalyst deactivation means that the loss of the activity and selectivity of the catalyst and it creates concerns and it continues in practice of industrial catalytic applications. Catalyst replacement or displacements have huge costs to the industrial

processes as billion dollars. Catalyst deactivation times are changes considerably, for instance, catalyst lifetime can be on the order of seconds in catalytic cracking operations in contrast to that the iron catalyst may have lifespan for 5-10 years approximately in ammonia synthesis. All in all, all catalyst will be decomposed and lost their integrity inevitably.

In general, the loss of activity in catalyst happens very slowly and it is well-controlled process. Some sort of catastrophic failure can be occurs depending on its designing hardware or process upsets. For instance, methane or naphtha steam reforming, it must be well considered in order to avoid higher operation temperatures in reactor or at steam-to-hydrocarbon ratios below critical values. In fact, great amount of carbon filaments can be produced under these conditions which filled the pores and voids of the catalysts, pulverize catalyst pellets and can shut down the process and all of these can be happened in few hours [8].

Catalyst deactivation is indispensable for most processes unfortunately, but some sort of its immediate or drastic results may be avoided, postponed or even reversed. Then, deactivation issues as extent, rate and reactivation are taken into consideration in researches, designing and operation of commercialized processes. There is significant motivation to obtain and indicate clearly the catalyst decay [8].

Mechanism of Deactivation

There are many pathways for decay of heterogeneous catalysts. For instance, if there is any one of dozen contaminants present on the feed, catalyst solid can be poisoned. Cracking/condensation of hydrocarbon reactants, intermediates and/or products produces a coke and/or carbon and they can foul the catalyst pores, surface and voids. In the treatment of a power plant flue gas, produced fly ash can dust and stuck the catalysts. Catalytic converters which are used for decreasing the emission from the gasoline or diesel engines may be fouled or poisoned by fuel or lubricant additives or engine corrosion protective products. When the catalytic cracking is occurred in higher temperatures, thermal degradation can happen in a way of active phase crystallinity growing, collapse of the support porous structure and/or solid-state reactions pf the active phase with the promoters. Additionally, oxygen or chlorine existing in the feed gas may be a reason for the formation of the volatile organic compounds of the active phases and it is followed by gas phase transportation from the reactor. In a similar manner, oxidation

state changes in active phase for catalytic reaction can be excited within the reactive gases in the feed.

There are many mechanisms of the solid catalysts deactivation and they are classified within the 6 mechanism types of decay as follows [8].

1. Poisoning
2. Fouling
3. Thermal degradation
4. Vapor compound formation or leaching by transportation from the surface of the catalyst or particle
5. Vapor-solid and/or solid- solid reactions
6. Attrition /crushing

Mechanisms 2 and 6 are occurred in mechanical manner and the others are in chemical approach when deactivation types are separated as thermal, chemical and mechanical.

The strong chemisorption of the reactants, intermediates, products or impurities on sites of the catalyst can cause poisoning [8]. As a result, poisoning has operational consideration as whether a species behaves as a poison depending upon its adsorption strength contrarily to the other species has a competition for catalytic sites. It can be an example that oxygen can be a reactant for partial oxidation of ethylene to form ethylene oxide on a silver promoted catalyst and poisoning effects in hydrogenation of ethylene on nickel promoter. Besides physical blockage of the adsorption sites, adsorbed poisons may change in the electronic or geometric structure of the surface [8]. Lastly, poisoning can be reversible or irreversible, and reversible poisoning example is the deactivation of the acid sites in fluid cracking catalyst by nitrogen compounds in the feed. Nonetheless, the affects can be severe; they can be separated within a few hours to days after the nitrogen is removed from the feed. In addition to the syngas of cobalt promoted Fischer-Tropsch catalyst, there can be similarities for nitrogen compounds (e.g. ammonia and cyanide) and, these surface species needs weeks to months' time periods before the lost activity of the catalyst is gained back again [11]. Mostly poisons can be irreversibly chemisorbed into the catalytic surface sites, thus sulfur on metals are investigated and discussed in detail later in this research. Whether the poisoning is reversible or not, the deactivation effects, as the poison is adsorbed on the surface, have similarities.

Many poisons occur in catalytic processes naturally, as feed streams are treated. There are some specifications of poisons in the feed, which must be kept on the desired value. See Table 1.1 for FTS specifications [8].

Table 1.1 The requirements of syngas cleaning for Fischer–Tropsch synthesis [7]

Impurity	Specification
$H_2S + COS + CS_2$	<1 ppmv
$NH_3 + HCN$	<1 ppmv
HCl + HBr + HF	<10 ppbv
Alkali metals (Na + K)	<10 ppbv
Particles (soot, ash)	"almost removed"
Organic components (tar)	below dew point
Hetero-organic components (S, N, O)	<1 ppmv

Coals includes great potential of the poisoning materials such as sulfur and other arsenic, phosphorus and selenium and they are placed in ash in general.

Poisoning mechanism which effect on the catalytic activity are several as indicated by a conceptual two-dimensional model for sulfur poisoning of ethylene hydrogenation on a metal surface (see Figure 1.2). As a starting point, at least one three or fourfold adsorption /reaction site adsorb the sulfur atom strongly in a physical manner and they are blocked in active sites. Secondly, strong chemical bonds create an advantage and it electronically improves its nearest neighbor metals and its next to-nearest neighbor atoms which modify their abilities of adsorbing and/or dissociate reactants molecules (at this manner H_2 and ethylene molecules), additionally these effects are not occurred beyond 5 atomic units [12]. Thirdly, restricting of the surface by strongly adsorbed poison can be occurred and it possibly causes important changes in catalytic properties, especially in reactions which are sensitive to the surface structurer. Besides, the adsorbed poison directly blocks accessibility of adsorbed reactants for one to another (a fourth effect) and finally prevents or gets slower the diffusion from the surface of adsorbed reactants (effect number five).

Two important keys for obtaining a clear understanding of poisoning phenomena include following items.

- Structure of the surfaces of poisons adsorbed onto metal surfaces determination
- Understanding how surface structure and then adsorption stoichiometry change with increasing coverage of the poison.
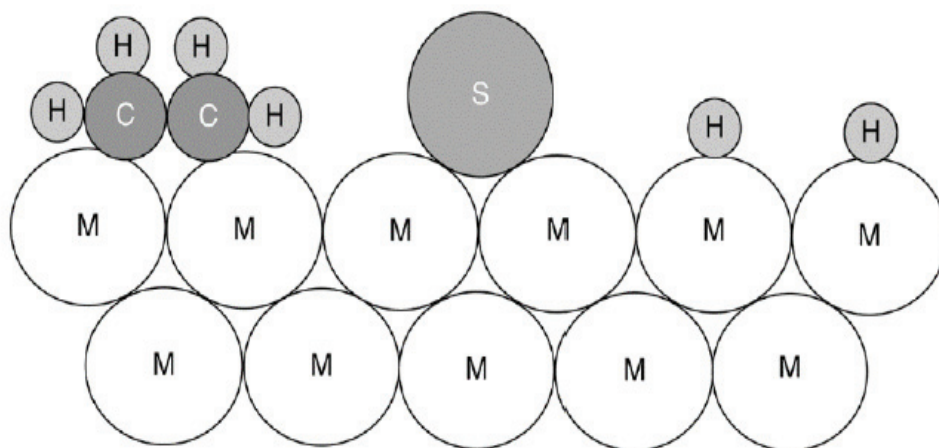
Figure 1.2 Model of S poisoning on metal surface [7]

1.2. Fischer- Tropsch Synthesis

Fischer-Tropsch synthesis (FTS) has drawn a great deal of interest in the recent decades from researchers, since it has been believed that liquid hydrocarbons' production through this promising clean technology is a potential alternative method which could solve the shortage of liquid transport fuels. Recently great interest has been generated in applying this relatively well-known technology to cellulosic biomass and agricultural waste, to convert them to linear- and branched-chain synthetic hydrocarbon.

1.2.1. Fundamentals of Fischer Tropsch Synthesis

Fischer Tropsch synthesis (FTS) is an important to alternate potentially clean technology and it is expected to solve shortage of the liquid transport. Different application has provided an area to use this technology. In addition, Bergius coal liquefaction and FTS of light hydrocarbons were developed relatively same time as 1910 to 1926. Firstly, Friedrich Bergius took Germany's abundant coal supplies that overcomes the lack of petroleum by synthesizing it, additionally Bergius invented high-pressure coal

hydrogenation in Rheinau- Mannheim within first and second decades of 20th century. Bergius set up the experiment as coal-oil paste by crushing and dissolving coals containing 85% carbon in heavy oil, and then he reacted this paste with H_2 at 200 atm and 673 K, where the products of this process were petroleum-like liquids. After this successive synthesis, Franz Fischer and Hans Tropsch have explored a process to transform coal into synthetic liquidized hydrocarbons at Kaiser Wilhelm Institute for Coal research (KWI) in Mulheim Ruhr in 1926. Firstly, Fischer and Tropsch hydrocracked the coal within the reaction it with steam to have synthesis gas (mixture of CO and H_2), after that converted that gases to petroleum-like synthetic liquid in between to 10 atm and 453 to 473 K .Fischer and his coworker preferred cobalt catalyst to design, and Tropsch achieves a successful process [13].

FTS composed of the paths within the indirect liquefaction process. Consequently, hydrogenation of CO and polymerization of carbide metal, wide range of products (hydrocarbons, oxygenates and water) are produced with a vast distribution in carbon number [2]. Figure 1.3 shows FTS production diagram.

The Fischer Tropsch synthesis consists of the exothermic reaction between H_2 and CO and it leads to water and a wide range of hydrocarbons (gas, liquid, waxes). The FT synthesis composed of mainly n-paraffins and α-olefins and additionally branched hydrocarbons and oxygenates within a minor extent. The reaction is indicated as follows [14]

$$CO + 2H_2 \rightarrow -CH_2- + H_2O \qquad \Delta H° = -165 \ kJ/mol$$

Selectivity of different hydrocarbons depends on the operation conditions such as temperature, pressure, feed composition and catalyst used. Hydrocarbons with long-chain are favored at low temperatures, high pressures and low H_2/CO ratio [2].

There are two main Fischer-Tropsch process which is shown in [2];

- High temperature Fischer-Tropsch (HTFT): this process operates between 300-350 °C with Fe-based catalyst. Short chain olefins oxygenate and hydrocarbons in the gasoline range are mainly desired products of this process.
- Low temperature Fischer-Tropsch (LTFT): this process operates between 200-240 °C and both Fe- and Co- based catalyst are used. Linear long chain paraffin (middle distillate and waxes) are the main desired products.
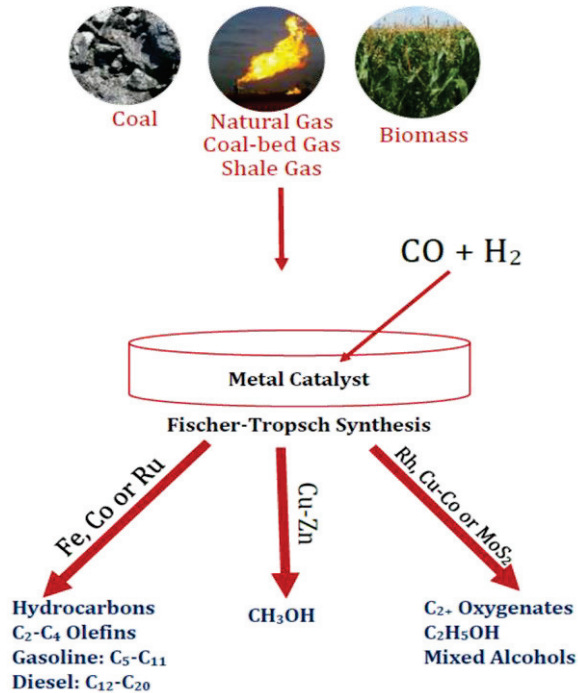
Figure 1.3 Fischer-Tropsch synthesis production diagram

The FT waxes will be hydrocracked later on to maximize the yield middle distillates (jet fuel and diesel cut) [7]. The FT synthesis is generally described as polymerization reaction that hydrocarbon chain grows by adding one monomer that includes C to another.

The mechanism consists of three steps that are initiation, chain growth and termination respectively. Process is separated into two types of mechanisms in which the chain growth proceeds with the aid of incorporation of CH monomers and the other type is that occurs with the aid of adding to other monomers (e.g. CO and/or enols). Generally, it could be accepted as parallel mechanism can occur simultaneously on the catalyst surface during FTS. Despite of the fact that there is no full agreement on the details about the mechanism for the formation of CH monomers. There are two monomer formation paths proposed. Satchler-Biloen mechanism or Direct CO dissociation is one of these; CO adsorbs and directly dissociates into C and O adatom-adsorbed atom. Then adsorbed C atoms have been hydrogenated and transformed into CH_2. Another pathway is H-assisted CO dissociation; H is connecting to CO before it dissociated [7].

A useful tool for estimating FT product distribution roughly, independent from the mechanism, is so-called Anderson-Schulz-Flory (ASF) model (see in Figure 1.5). This model has just one assumption that the possibility of a chain grows (α) is independent of the hydrocarbon chain length (n). According to this assumption, it is possible to obtain an

equation relating the probability of chain growth (α) and the mole fraction (X_n) of hydrocarbons with the same number of carbon (W_n).
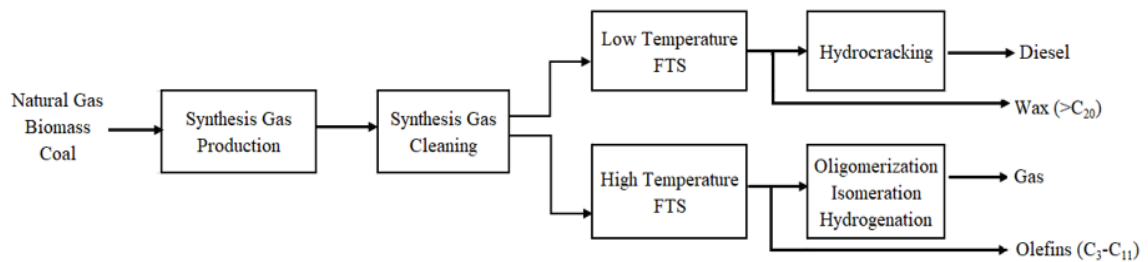
Figure 1.4 Overall process for production of liquid fuels by Fischer-Tropsch synthesis[3]

1.2.2. Reactors for Fischer-Tropsch Reaction

The Fischer Tropsch synthesis of liquid fuels from synthesis gas was discovered in the second decade of 20th century in Germany, and it was applied to industrial scale operation within a short period of time. Fixed-bed reactors are used technically with an internal water-cooling system as well, different kind of reactor concepts for low-temperature FTS was tested in the meantime. These possibilities lead that, only two reactor types are mainly used commercially. Shell uses the fixed-bed reactor technology for all present and planned facilities. This reactor type is robust and can be sized up easily by investigations on a single tube. Sasol discovered the bubble column reactor and this type of reactor provides advantages about effectiveness and heat removal. This leads for a higher average temperature in the reactor and thus a higher space-time yield. Moreover, considerably higher reactor capacities and lower reactor costs contrarily to multitubular reactors are feasible. Slurry bubble columns have disadvantages and some challenges as well, and it concerns the necessity separation of suspended catalyst from the liquid products [3].

In principle, different reactor technologies are applicable for operating the highly exothermic FTS. Some of these concepts have already been applied on the lab-scale, pilot plant and industrial scale. One can distinguish between the so-called high temperature process, where gaseous products are formed in moving bed reactors and the low-temperature process, in which liquid products are also present under reaction conditions. In these, more developed low-temperature processes multitubular and slurry bubble column reactors are applied industrially. In the same manner, both reactor technologies

have disadvantages as well. High pressure drops, low catalyst utilization and insufficient heat removal effects fixed bed multitubular reactor in a bad way, whereas the slurry bubble column reactor have requirement for catalyst separation, behavior of lower ideal residence time, and highly demanding size-up. (See in Table 1.2) .These disadvantages lead to researches towards improved reactor technologies that may become industrially applicable in a media and long term approaching [3].
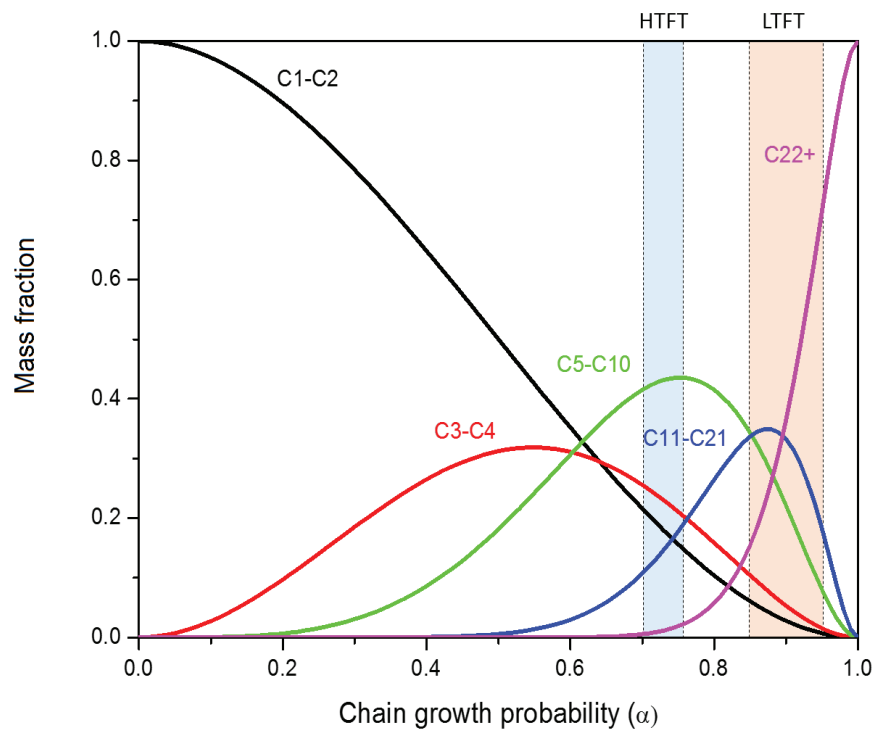
Figure 1.5 Anderson-Schulz-Flory FT product distribution as function of the chain growth probability [7]

In the case of exothermic reactions, multitubular reactors are used mostly. These types of reactors easy to apply and to design reason for similarities of the parallel tubes' behaviors. On the other hand, multitubular reactors have drawbacks. In order to minimize pressure drop, catalyst dimensions must be chosen between 1 and 3 mm. catalyst utilization is decreased resulting of that and it leads reduction on product selectivity as undesirable effect. Furthermore, in the case of tube diameters as several centimeters as used in industry can cause hot spot formation. In order to prevent damaging of the catalyst, the temperatures of both feed and cooling medium must be selected significantly lower than the maximum possible temperature. This raises to a decreasing in the reactor productivity. Furthermore, capital cost of multitubular reactors are quite high.

The second reactor type that used in industry for FTS is the bubble column reactor with suspended catalyst. In slurry bubble columns, fine catalyst powders within the dimensions from 10 to 200 μm are used [7]. The effect of internal mass transfer is negligible and optimal activity and selectivity can be achieved. Isothermal operation is almost succeeded with efficient heat removal from the reactor. Despite applicable catalyst fraction is up to %25 by volume, the reactor production capacity of a slurry bubble column should be higher due to the enhanced catalyst usage and higher average reactor temperature. FTS reactors are shown in Figure 1.6.
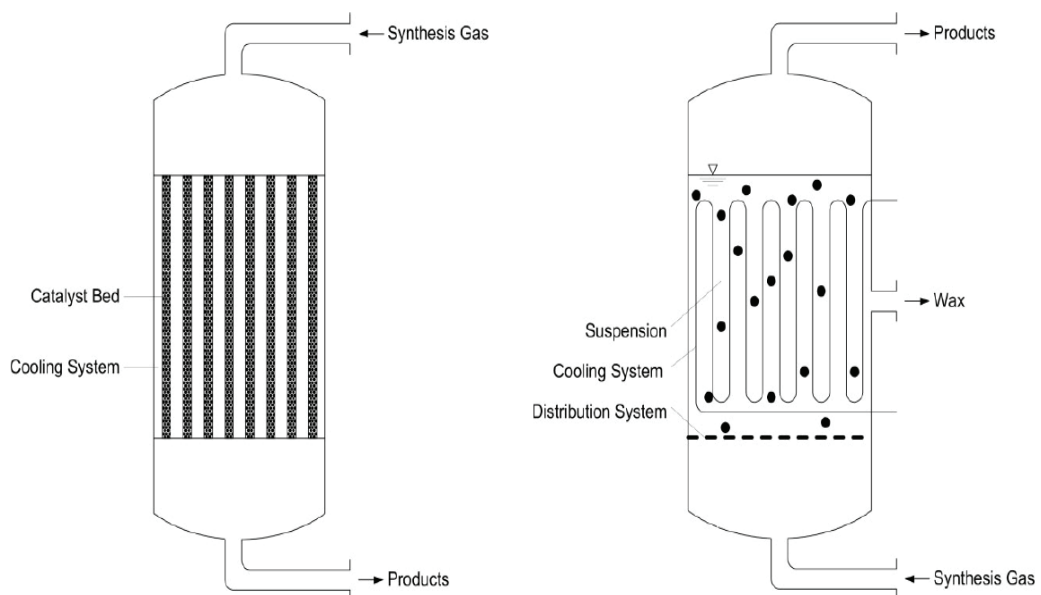
Figure 1.6 Technically established reactors for Fischer-Tropsch synthesis (left: multitubular fixed bed reactor, right: slurry bubble column reactor) [3]

1.2.3. Fischer-Tropsch Catalysts

Selectivity of the product of FT synthesis can be change over the wide range. Formulation of catalyst, system of performing the synthesis process and reaction conditions, is the main factor, which effects the distribution of product in FT synthesis. The catalyst chosen for the hydrogenation process affects probability of chain growth in FT synthesis. Additionally, catalyst type, probability of chain growth mechanism on the catalyst surface has affected by the catalyst's promoter level, temperature, and composition of feed gas as well [13].

1.2.4. Cobalt Based Fischer Tropsch Catalysts

A cobalt based catalyst is favorable for industrial applications depending upon its significant specifications. Cobalt catalyst has high selectivity over long chain alkanes; besides it has low selectivity to oxygenate products and alkane, in addition high deactivation resistance, long-life time and relatively low price of this catalyst is a reason for accepting it to be utilized for FT biodiesel generation. Cobalt based catalyst highly active at low temperature, as a result it is efficient and capable catalyst type. Besides, a cobalt catalyst has durability about 5 years on stream contrarily to 6 months in the case of an iron catalyst. Co-based catalyst generally yields higher production rate of long chain synthetic hydrocarbon. The FTS process with Co-based catalyst at a normal pressure and temperature of 200-300°C produces linear olefins as main product. Small amount of non-linear product which composed of commonly monomethyl branched compounds are produced at this temperature range. High pressure FTS with Co-based catalyst produces less olefins in the mean of alkanes' content depending upon the increase of molecular weight. Probability of a chain growth is between 0.5-0.7 for an iron catalyst and this number is placed between 0.7-0.8 for Co-based catalyst. This process work well with this conditions and additionally H_2/CO ratios nearly [2].

Co based catalyst is mostly used in special companies that given in Table 1.2 below and companies prefer Co based catalyst depending upon the suitability in the production of middle distillates with a high cetane number. The mainly carriers that used commercially are γ-Al_2O_3, SiO_2 and TiO_2 (mainly anatase). Methods of depositing the cobalt on the surface of these carriers differs from one to another, but the most common method is impregnation of the carrier with a liquid solution containing Co_3O_4 nanoparticles. The active phase for FT is Co^0, as a reason for the fact that the catalyst needs to be reduced prior to reaction [2].

Spinel compounds are difficult to reduce, with the aid of this information small nanoparticles interact strongly with support and form spinel compounds. This phenomenon is significantly important in the manner of Co/Al_2O_3 catalyst. To reduce Co/Al_2O_3 species temperature should be as high as 700 ^{o}C. In order to facilitate the catalyst reducibility, second metal such as Pt, Re, Ru are added ad these metals are usually called reduction promoters. Small amounts of metal oxide (structural promoters) can be added to the carrier (e.g. Zr, Ti, and La) alternately. There are many other structural

promoters that can be used to improve FT selectivity and many other properties. As an example, Mn promoted formation favors of long chain hydrocarbons and olefins. Even so, it should be realized that excess amount of promoter may have an adverse effect. There is a list of commercial-type cobalt catalysts and their composition below in Table 1.3 [2].

Table 1.2 Advantages (+) and disadvantages (–) of established reactors for FTS

	Fixed bed reactor	Bubble column reactor
Pore diffusion	-	+
Catalyst content in reactor	+	-
Gas-liquid mass transfer	+	-
Isothermal behavior	-	+
Catalyst exchange	-	+
Catalyst attrition	+	-
Need for liquid-solid separation	+	-
Scale-up	+	-
Reactor costs	-	+

1.3. Surface Science Approach

Surface chemistry, which is challenging and promising field, considered at the boundary between the solid state and the liquid or gas phase and it is an intersection point between condensed matter physics and the chemistry. The phenomena at solid-gas or solid-liquid interface are more complex for that reason. A chemical reaction which takes place on the surface, for example, shows the same behavior and complexity as ordinary gas phase reactions and, additionally the common electron conservation laws do not apply the reason for that the metal provides a semi-infinite source of electrons at the Fermi level. New approaches are required in order to have improvement and to describe the surface chemistry. Surface chemical reactions need to be understood in order to have an insight for many surface phenomena including semiconductor processing, corrosion, electrochemistry, and heterogeneous catalysis. Heterogeneous catalysis has been

accepted to be a prerequisite for more than 20% of all production in the industrial world [10], and it will have more importance in the years to come expectedly. The development of sustainable energy solutions represents one of the most important scientific and technical challenges for recent years, and heterogeneous catalysis is located at the center of the case. Surface science experiments do not show greater importance in providing a quantitative description of surface phenomena [16]. Density functional theory calculations which depends on the computational surface science provide an insight and guidance and verification of the proposed concepts. It is important to have an information about which properties indicates clearly the activity and selectivity of a catalyst and to be able to use calculations to search for new catalyst leads.

1.3.1. Density Functional Theory

Density functional theory (DFT) is a quantum mechanical simulation method to obtain accurate thermodynamic and kinetic properties, including adsorption, desorption, diffusion and chemical reactions. Atomic and molecular adsorptions are effective in probing surface active sites and surface reactivity, and the binding energies are considered fundamental properties for catalyst screening in rational catalyst design.

Two different approaches are indicated to the calculation of the electronic structure and total energies of molecules and solids. The first one is the wave function-based methods [16] and the second one is Density Functional Theory Methods (DFT) [17]. The previous, that can be very definite if a high level of configuration interactions is involved, is currently restricted to 10-100 electrons. When the consideration of the transition metal surfaces is taken, this limits the number of atoms which can be treated to 10 since each of the transition metals have the order as 10 valence electrons. These methods are seemed nonpractice for using in common treatments of the complex systems which needed to model catalyst. There are unique ways of the inserting accurately indicated region into a less accurately described environment region, that can increase the system sizes and wave function-based theory becomes useful method at this time [17]. These calculations costs as computational work and the limited size of the systems that performed shows that, for a surface science and catalysts content, they can be accepted as benchmarks and they can be used as measured and defined the accuracy of the less computationally demanding DFT methods.

Table 1.3 Cobalt FT catalysts used and/or patented by FT synthesis companies [2]

Company	Support	Reduction Promoter	Structural Promoter
Sasol	γ-Al_2O_3	Pt	Si
Shell	TiO_2		Mn, V
GTL.F1 (Statoil)	$NiAl_2O_4$	Re	
ENI/IFP/Axens	γ-Al_2O_3		Si
Nippon Oil	SiO_2	Ru	Zr
Syntroleum	γ-Al_2O_3	Ru	Si, La
BP	ZnO		
Exxon Mobil	TiO_2	Re	γ-Al_2O_3
ConocoPhilips	γ-Al_2O_3	Ru, Pt, Re	B
Compact GTL	Al_2O_3	Ru, Pt	
Oxford Catalysts/Velocys	SiO_2	Pt, Re	Ti

Density functional theory explains the determination of the ground state electron density and total energy by solving a set of one electron Schrodinger Equations (the Kohn-Sham equations) instead of the complicated many-electron Schrödinger equation. There are several methods used to solve the Kohn–Sham equations, as a shortcut, they can be characterized by the model, which used to describe the surface with the aid of the basis set. Kohn-Sham equation and it is given as follows:

$$E[\rho] = T_S[\rho] + \int dx v_{ext}(r)\rho(r) + E_H[\rho] + E_{xc}[\rho]$$ **Equation 3**

Where :

ρ : Electron density of the system

$E[\rho]$: The ground state energy of the system

$T_s[\rho]$: Kohn-Sham kinetic energy

v_{ext} : The External potential acting on the integrating system

E_H :   The Coulomb Energy of the system

E_{xc} :   The exchange-correlation energy of the system

Equation 3 enables the calculation of the kinetic energy and the Coulomb interaction terms by lumping all the unknown terms such as exchange energy, correlation energy and the correction of the kinetic energy due to electronic interactions in one term, the so-called exchange-correlation functional. DFT states that the ground state energy could be solved exactly provided that the exchange correlation term could be solved. However, the exchange-correlation term cannot be calculated exactly and thus has to be approximated. There are different approaches for approximating the exchange-correlation energy, the main two being the Local Density Approximation (LDA)[18] and the Generalized Gradient Approximation (GGA)[19]. Mostly, the interactions between atoms depend on the valence electrons, such that core electrons are not needed explicitly in the computations. This property led to the pseudopotential approach where the core electrons are described by an effective potential, i.e. lumped in a pseudo-potential. Ultra-soft pseudo-potentials can yield accurate energies with good efficiency[20]. The important point is that the accuracy of DFT depends on the careful choice of the exchange-correlation functional. That is why one has to be careful while comparing the experimental results with DFT obtained ones, and even while comparing the DFT results with each other. A detailed discussion about the topic can be found elsewhere[20].

The advantage of DFT is that Kohn-Sham equations describing a system can be solved practically up to around 100 atoms, since it demands less computational power per atom compared to other quantum mechanical techniques. Many different chemical properties can be calculated accurately by DFT such as adsorption energies and geometries, adsorption structures, geometry and energy of transition states, vibrational frequencies, etc. We have used the periodic, plane wave based, slab approach implemented in Vienna Ab-initio Simulation Package(VASP)[20] to model the catalytic surfaces that are used in the study. This brings the advantage of having the best available model to compare with experimental data obtained on single crystal surfaces. The combination of DFT modelling gives a wealth of atomic scale information about the catalyst surface such as stability and identity of reaction intermediates, which is often difficult to obtain experimentally, and the determination of transition states for the catalytic surface reactions, which provide valuable information about the catalytic activity

and can be compared with experimental data in those cases where it is possible to measure reaction rates of elementary steps on single crystal surfaces.

The Model Used to Describe the Surface

The calculations cannot indicate all the atoms in a solid or a catalyst particle as a result common solving strategy must be chosen to limit the number of atoms processed explicitly. Two basic types of methods exist as Cluster and Slab methods which are indicated below.

Cluster Methods, which explain only a restricted cluster of the surface atoms with the hope that the surface atoms further away from the adsorbates of interest are not much significant. Slab methods works with description of the surface as a slab with a periodic structure among the surfaces. The surface unit cell size determines the computational effort, and the unit cell had better to be selected as large enough in principle, thus the adsorbates in neighboring unit cells do not interact.

The two types of models are illustrated (see Figure 1.7). The slab method is a choice for the boundary conditions in the cluster approach, which is generally found to shows the surface properties better than the cluster approach for a given number of atoms in the super cell or the cluster, respectively. Only a limited number of atomic layers can be involved for both methods. In addition to that, there are Greens function-based methods that can be processed a single adsorbate on a semi-infinite substrate [21], but they are not common and wide usage.
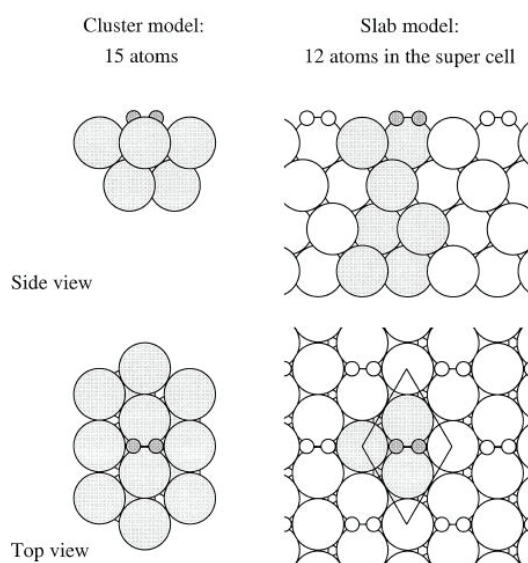
Figure 1.7 The slab and cluster models[21]

1.4. Objectives of the Study

Based on the literature review presented, despite the common understanding of sulfur as a catalyst poison, there is no consensus in literature about why it acts as a poison and how it effects the elementary reactions on cobalt catalyst surfaces for Fischer-Tropsch Synthesis. This is mainly because such experimental investigations are prone to errors or different conclusions as a result or reactor, operating conditions and catalyst preparation procedures. Therefore, a fundamental explanation of the interaction of sulfur species with reactants and intermediates of FTS on cobalt surfaces that are found on fcc cobalt nanoparticles, and the effect of sulfur on the elementary reactions of FTS, can help to explain the intrinsic effect on sulfur on cobalt catalyzed FTS. Therefore, the aims of the study can be summarized as to answer the following scientific questions:

i. What are the main S species that exist on the surface as a result of H_2S (the main sulfur source molecule in the reactant feed) adsorption and decomposition on Co(111) surface, the most abundant surface found on an fcc-Co nanoparticle?

ii. How does the S species on Co(111) effect the adsorption energies/sites of reactants and intermediates of FTS?

iii. How does S species on the surface affect the main elementary reactions of FTS ?

CHAPTER 2

LITERATURE SURVEY

Sulfur is the unwanted component for the FT reaction, which comes from the feed [3]. Sulfur is toxicant for metals as it adsorbs on the catalytic sites strongly. The result of this powerful bonding is usually physically blocked sites and electronic modification of neighbor atom [4,22–27]. Sulfur is thought to cause deactivation and it presents generally in the fresh feed. Sulfur is contained a lot at raw synthesis gas that derived from biomass or coal, whereas sulfur usually removed from the natural gas before the reforming part. Sulfur may also come from corrosion inhibitors that occasionally added. In any cases, traces of sulfur can possibly reach FTS reactor, might cause an operational upset [28]. As a result, the effect of the sulfur in different molecular forms studied at the beginning of the development of FT technology. Fischer proposed upper limit for sulfur concentration in the feed as (1-2 mg/m^3) [29]. This result came from researches that have been done for the process development in the field of Co-based FTS technology. Madon and Seaew indicated the literature concerning effects of sulfur in 1977 [29]. They presented several studies carried out for more than four decades dealing with sulfur effects on different catalyst for FTS. Researches indicated that Co-based catalyst has a promotion effect with adding sulfur in form of H_2S and CS_2 in very low concentrations (0.15 to 0.4 % by catalyst weight). Low concentrations of sulfur content increase the lifetime of catalyst, selectivity is increased towards heavier hydrocarbons as well. Nevertheless, further addition of sulfur result in complete catalyst deactivation. Sulfur poisoning studies are done at in-situ methods, showing that H_2 adsorbs on stronger on metallic tubes, but it is also corrosive, toxic and flammable. The selection of sulfur carrier is an important subject since there is a significant difference between adsorption phenomena of organic and inorganic sulfur contained molecules. An appropriate sampling procedure is essential for the accuracy of such studies, due to expected intraparticle and reactor poisoning gradient (especially for PFR) [30,31].

The effect sulfur on activity and selectivity of FTS has been investigated by both in-situ [32–34] and ex-situ methods [35–38] (See on Table 2.1). Observing the effect of the sulfur with in-situ methods are difficult [34]. H_2S has the strong adsorption on the reactor's

metallic tube, so determination of sulfur amount on the catalyst sample is difficult. Sulfur concentration gradient is formed because of high adsorption capacity of H_2S. Therefore, activity and selectivity of FTS catalyst evaluation get complicated [31]. Compared to this, in ex-situ method, a known amount of sulfide introduced to the catalyst which allows to track the sulfur amount. This procedure provides more homogeneous sulfur distribution both on the catalyst surface and in the reactor. However, there might be different Co-S interactions in ex-situ procedures than those under normal reaction conditions [3,31,35–38].

Table 2.1 Effect of sulfur on selectivity of FTS

Reference	Year	Catalyst	Poisoning	Reactor	SC_{5+}	o/p^a
[32]	1985	Co/SiO_2	In situ H_2S	Fixed-bed	↑	n.a.
[35]	2007	Co/Al_2O_3	Ex situ $(NH_4)_2S$	Fixed-bed	↓	↑
[39]	2008	Co/TiO_2	Ex situ $(NH_4)_2S$	Fixed-bed	↓	n.a.
[34]	2010	Co/Al_2O_3	In situ $(CH_3)_2S$	CSTR	↓	↓
[33]	2011	Co/Al_2O_3	In situ H_2S	Fixed-bed	-	↓
[40]	2014	Co/SiO_2	In situ $C_4H_{10}S$	Fixed-bed	↓	↑
[28]	2015	$Pt-Co/Al_2O_3$	Ex situ $(NH_4)_2S$	Fixed-bed	↓	↓
[41]	2016	$Pt-Co/Al_2O_3$	In situ H_2S	CSTR	↑	↓

↑ : the selectivity increases with the addition of S

↓ : the selectivity decreases with the addition of S

n.a. : effect of S on that parameter was not assessed or not reported

- : the selectivity is practically unaffected with the addition of S

^{a} : Olefin to paraffin ratio

2.1. Experimental Studies for Effect of Sulfur on Activity and Selectivity of Fischer-Tropsch Synthesis Catalyst

Bartholomew and Bowman studied effects of sulfur by introducing 0.5-0.8 ppm H_2S in the reactor feed through Teflon lines. For the silicate supported cobalt catalyst has a decline in catalytic activity for the entire range of sulfur content feed. The decline

appeared to be more intense for concentrations between 0.5 and 2 ppm, while less for 5-6 ppm of H_2S. A possible explanation of this unexpected trendline was that at higher sulfur concentrations, a different structure or multilayer of surface of sulfide were created. Catalyst selectivity was also shifted resulting of sulfur addition increased to production of heavier hydrocarbons ($>C_4$). A possible reason for the increased selectivity towards higher weight products could be the selective adsorption of the H_2S on sites which normally adsorb H_2, resulting in a hydrogen deficient surface. Water production decreases, which is a result of lower conversion, and normally affects the product distribution in the opposite direction[32].

Curtis et al (1999) did a study based on the low amount of sulfur may improve the catalytic activity and selectivity towards olefin and heavier hydrocarbons [42,43]. The studies were done for iron-based FT catalyst. The authors have made experimental studies for cobalt based catalysts with use of two different supports, which are TiO_2 and SiO_2. For sulfur source; $(NH_4)S$, $(NH_4)SO_4$ and $(NH_4)SO_3$ were used at different (100-2000 ppm) levels. First, Co/TiO_2 catalyst was tested for bare, 100 ppm and 2000 ppm sulfur levels. Amount of sulfur addition can change the results of experiment. So, first trial was done sulfur loaded before the catalyst, second S is loaded with catalyst, and finally it was loaded after cobalt catalyst. According to the IR data, low ppm levels of S (100 ppm) increases the peak intensity of hydrocarbons when sulfur was loaded after cobalt catalyst. At high levels of sulfur (2000 ppm), the peak intensity decreases when compared with bare and 100 ppm catalysts. The results do not change with sulfur loading methods. Results of these experiments have shown that low amounts of sulfur (< 200 ppm) increases the catalytic activity, while high amounts of sulfur (2000 ppm) decreases the catalytic activity. Second set of experiments were done for same catalyst with different sulfur sources (SO_3, SO_4). At these experiments, hydrocarbon peak intensity was the highest at bare catalyst when compared with 100 ppm S loading with Co/TiO_2 and 2000 ppm S loading with Co/TiO_2 catalysts. When the support was changed with SiO_2, catalytic activity decreases 50% compared with TiO_2 supported catalysts with same amount of sulfur loading.

Previous experimental studies were related to the addition of sulfur contaminants in different forms and amounts to the reactor to examine the effect of sulfur on the activity and selectivity of the FTS catalyst. As an alternative study, Coville et al (2001) were investigated that addition of sulfur with another substance could affect the poison effect

of sulfur. The authors have studied intensively the effects of sulfur addition while catalyst were prepared. These studies indicated the effects of the additives such as boron, zinc that behaves as a sulfur sink. Diffusion reflectance infrared Fourier transformed spectroscopy (DRIFTS) and temperature programmed reduction (TPR) that were operated on TiO_2 and SiO_2 supported cobalt catalysts resulted that total range of sulfur loading (100-2000 ppm) CO adsorption inhibition is observed. Additionally, in the range of 200-2000ppm sulfur, raising in the reduction temperature of the sulfide samples was detected. Another study catalyst activity by using IR suggested that sulfur loading had a promotional effect for concentrations lower than 200 ppm [36]. Catalyst activity and selectivity increase is observed towards methane at such concentrations. Li and Coville showed that the additive did not affect the catalyst's resistance to sulfur at low concentrations (100-200ppm) with $(NH_4)_2S$ as the sulfur source for a boron treated catalysts. On the other hand, the reaction rate was twice as high as contrarily to the boron-free catalyst with the same sulfur loading at higher concentrations (500ppm). The selectivity is also affected by the sulfur as well, leading to the lower chain growth possibly. Boron was selected reason for its electron acceptance nature which neutralizes the electronic density introduced by sulfur addition, in this case sulfide ion are accepted as electron donors. The effect of zinc additive has been researched recently, and it showed the importance of the step-in which sulfur is introduced to the system during the presulfidation procedure. Sulfide zinc containing Co/TiO_2 catalyst showed about 45% improved activity in contrast to sulfided catalyst without zinc. The selectivity for the sulfided catalyst was shifted through the lighter hydrocarbons as agreed with the previous results [37].

Visconti et al (2007) reported on the effect of sulfur poisoning of an Al_2O_3 supported Co catalyst. Sulfur in the range 0-2000 ppm was added ex-situ to the catalyst by incipient wetness impregnation of ammonium sulfide. This range corresponds to nearly 50.000 h on the stream, with an assumption that the feed composed of 0.02 mg/m^3 of sulfur and a space velocity of 2000 cm^3 (STP)/h.g$_{cat.}$ The catalyst reducibility, activity, hydrogenation ability and selectivity were experimentally estimated. The results indicated that no morphological changes in the catalyst structure. Despite of the fact that, negative effect on catalyst reducibility and catalytic activity were observed in the total range of sulfur addition. In the same manner, the product selectivity altered towards lighter hydrocarbons and CO_2 production. The results are expected as selective poisoning by sulfur atoms carrying different interest at different loadings. Attempting of the model

sulfur effect on the conversion rate was indicated as well. The ex-situ researches agreed with that sulfur additive effects the reducibility, activity and selectivity of the catalyst shifting to lighter hydrocarbons [35].

Pansare et al. (2010) stated a study in which they added 50, 300, 600 and 1100 ppbV levels of di-methyl sulfide to the feed by wetness impregnation method (ex-situ method) to a cobalt catalyst performed in a CSTR at 220° C and 25 atm [34]. They reported that at 50 ppb S levels the sulfur did not negative effect the catalytic activity that is CO conversion. However, as they increased the sulfur levels, they did observe a negative effect on CO conversion. This relationship is presented in Figure 2.1.
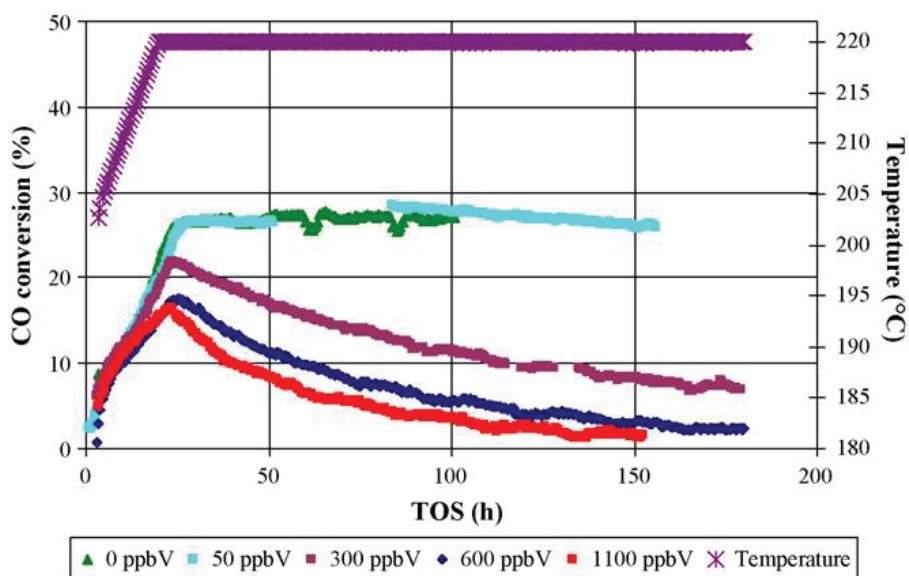
Figure 2.1 CO conversion with varying sulfur loading [34]

Based on the Figure 2.1, low amount of sulfur (50 ppbv) and no sulfur content has the same trend based on the TOS data. However, it was observed that increasing sulfur as 300 ppbV, 600 ppbV and 1100 ppbV decreases linearly the CO conversion. This situation is same for C_{5+} selectivity which is presented in Figure 2.2. However, methane selectivity has inverse trend with effect of sulfur on CO conversion and selectivity of C_{5+} that is shown in Figure 2.3.

Based on the Figure 2.2, increasing sulfur content (>300 ppbV) has a negative effect on the C5+ selectivity. However, at low amount of sulfur such as 50 ppbV, has the same effect with no sulfur content situation.

Based on the Figure 2.3, has the inverse situation as effect of Sulfur on CO and C_{5+} selectivity. Because high amount of sulfur (1100 ppbV) has the highest CH_4 selectivity as nearly 60% when compared no sulfur content situation which has nearly 20 % CH_4 selectivity. The study shows the similarities with other studies which suggest sulfur decreases the catalytic activity of catalysts and selectivity of long chain hydrocarbons but increases the selectivity towards long chain hydrocarbons [35,36].
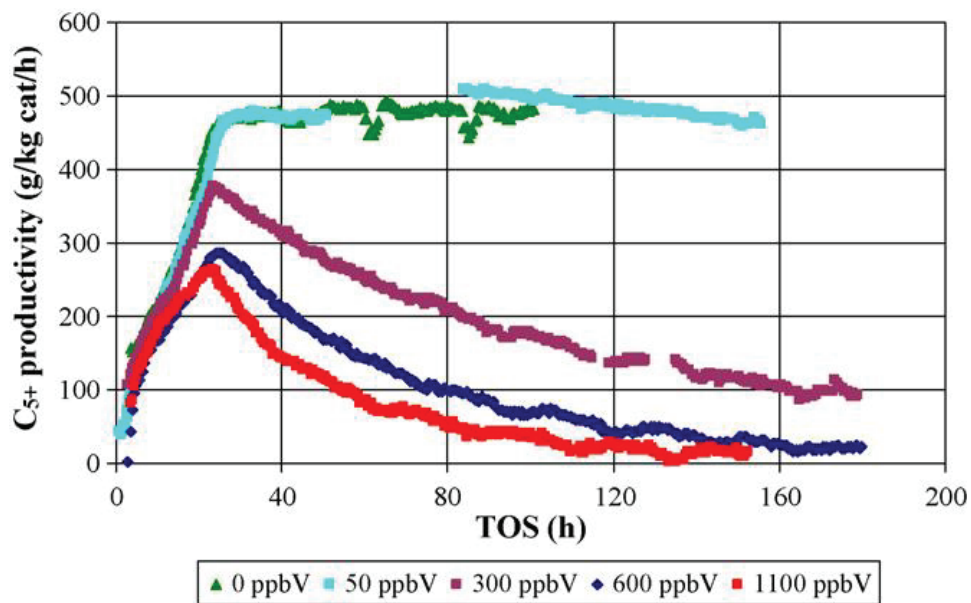
Figure 2.2 C5+ selectivity with varying sulfur content [34]
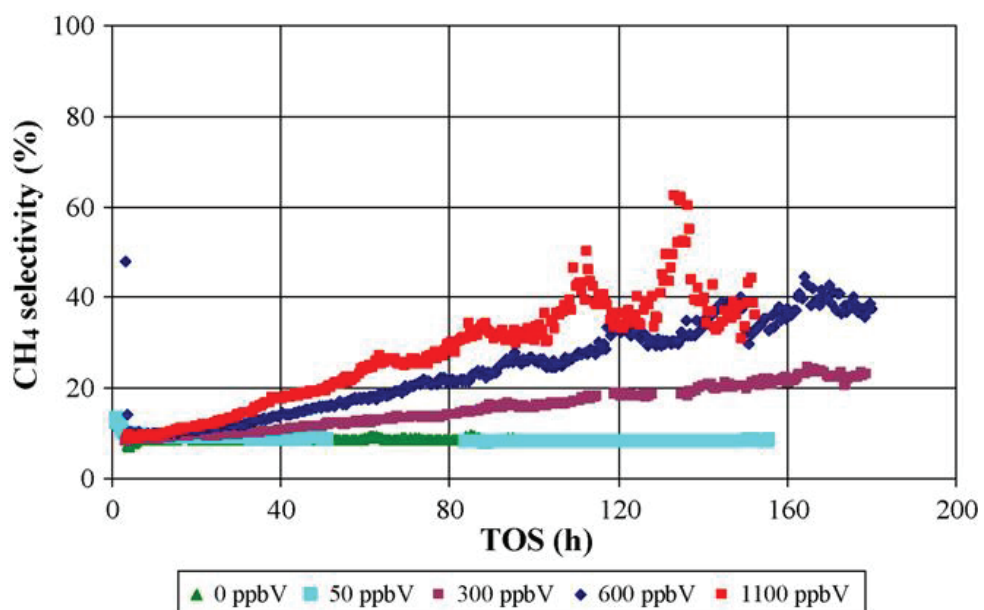
Figure 2.3 CH4 selectivity with varying sulfur content [34]

28

The promoter effect of the small amount of the sulfur is more questionable. Barrientos (2016) and coworkers did an experiment for this subject. In this method, assuming all sulfur fed into the reactor chemisorbs irreversibly on the catalyst surface and 4 catalysts were prepared with different sulfur amount. The Sulfur amounts are 10, 100, 250 and 1000 ppmv of sulfur and they were called as S10, S100, S25 and S1000 respectively. These amounts of Sulfur correspond to 250, 2500, 6250, and 25000 hours on stream for a gas hourly space velocity (GHSV) of 2 NL/h-gcatalyst and a Sulfur concentration in syngas of 20 ppbv. Experiment was operated at 20 bar and 210 $^{\circ}$C and using the H_2/CO ratio of 2.1. In addition, to make an accurate comparison of the different samples, the GHSV was adjusted to achieve CO conversion of 30 %. The tests lasted for 200-300 hours in order to reach steady state conditions for both activity and selectivity [28].

The relative activity of the catalyst was indicated as a function of the sulfur loading in the catalyst and the sulfur loading/sulfur capacity which is sulfur coverage. Based on the experimatal data, a deactivation model was referred in case of the loss activity as the function of sulfur coverage.

The deactivation model [28]

$a=(1-\theta s)^{\delta}$

a: Relative activity

θs: The sulfur coverage

δ : The deactivation order

According to the Figure 2.4, sulfur has a negative effect on catalyst activity. Main effect of sulfur is surface blockage of the catalyst, which leads to complete deactivation. The relative activity model was remained incapable of determination of S/Co adsorption stoichiometry. The S/Co adsorption stoichiometry increases with sulfur coverage. This fact implies that a proper understanding of this variation of the S/Co adsorption stoichiometry is required to determine the available Co metallic area (or the real sulfur coverage) for each poisoned sample. The model assumes that the activity of the catalyst is negligible at S/Co* = 1, as evidenced in other experimental studies. The deactivation order "δ" found using this equation is 3.78.

The 2nd model:

$a = (1 - S/Co^*)^{\delta}$

S/Co*: The sulfur to cobalt active site ratio
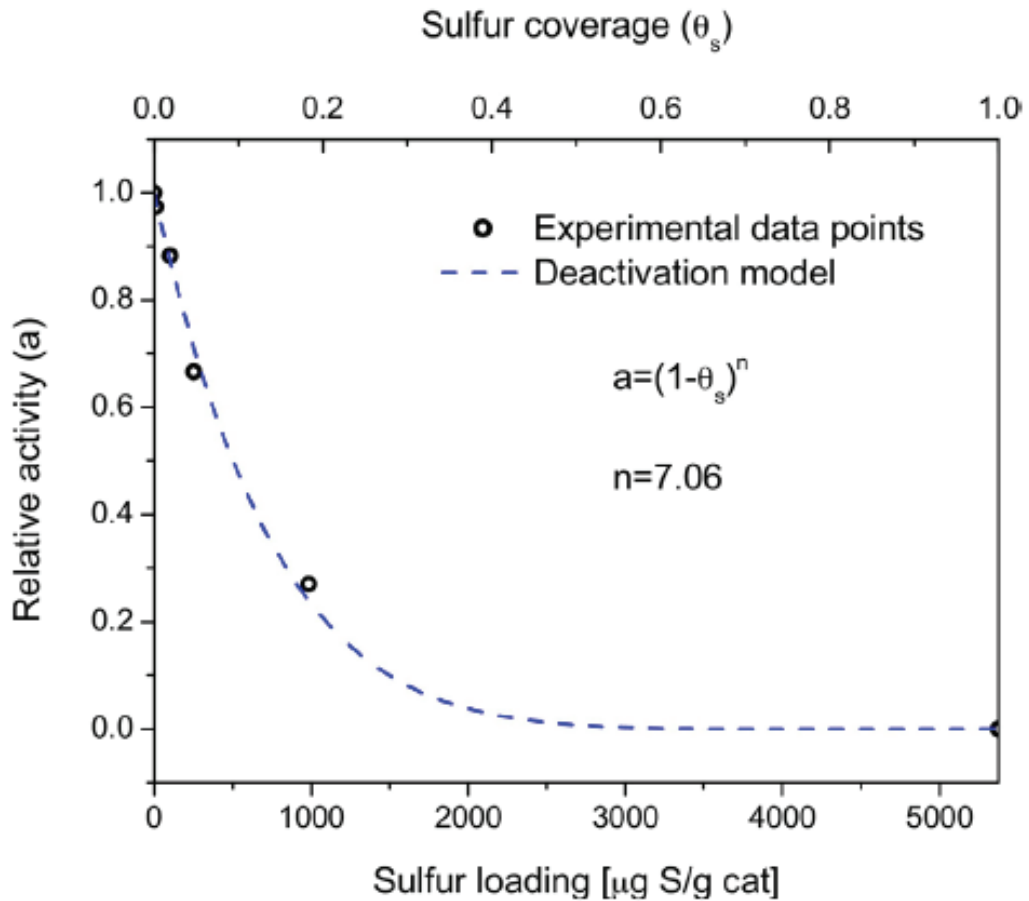
Figure 2.4 Relative activity as a function of the sulfur coverage and capacity [28]

This model which is presented in Figure 2.5, is coincide in situ poisoning studies from Bartholomew et al. using Co/SiO_2 catalysts. The effect of sulfur on selectivity is more complicated for understanding. Because there are various issues which must be take account for a proper assessment of this effect. It must be considered that the FT selectivity is related to the CO conversion. It affects the activity of catalyst and catalyst activity decreases with sulfur poisoning, which was reported in previous section. Another important criterion is the strong chemisorption of S on cobalt since poisoning is studied in fixed bed reactors by in-situ procedures. In this perspective, sulfur chemisorbs basically at the inlet of the catalyst bed leading to two reactor zones. First one which is totally deactivated and increases in size with time on stream and other one that behaves as a

nearly S-free catalyst. Finally, the selectivity of catalyst is same as on a catalyst which has not been poisoned. The selectivity to C_1, C_2, C_3, C_4, C_{5+} and CO_2 is presented in Figure 2.6. The selectivity to methane increases significantly with increasing S content. Sulfur also gives a slight increase in the selectivity to C_2-C_4 hydrocarbons. As a result, the selectivity to long chain hydrocarbons (C_{5+}) decreases with increasing S concentration in the catalyst. The selectivity to CO_2 was found negligible for all the samples and presented no appreciable trend with increasing S content.
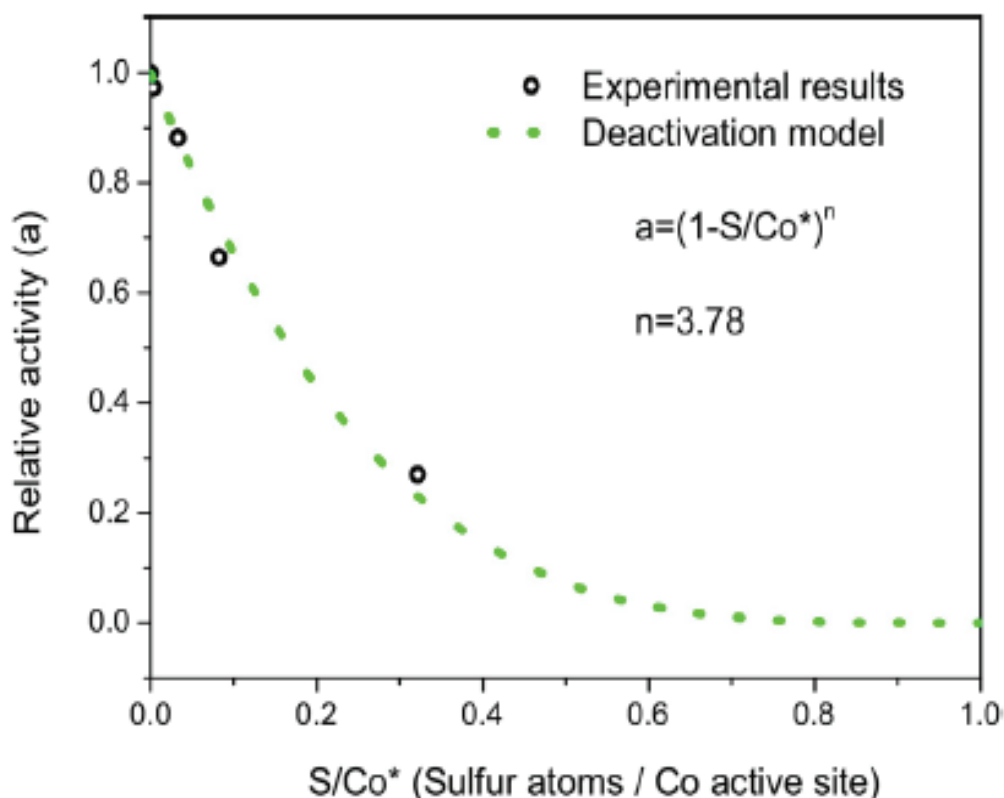
Figure 2.5 Relative activity as a function of the sulfur-to-cobalt active site ratio [28]

To conclude, the selectivity of short chain hydrocarbons, which is mainly methane, increases with increasing sulfur amount and sulfur favors olefin hydrogenation. This effect can be explained with hydrogenation activity of cobalt sulfide and a possible electronic modification of neighboring S-free cobalt atoms. However, there is no exact definition about effect of S on selectivity because of the lack of scientific agreement. These might be due to the use of different catalysts, poisoning agents, poisoning methods, type of reactor and perhaps, an underestimation of CO conversion effects on the FT selectivity.
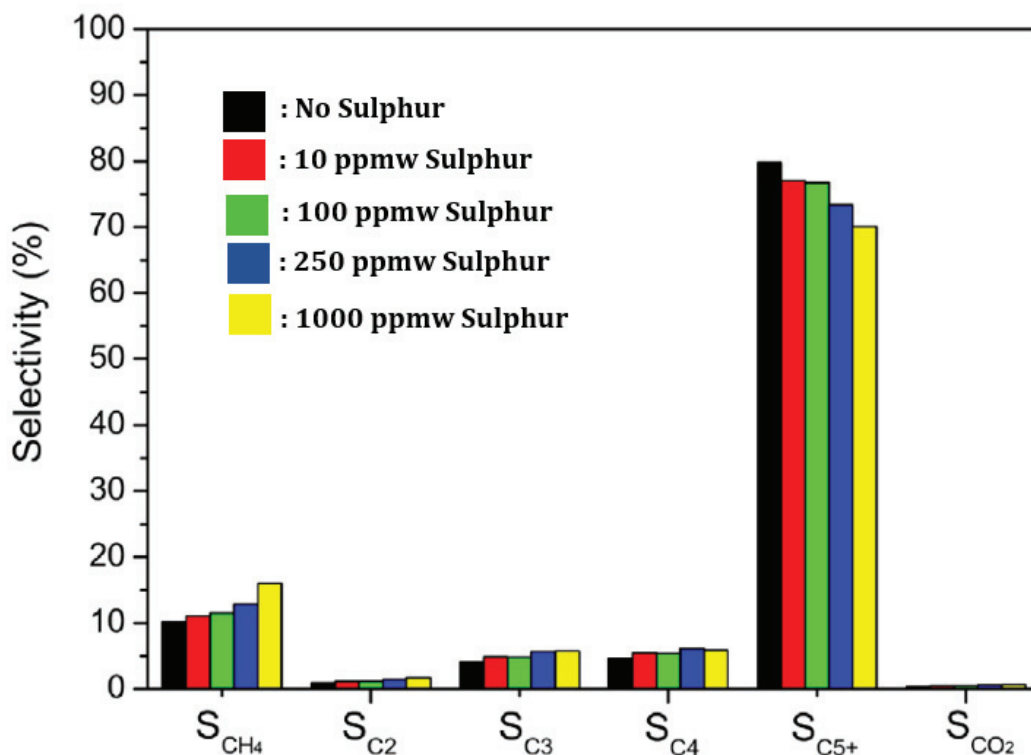
Figure 2.6 Effect of sulfur on the selectivity to different hydrocarbons and CO_2. Results obtained at 210 °C, 20 bar, inlet H_2/CO=2.1 and at a CO conversion=30 % [28]

2.2. Surface Science Studies for Effect of Sulfur on Activity and Selectivity of Fischer Tropsch Synthesis Catalyst

Surface science studies provide fundamental understanding of effect of sulfur on activity and selectivity of FTS catalyst. . CO and H_2 are the main reactants of FT reactions. To understand the effect of sulfur on these reactants, Lahtinen and coworkers (2004) stated two studies, are as follows. The first one is effect of CO and sulfur additives on $D_2/Co(0001)$ system. The study aims three fundamental subjects that are; firstly to observe pure hydrogen adsorption on Co(0001) surface, secondly H and CO co-adsorption on Co(0001) surface and finally, hydrogen adsorption on sulfur pre-covered Co(0001) surface to understand the effect of sulfur.

Experiments are operated ultra-high vacuum stainless steel chamber with base pressure 2.10^{-10} Torr. To obtain pure sulfur layer, decomposition of H_2S was operated at desired temperature followed by annealing to 650 K because of removing of hydrogen on the surface. The hydrogen adsorption on Co(0001) and effect of CO and sulfur on the

hydrogen adsorption were studied by XPS, TDS, WF measurements and LEED. Work Function measurements shows an increase of 200 mV on the deuterium adsorption because of electronegative character of deuterium. Therefore, hydrogen (deuterium) behaves as electron acceptor on the surface. Additionally, hydrogen can adsorb on and desorbs easily on cobalt surface because it has 33 kJ/mol binding energy. Finally, saturation coverage of hydrogen on cobalt surface is determined as 0.17 ML at 320 K and 0.27 ML at 180 K from TDS measurements. For effect of CO adsorption on deuterium adsorbed cobalt surface, the amount of adsorb deuterium decreases 50% from the initial amount of deuterium because of both repulsive interactions between CO and deuterium atoms and CO replaces with deuterium atoms.

Finally, researchers stated that increasing sulfur coverage decreases the hydrogen adsorption on the Co (0001) system. Because sulfur blocks the hydrogen adsorption sites and shifts the hydrogen energetically less favorable adsorption sites. The sulfur effect is shown in the Figure 2.7.

As shown in Figure 2.7 , the D_2 desorption rate that is coverage of D_2 on Co(0001) decreases linearly with increasing sulfur coverage from 0 to 0.25 ML. The inset on the graph shows this relationship. Blocking of adsorption sites of deuterium by sulfur causes the decreasing of deuterium coverage on cobalt surface. Second result from Figure 2.7 is related to temperature values.

As shown in Figure 2.7, increasing sulfur coverage from 0 to 0.25 ML causes a shifting on desorption temperature from 375 K to 290 K. This is a result of that hydrogen places energetically less favorable adsorption sites because of sulfur. As a result sulfur is a poison for the hydrogen adsorption on cobalt surface [44]. The second study [45] of the same group is related to effect of sulfur poisoning on CO adsorption on the Co(0001) surface. The experimental procedure is same as the previous study. For saturation sulfur coverage, 0.25 ML [26] was used. For CO adsorption on the Co(0001) surface, CO can adsorb and desorbs on the surface, however CO dissociation was not observed. For 0.25 ML Sulfur pre-coverage, CO saturation coverage decreased from 0.54 ML to 0.27 ML. The activation energy of desorption for CO decreased from 113 kJ/mol to 88 kJ/mol and it was observed weak CO bond to the surface. The trend of CO/S/Co(0001) was a combination of steric and electronic effect.

Sulfur has short-range effect on the catalyst surface. The short-range effect is that

one sulfur atom blocking effectively 1.2 CO sites for this system [4]. Similar to this for Ni(111), one S atom blocks 2.1 CO sites [23], on Ni(100) where one S atom blocks 1.4 CO sites [24] or about 10 Ni sites [25]. On Pd(100) surface, the blocking is not linear and more efficient with small S coverage [26,27]. This means that, sulfur blocks neighbor active sites on the surface. This finding can be supported with the study of Lahtinen at 2005. The study shows the change of charge density of sulfur and this change gives information about interaction of sulfur with next neighbor cobalt atom, see on Figure 2.8. The study aims that to observe local adsorption structure of sulfur on cobalt surface. They formed a p (2x2)-S structure on Co(0001) surface using the DFT and LEED measurements. As a result, fcc sites are energetically favorable for sulfur atoms compared with bridge, hcp and top sites. The adsorption energy of fcc, hcp, top and bridge site are -5.35 eV, -5.33 eV, -4.12 eV and -5.15 eV respectively.
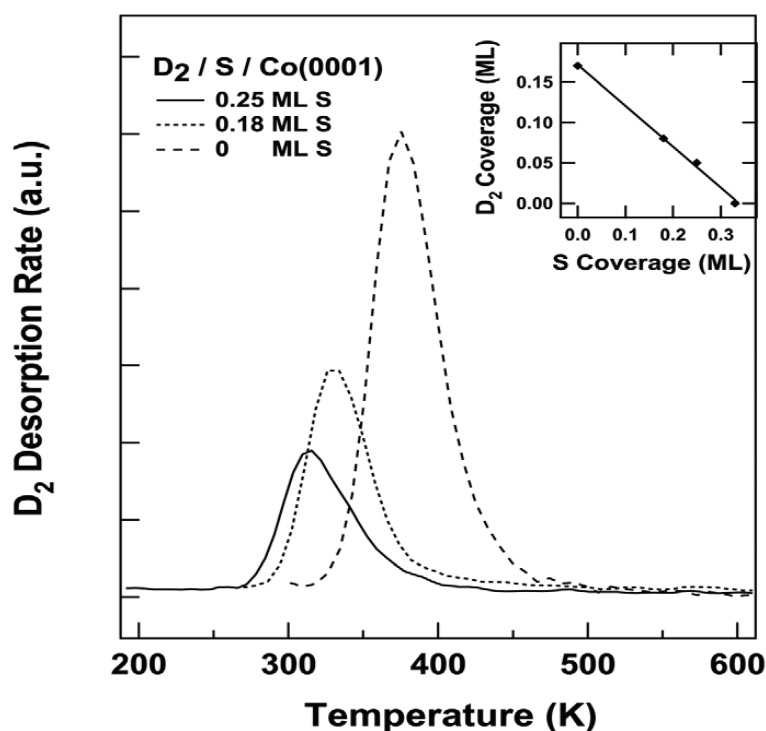
Figure 2.7 TDS signal for 200 L of D_2 for increasing sulfur coverage [44]

Based on Figure 2.8 , the interaction takes place between the topmost Co surface atoms and the adsorbed S atoms. The S adatom is slightly bound to the next neighbor Co surface atom, but there are only small changes in the electronic structure near the other Co atoms, based both on the LDOS and charge density. It can be said that about the

poisoning effect of S on Co(0001) as the S atom effectively blocking the site it is located at but leaving the other sites still active.
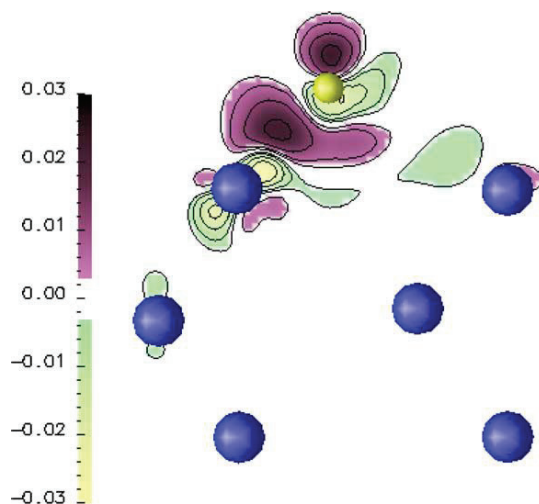
Figure 2.8 Changes in the charge density due to S located at the

fcc site on Co (0001).The successive contours correspond

to ±0.003, ±0.006, ±0.012, ±0.020 electrons /Å^{3}

Lahtinen et al (2005) stated the effect of elemental sulfur on cobalt system and they proposed that 0.25 ML sulfur pre-coverage has poison effect on the cobalt catalysts. As the same manner McAllister et al (2005) did a study to determine the amount of sulfur which can poison the CO methanation. The authors investigated elemental sulfur hydrogenation pathway, where elemental sulfur converted into H_2S on Rh(211) surface [46]. Generally, the remainder of experimental and DFT studies are focused on H_2S dissociation on the surface [47]. This is due to H_2S being the main sulfur source for the FT reaction. This study aims to answer the difference between S, C and O hydrogenation mechanism. Because carbon leaves the surface as CH_x products [48] and O leaves the surface as water or OH [49] , but sulfur does not leave the surface as H_2S. To answer this question, Sulfur hydrogenation was investigated in the article the overall hydrogenation reaction consists of two elementary reactions. First reaction is S+H→HS with 1.53 eV activation barrier and the second reaction is HS+H→H_2S with 1.43 eV activation barrier. For the reverse barriers, there is a decrease which are 0.32 eV and 0.01 eV, respectively. The results show that elemental sulfur does not leave the surface as H_2S. In addition to this, the second question of this article is that to observe effect of sulfur on CO

35

methanation for step surfaces. The adsorption energy of sulfur, which is 6.00 eV, indicates strong chemisorption with the surface and it adsorbs on the defect sites. This value is 5.35 eV for Co (0001) surface [4]. Reaction takes place on the defect site. However, sulfur covers the defect site, which interrupts and therefore poisons the reaction. Defect site is covered by sulfur, so CO methanation is blocked by sulfur. This finding proved that sulfur blocks the active site of the catalyst, so it causes poison effect [4].

Properties of sulfur adsorption on the metal surfaces have an important criteria for understanding the poisoning effect of sulfur on metal catalyst [15]. Based on this, coverage effect studies are important for interpreting the poison effect of sulfur on metal catalyst. Furthermore, Ma et al (2010) did a study which is related to the sulfur adsorption on the Co (0001) surface with different coverages, from 0.11 ML up to 1 ML. The relationship between sulfur coverage and adsorption energy is shown in Figure 2.9. The authors have stated that, S prefers to adsorb in hollow sites with -5.2 eV adsorption energy. This is the strong chemisorption because of strong interaction between S-Co at lower coverage. At higher coverage, the strong S–S interaction is dominating, so it leads to the formation of S_2 species.

Based on the Figure 2.9, adsorption energy of sulfur increses numerically but energitically gets weaker with increasing surface coverage. Sulfur forms strong covalent bond with surface at low coverages ($\theta_s < 0.33$ ML) and the dominant mixing is between Co (3d) and S(3p).

Tang et al. stated that, the most important part for the understanding of sulfur poisoning on the metal surface H_2S splitting [50].They compared H_2S dissociation between step and flat surfaces. Finally, they indicate that on each surface examined, the dissociative adsorption easily leads to formation of elemental sulfur from initial molecular adsorption of H_2S. They investigated that, first dissociation reaction which is formation of HS disproportionation reaction is not a favorable pathway. Beside this, authors say that deficient sites (step surface) are known as the most active sites of Cu-based catalyst in the absence of the sulfur containing. Jiang et al. stated that atomic sulfur causes the poison effect on FTS catalysts. This can be explained with dissociation of H_2S on metal surface with using DFT. H_2S dissociation takes place in two steps;

$$First\ Step：H_2S \rightarrow HS + H$$

$$Second\ Step：HS \rightarrow S + H$$
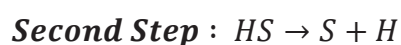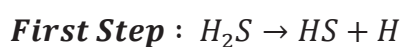
Adsorption of H_2S is very low (-44 kJ/mol at bridge site) which means it is easily breakdowns HS (intermediate product) and H then HS breakdowns S and H. Based on this, H_2S cannot be the reason of poison for the FTS catalyst. However, HS and S can be strongly adsorbed on the surface, so these species are not removed from surface easily. According to this, HS and S can be the reason of the sulfur poisoning. In the Figure 2.10 H_2S dissociation on Fe (100) surface is shown.[51]
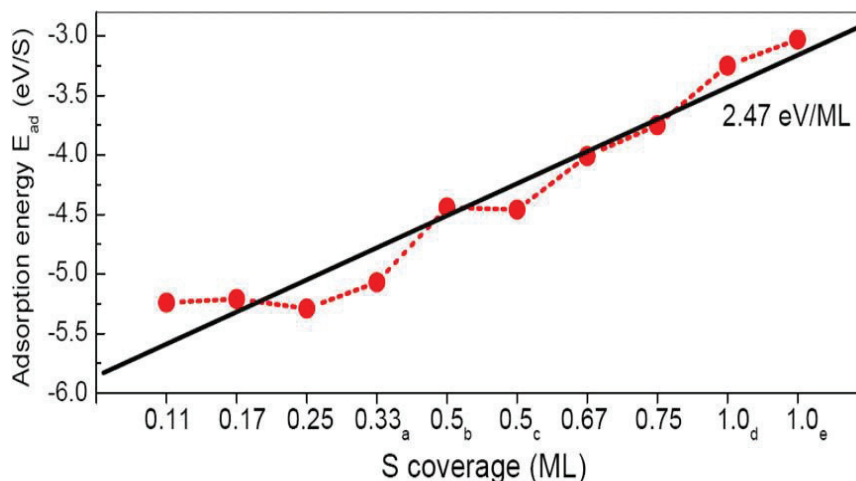
Figure 2.9 Adsorption energies of Sulfur as a function of Sulfur coverage (the bold line is the linear fit)[15]

According to the Figure 2.10 the electronic interaction of H_2S with Fe surface is weak, HS have a stronger interaction with Fe surface compare with H_2S, and dissociative S adsorption is the strongest.
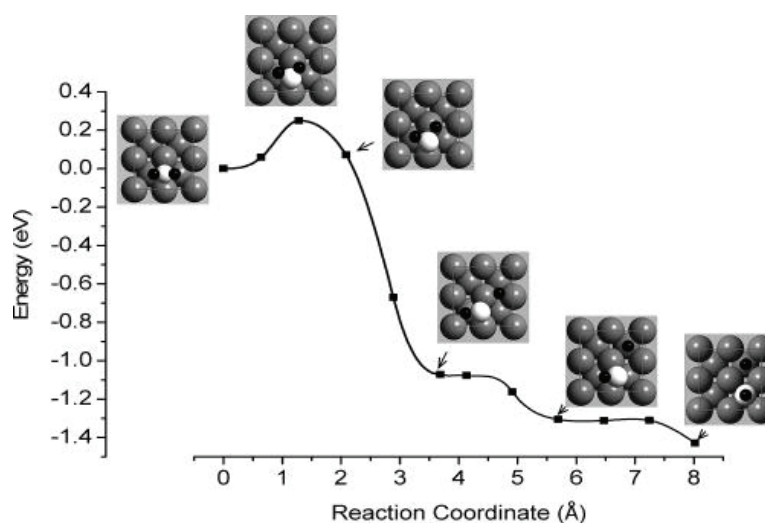
Figure 2.10 Adsorption and dissociation of H_2S on Fe (100) surface[51]

CHAPTER 3

COMPUTATIONAL METHODOLOGY

In this chapter, a short summary of the computational methods used in this study is covered. For computational tool, Density Functional Theory (DFT) is used. The principle and physical background of each technique is introduced. During the study, effect of sulfur covered on 0.25 ML and 0.11 ML Co(111) surface was investigated. Calculations were done by Vienna Ab-Initio Simulation Package (VASP).

Bulk Optimization
- Volume Relaxation
- ENCUT Optimization
- KPOINT Optimizaiton

Clean Surface and Molecule Optimization

Adsorption Energy Calculation
- Adsorption
- Co-adsortption
- Zero-Point Enery Calculation

Transition State Calculation
- Nudge Elastion Band (NEB) Calculation
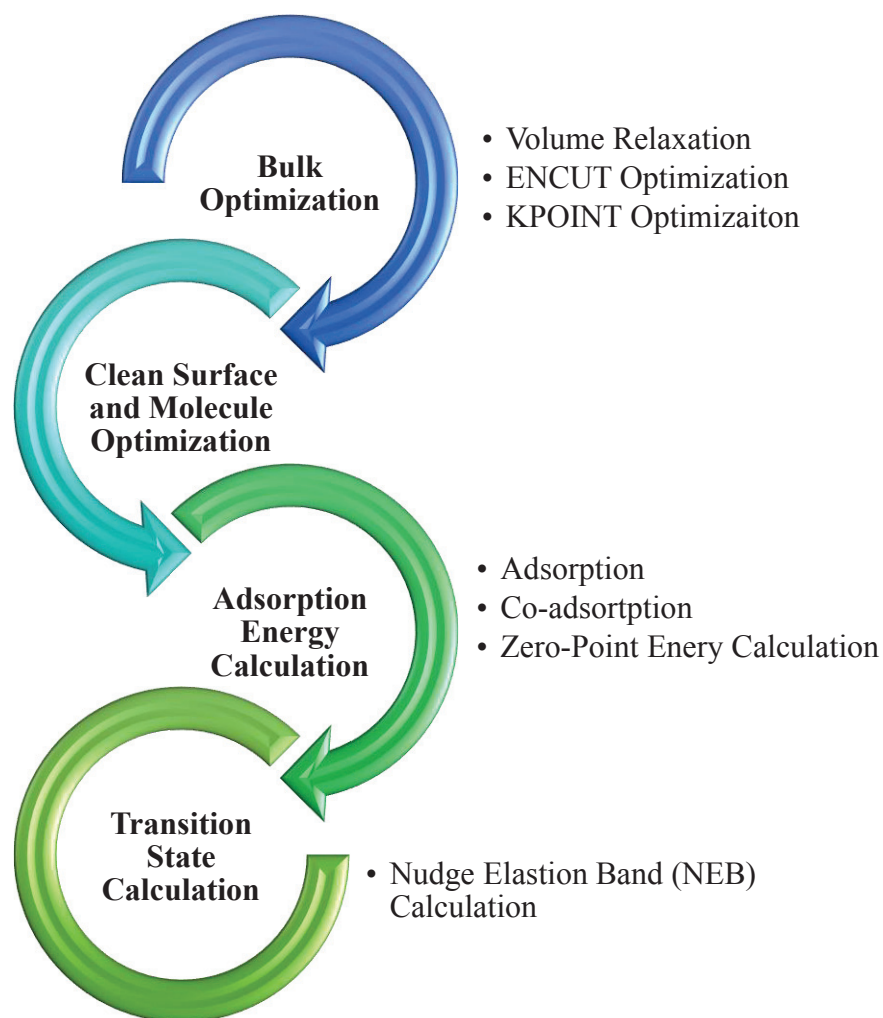
Figure 3.1 General schema for Calculation Steps

Table 3.1 Fundamental Input Files of VASP[52]

File Name	Description
INCAR	It is the central input file of VASP, to tell the calculation file what to do and how to do it.
POTCAR	It contains information about the atoms and their mass, their valence and energy of the reference configuration for which the pseudopotential was created.
KPOINTS	It is the mesh size for creating the k-point grid
POSCAR	This file contains the lattice geometry and the ionic positions of atoms.

Table 3.2 Fundamental Output Files of VASP [52]

File Name	Description
OUTCAR	It is the main output file. All energy values, vibrations and etc are placed in here
CHGCAR	Contains charge density, lattice vectors and atomic coordinates. It contains also one-center occupancies
CONTCAR	It is the the updated POSCAR file after each calculation, whether ionic movement was performed or not.

3.1. Bulk Optimization

Bulk optimization is the first step of the calculations. It contains volume relaxation, ENCUT optimization, and KPOINT optimization. Volume relaxation is a tool to determine the lattice constant for bulk structure. It was calculated as 3.516. Also, bulk Co has face-centered cubic structure.

Surfaces that are p(2x2), p(3x3) created in Materials Studio software program by using lattice constant and entering space group, which is FM-3M for cobalt. Bulk contains 4 cobalt atoms in each layer and the layer number is the thickness of the bulk. In this study, 5 layers were used for p(2x2), p(3x3) Co(111) surfaces. The vacuum thickness was 15 Å. ENCUT optimization is done to determine the maximum cut-off energy. ENCUT energy value must be greater than the all atoms ENCUT energy values. Finally, ENCUT

value was calculated at 600 eV as an optimum value. Then, KPOINTS optimization was done and found as 19 19 19. Bulk optimization was completed.

3.2. Clean Surface and Molecule Optimization

This chapter is related with clean surface optimization steps and molecule optimization analogy.

3.2.1. Clean Surface Optimization

This step is done for optimizing the surface, which is created on Materials Studio software. The correct input files and input command are important for achieving accurate results. In this study, cobalt is used as catalyst surface. Cobalt is a metal element, so this is important for the calculation. These metallic properties must be remarked in the INCAR file. These are, IBRION, ISIPIN, MAGMOM values which shown in Table 3.3.

As mentioned on the Table 3.1., there are 4 INPUT Files. INCAR File is same as Table 3.1 KPOINT value for clean surface optimization is calculated as the following.

For 0.25 ML (p (2x2)) Co (111) surface;

$$\frac{19}{(2x2)} \cong 5$$

- 19 is the optimized KPOINT value at bulk optimization.
- KPOINT value are calculated as 5 5 1 for 0.25 ML, 3 3 1 for 0.11 ML (p (3x3)).
- POSCAR File is the geometry of the surface. For clean surface optimization all atoms kept relaxed. Finally, POTCAR File is formed similar order of POSCAR file.

3.2.2. Molecule Optimization

The molecule optimization provides the calculation of molecule's energy at gas phase. It is used during the calculation of adsorption energy of related molecule INCAR file is same as clean surface optimization with no differences, which are dipole correction and magnetic value. For molecule optimization, IDIPOL is equal to four and MAGMOM

value is not written here because, MAGMOM value is valid only for metals.

Table 3.3 Sample INCAR File for calculation [53]

TAG	JOB
ISTART =0	Start job
ENCUT = 600	Cut-off energy
ISMEAR = 1; SIGMA = 0.2;	Determines how the partial occupancies are set for each orbital. SIGMA determines the width of the smearing in eV.
EDIFF = 1E-4	The relaxation of the electronic degrees of freedom will be stopped if the total (free) energy change and the band structure energy change between two steps are both smaller than EDIFF.
EDIFFG = -0.01	defines the break condition for the ionic relaxation loop
NSW = 999	Sets the maximum number of ionic steps.
POTIM = 0.5	time-step for ion-motion
IBRION = 2	**determines how the ions are updated and moved, IBRION = 2 is for first trial**
ISPIN = 2	spin polarized calculation (2-yes 1-no)
MAGMOM = 20*3	**specifies the initial magnetic moment for each atom** **20 = #of cobalt atoms in bulk, 3=**
LDIPOL = .TRUE.	switches on corrections to the potential and forces in VASP True means switch on, false means switch off.
IDIPOL = 3	Switches on monopole/dipole and quadrupole corrections to the total energy.
GGA = RE	*Tags for VDW Functional*
LUSE_VDW = .TRUE.	
AGGAC = 0.0000	
LASPH = .TRUE.	

3.3. Adsorption Energy Calculations

Adsorption energy calculation is separated into two sections. First one is bare adsorption, where molecules adsorb on the bare Co(111) surface. Second one is co-adsorption, where molecules adsorb on the surface with another molecule.

3.3.1. Molecule Adsorption Energy Calculations

Adsorption energy calculation on bare Co(111) surface provides the determination of most stable adsorption sites and adsorption energy on that site. For 0.25 ML bare Co (111) surface is presented in Figure 3.2.

Adsorption sites are presented in Figure 3.2. The adsorption energy is calculated as Equation 4.

$$(E_{ads})_i = E_{(slab+i)} - (E_{slab} + E_{i_{molecule}})$$ **Equation 4**

$(E_{ads})_i$	:	adsorption energy of species [eV]
E_{slab}	:	Co (111) surface energy [eV]
$E_{i,molecule}$	:	energy of molecule in gas phase [eV]
i	:	Species
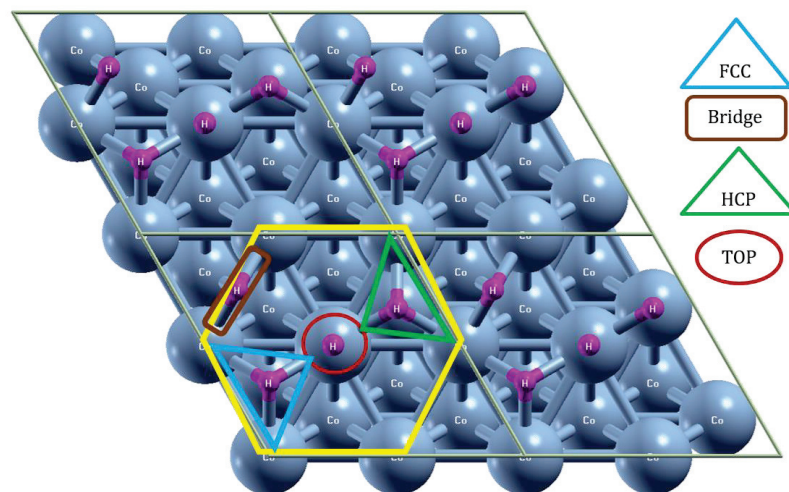
Figure 3.2 Adsorption Sites for 0.25 ML Co (111) surface

3.3.2. Co-adsorption Energy Calculation

Co-adsorption calculation is done to determine how sulfur affects the adsorption sites and adsorption energies of species when they adsorb on surface together with sulfur. Besides, adsorption sites are determined based on their proximity from the sulfur.
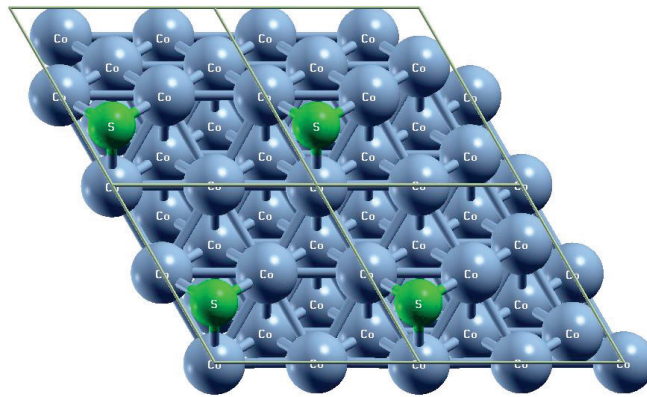
Figure 3.3 0.25 ML Sulfur Covered Co (111) surface

In Figure 3.3, shows regions of adsorption sites around sulfur. 0.25 ML has high sulfur coverage compare to the 0.11 ML sulfur covered Co(111) surface. So, all species must be placed on adsorption sites that are close to sulfur. For 0.11 ML sulfur covered Co(111) surface, there are two regions. These are close and far region from sulfur.
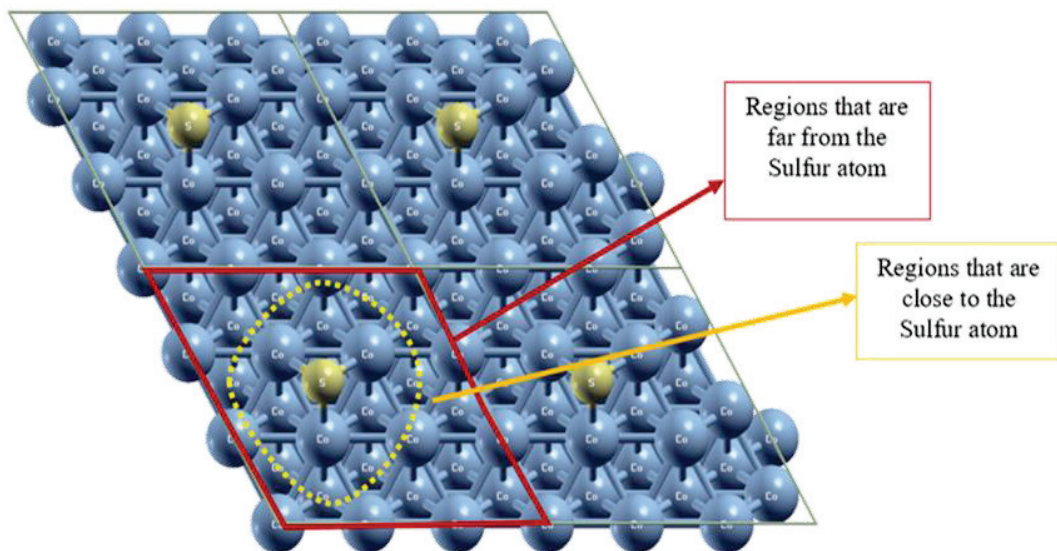
Figure 3.4 0.11 ML Sulfur Covered Co(111) surface

The co-adsorption energy is calculated as Equation 5.

$$E_{(x \, ads \, on \, i)} = E_{(slab+x+i)} - (E_{slab+i} + E_{x_{molecule}})$$

Equation 5

$E_{(x \, ads \, on \, i)}$	:	adsorption energy of species [eV]
E_{slab+i}	:	S+Co (111) surface energy [eV]
$E_{x\_molecule}$	:	energy of molecule in gas phase [eV]
i	:	Sulfur atom
x	:	species (C, O, H, CO, CH_y, C_2H_y, H_2O, OH)

3.3.3. Zero Point Energy Calculation

The next step after the adsorption calculation is vibrational analysis. Zero-point energy is calculated with the aid of vibrational frequency analysis. The INPUT Files that are mentioned previous sections are valid in here. However, IBRION tag is changed as 5 instead of 2 compared to the adsorption calculation. This special condition is valid for vibration analysis calculation. For POSCAR file, all metal atoms kept fixed and only adsorbates kept relax.

After the calculation, the output file has 3 vibrational frequency for each atom. For example, OH molecule has 6 vibrational frequency values (2 atoms, 3 vibrational frequencies). In general, energy of a body and a system is defined as the motion of the system at the given position of the system. The general equation is shown below.

$$E = \frac{1}{2} mv^2 + mgh$$

Equation 6

In thermodynamics, the energy of the system depends on absolute temperature (T) of the system. In the ground of thermodynamics, the motionless system at absolute zero has zero energy. But in quantum mechanics, the energy of a system is always related with the expectation value of Hamiltonian operator, which is given by formula below.

$$E = \frac{1}{2}hv + \frac{hv}{e^{\frac{hv}{kT}} - 1}$$

Equation 7

E	:	energy value [eV]
h	:	Plank's constant [$4.15*10^{-15}$ eV.sec]

44

k : Boltzmann constant [$8.617*10^{-5}$ eV/K]

T : Temperature [K]

v : frequency [sec^{-1}]

Based on the Equation 7, T is equal to zero. In this case, $e^{hv/kT}$ is diverging to infinite so $hv/(e^{hv/kT}-1)$ term becomes zero. So Equation 7 is replaced as shown below.

$$E = \frac{1}{2} hv \qquad \qquad \textbf{Equation 8}$$

Based on the Equation 8, the zero-point energy is calculated. Below, sample calculation is presented for ZPE calculation. Vibration values are added into sigma corrected adsorption energy of each species. This is formulized as,

$$E^{ZPE} = (E^{SCE}_{slab+adsorbate} + E^{ZPE}_{slab+adsorbate}) - E_{slab} \qquad \textbf{Equation 9}$$
$$- (E^{SCE}_{adsorbate} + E^{ZPE}_{adsorbate})$$

SCE refers sigma corrected energy, and $E_{adsorbate}$ refers adsorbate's energy at gas phase. Sample calculation is shown below for zero-point energy.

Zero Point Energy for CO Molecule:

Adsorption energy calculation based on Equation 4 :

$$(E_{ads})_i = E_{(slab+i)}(= 79.609) - \left(E_{slab}(= -67.019) + E_{i_{molecule}}(= -11.356)\right)$$
$$= -1.234 \ eV$$

Vibration calculation based on Equation 8:

Table 3.4 Frequency result from VASP

1 f =	1954.9	cm^{-1}	242.377	meV
2 f =	439.841	cm^{-1}	54.5333	meV
3 f =	371.754	cm^{-1}	46.0916	meV
4 f =	360.628	cm^{-1}	44.7121	meV
5 f =	165.981	cm^{-1}	20.579	meV
6 f =	48.348	cm^{-1}	5.9944	meV
			414.287	**meV**

414.287 meV is the summation of 6 frequency values. Based on the Equation 8, hv term was calculated with unit of meV. If 414.287 is divided by 1000 meV converts to eV. Finally, the energy value in eV (0.414287) is divided by 2 that is taken from formula, ZPE of $E_{slab+adsorbate}$ is calculated as 0.20714 eV. The same procedure is used for ZPE of CO molecule at gas phase and it is calculated as 0.211 eV. When the results placed into the Equation 9, ZPE of CO was calculated as -1.24 eV.

3.4. Transition State Calculation

Transition state has an importance in surface science to obtain and explain minimum energy paths (MEPs) and describing atomic diffusion, molecular diffusion or reaction on a given potential energy surface (PES). It is required to find those elusive transition states and obtain certain energy barriers to determine kinetics in catalysis. These calculations likewise include the research for the saddle point along the reaction coordinate for the pre-set initial and final states. A first-order saddle point should be a maximum through the reaction coordinate, but a minimum in all other directions. A number of transition state research techniques are available in the literature, and have been reported by Henkelman et al.[54]. When the initial and final states are specified, the Nudged Elastic Band (NEB) [55] may be the most frequently preferred method, and is widely applicable in VASP, CASTEP, GPAW, Quantum Espresso and suchlike that. The Synchronous Transit method [56] has been incorporated into DMol[3] and CASTEP. The conjugate peak refinement (CPR) [57], and the Ridge methods [58] have been developed to find fluid phase transition state and energy barriers, and are included in programs, such as CHARMM. When the initial state is specified, dimer method [54], is more useful for calculations. The dimer method is available in software, such as VASP. In the following sections, the NEB is explained in detail.

3.4.1. Nudged Elastic Band (NEB) Method

In the NEB method, a geometric interpolation (or string of images) between the known reactant (R) and product (P) are generated and relaxed. At the beginning, the locations of intermediate images can be generated with the aid of simple linear interpolation. After that, subsequent optimizations will relax the images to the real MEP. Therefore, NEB is preferable to map out the MEP in a field of the potential energy.

Multiple saddle points can be indicated and specified using NEB as well. The true force on each individual image in the elastic band is separated into a perpendicular and a parallel component to the MEP during relaxation. A nudging force, which is perpendicular to the pathway, is used to ensure that there will not be severe corner cutting at the curve of the MEP. The modified Climbing Image NEB (CI-NEB) method can move the highest energy image towards the energy uphill in order to avoid the slip of the image near the saddle point, by turning off the nudging force completed and keeping only the inverted parallel component. Consequently, the image can maximize its energy among the band and minimize among all other directions at the same time. When this image converges in theory, this image will fall to the saddle point exactly. If the maximum image is away from the saddle point at first, and the climbing image was used from the outset, the path would develop quite different spacing on each side of the saddle point.[59]

The NEB Calculation procedure is following.

- The initial and final adsorption files are optimized at previous sections. For instance; to determine CO dissociation barrier (CO → C+ O) CO adsorption on Co (111) surface is selected as initial geometry and C and O co-adsorption situation is taken as final geometry for NEB calculation.

- Images are formed from the initial and final geometries. A video is formed to observe the movement of reaction on surface. The reaction must move in shortest way because, the shortest way provides the minimum energy.

- INCAR File is organized for NEB Calculation given in Appendix B2.

- Run the calculation file. End of the calculation, a volcano curve is plotted based on each image's energy values. The top of volcano curve is selected as approximate transition state candidate. In addition, top of volcano curve alone is not enough criteria for selecting transition state candidate. As the second criteria, video of movement of reaction is formed by CONTCAR files of 8 images'. If the video progresses as initial video, the top of volcano curve' image is selected transition state candidate.

- Selected imaged ae optimized as adsorption calculation. If it same or close to same as transition state candidate, vibrational analysis is done. If it has one imaginary frequency, it is selected as Transition state for the reaction.

- Finally, transition state graph is plotted as adsorption energy versus reaction coordinates. Energy values of forward, reverse and heat of reaction is determined.

CHAPTER 4

RESULTS

4.1. H₂S Dissociation on Co(111) surface for 0.25 ML Coverage

In this study, H_2S dissociation was calculated. This calculation gives information about whether H_2S or its dissociation products, HS or atomic S is likely to be found on the Co(111) surface. Potential energy diagram (PED) for H_2S dissociation is presented in Figure 4.1. The information about the adsorption energies of sulfur species for step and flat surface is given in Table 4.1.

Table 4.1 Adsorption Energies and sites of Sulfur species for
0.25 ML and 0.11 ML coverages on Co(111)

Surface	Unit Cell	Adsorption Energy [kJ/mol] *(Adsorption Site)*		
		S	**HS**	**H₂S**
Co(111)	p(2x2)	-480 *(fcc)*	-275 *(bridge)*	-34.2 *(top)*
			-240 *(fcc)*	
		-479 *(hcp)*	-236 *(hcp)*	
	p(3x3)	-488 *(fcc)*	-266 *(bridge)*	-32.2 *(top)*
			-233 *(fcc)*	
		-472 *(hcp)*	-229 *(hcp)*	
Co(211)	p(2x2)	-520 *(step site)*	-318 *(bridge-step edge)*	-59.8 *(top-step edge)*
		-501 *(hcp-step edge)*	-271 *(top-step edge)*	
		-483 *(fcc- step edge)*	-264 *(fcc- step edge)*	
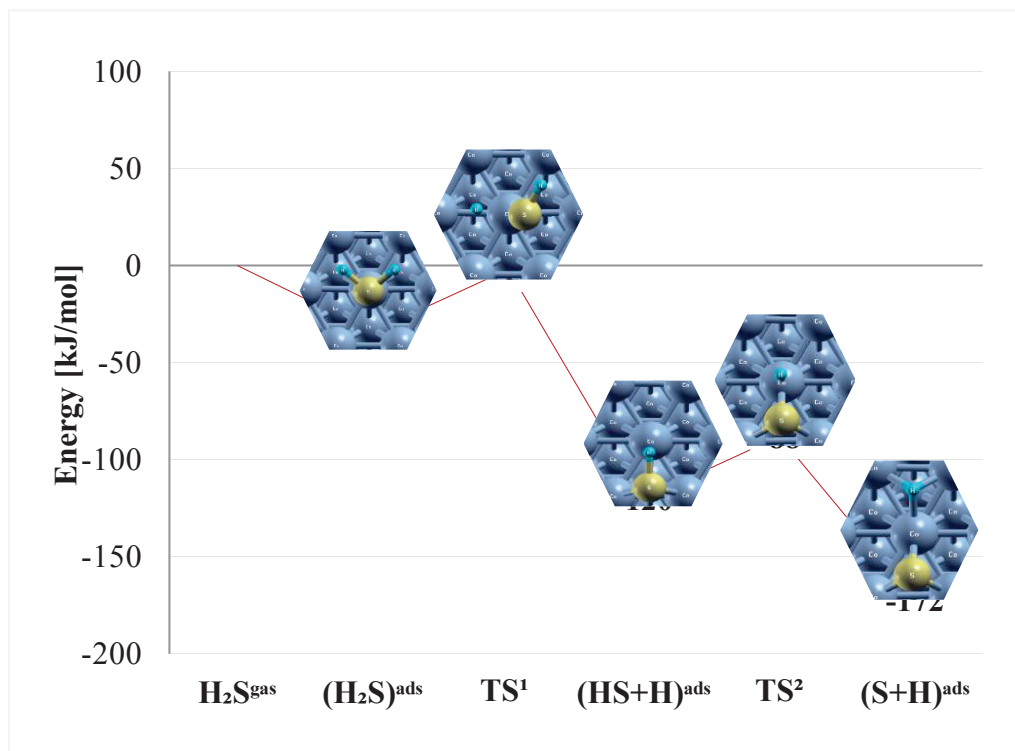
Figure 4.1 Potential Energy Diagram for H₂S Dissociation

Based on the analysis of Temperature Programmed Desorption spectra under Ultra-High Vacuum conditions (i.e. using the Redhead Equation), an adsorption energy/activation barrier of 100 kJ/mol corresponds to desorption/reaction peak temperature of 400 K (123°C)[9]. Although the relation is strictly valid for UHV conditions and 1st order desorption/reaction, it provides a rough estimate for the temperature that the reaction would take place based on its activation barrier. For the low temperature FTS conditions, temperature is typically around 250 °C, which means that reactions with an activation barrier below 130 kJ/mol would easily proceed on cobalt catalyst surfaces. Based on this analysis and Figure 4.1, H₂S easily dissociates to elemental S on bare Co(111) surface, indicating the main component that induces S poisoning is the atomic S. H₂S dissociation is also examined on the carbon and oxygen covered Co(111) surfaces, to evaluate if H₂S would also dissociate under FTS conditions on more crowded surfaces. Results are presented in the Figure 4.2.

According to the Figure 4.2, HS easily dissociates into elemental sulfur on bare, C and O covered surfaces, so the main S species that can be found on cobalt surfaces is atomic S. When reverse and forward reactions are compared, reverse activation barriers are lower than the forward reaction barriers, which indicates that HS can also be present

49

on the surface at low amounts. A full analysis of the coverages of S/HS would need a detailed kinetic modeling of the complicated reaction network, which is beyond the scope of this thesis.
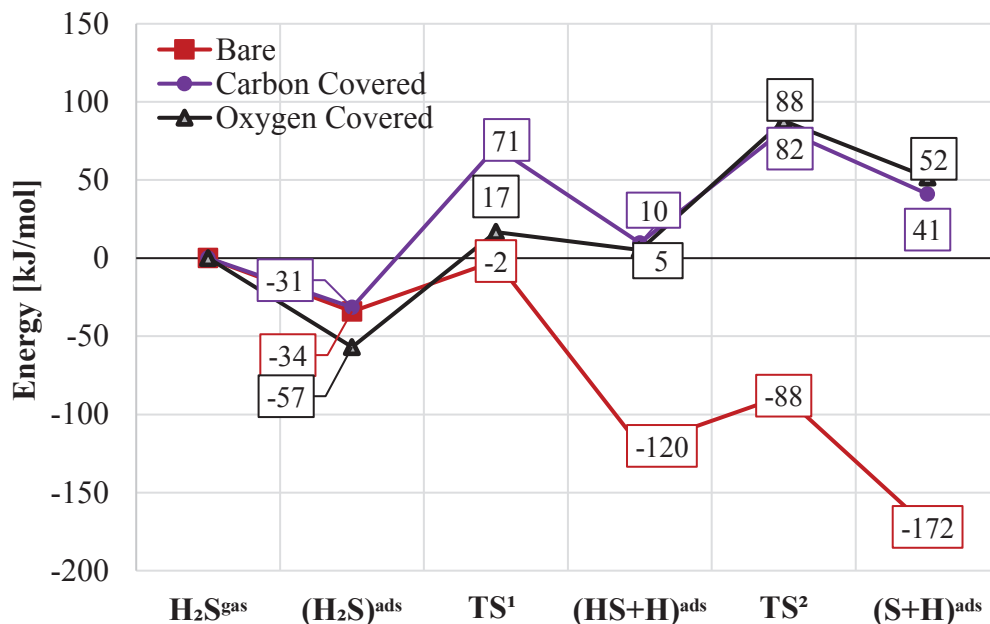
Figure 4.2 Potential Energy Diagram for H_2S Dissociation for 0.25 ML bare, Carbon, Oxygen and covered Co(111) surface

Table 4.2 H_2S Dissociation Barriers and reaction enthalpies for forward and reverse reactions for 0.25 ML bare, Carbon and Oxygen covered Co(111) surface

Surface	1st Dissociation Reaction $H_2S \rightarrow HS + H$	2nd Dissociation Reaction $HS \rightarrow H + S$
Bare	E^a_f = 32 kJ/mol E^a_r = 118 kJ/mol	E^a_f = 32 kJ/mol E^a_r = 84 kJ/mol
	ΔH_{rxn} = - 86 kJ/mol exothermic	ΔH_{rxn} = -52 kJ/mol exothermic
Carbon Covered	E^a_f = 102 kJ/mol E^a_r = 61 kJ/mol	E^a_f =72 kJ/mol E^a_r = 41 kJ/mol
	ΔH_{rxn} = 41 kJ/mol endothermic	ΔH_{rxn} = 31 kJ/mol endothermic
Oxygen Covered	E^a_f = 74 kJ/mol E^a_r = 12 kJ/mol	E^a_f =83 kJ/mol E^a_r = 36 kJ/mol
	ΔH_{rxn} = 62 kJ/mol endothermic	ΔH_{rxn} = 47 kJ/mol endothermic
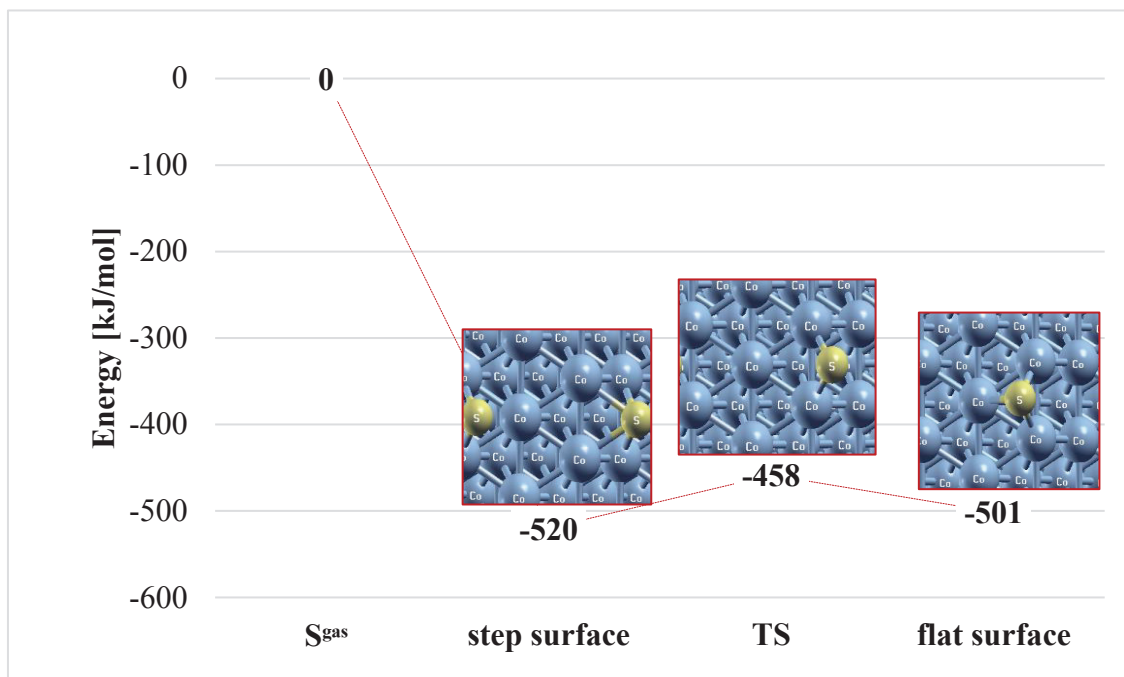
Figure 4.3 Potential Energy Diagram for diffusion of elemental sulfur from 0.25 ML Co(211) to Co(111)

Based on Figure 4.3, diffusion barrier of sulfur is 62 kJ/mol, which means sulfur, which can also be found on the step sites of cobalt nanoparticles (such as the Co(211) surface) can also be found on flat surfaces such as Co(111).

4.2. Effect of S and HS on the Adsorption Energies of Reactants and Intermediates of FTS for 0.25 ML and 0.11 ML Coverages on Co(111)

The coverage of sulfur can change its effect on adsorption energies of species, so coverage dependent sulfur effect is investigated in this section.

Based on the Figure 4.1, H_2S can easily dissociate on the cobalt surface to elemental sulfur and HS. So, effect of sulfur and HS on the adsorption energies of CO and H which are the main reactant of the FT reaction, OH and H_2O which are important for the water formation and CH which is the monomer of the hydrocarbon chain was examined. According to the Figure 4.5, due to sulfur and HS, adsorption energy of species decreases while this negative effect was reduced at 0.11 ML covered Co(111) surface. In addition to this, HS increases the adsorption energies of all species.
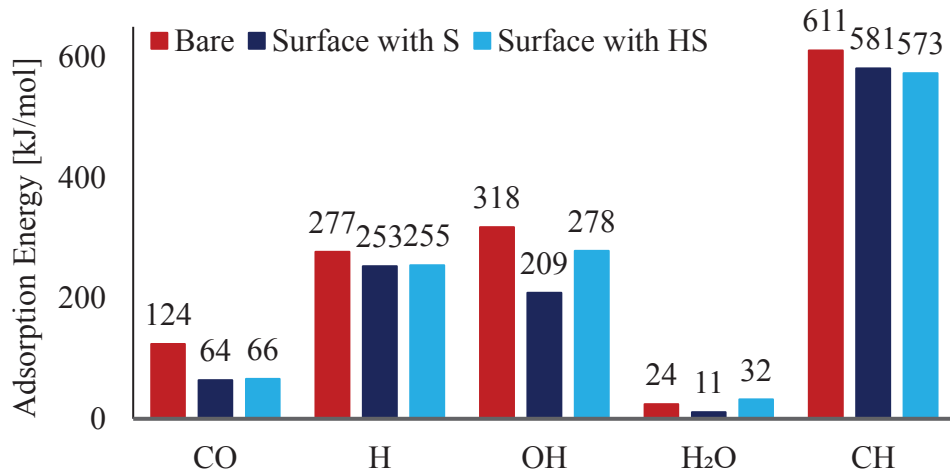
Figure 4.4 Effect of S on adsorption energies of species on 0.25 ML S covered Co(111) surface

Figure 4.4 and Figure 4.5 shows adsorption energies of main species on 0.25 ML and 0. 11 ML S and HS covered Co(111) surface. 0.11 ML HS coverage shows positive effect (promoting effect) on adsorption energies of species. However this effect is expected to be limited due to low concentrations of HS that could be found on Co(111), based on the activation barriers presented in Figure 4.2. This point will be investigated in detail, including other (lower) coverages, as a follow-up study of this thesis. So, in the Table 4.3, adsorption Energies and adsorption sites of species are presented only 0.25 ML and 0.11 ML sulfur coverage.
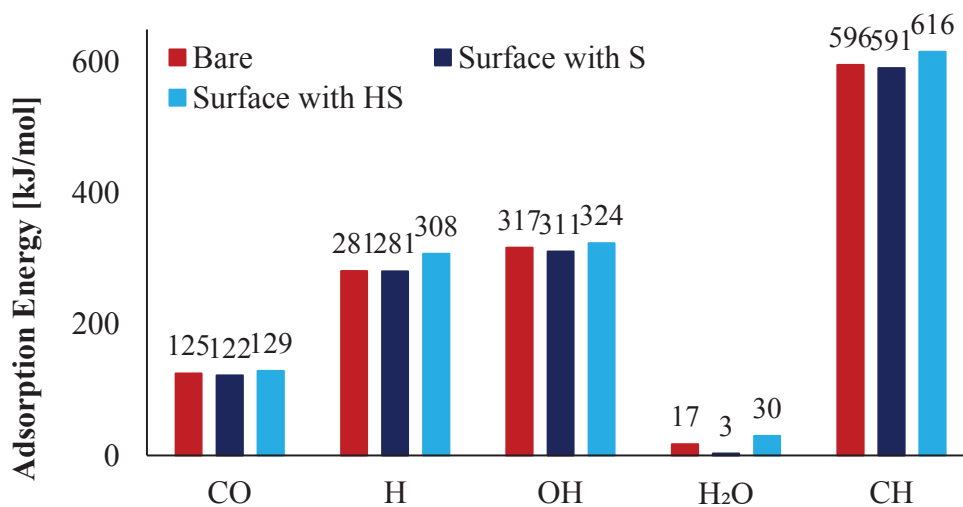
Figure 4.5 Effect of Sulfur and HS on adsorption energies of species on 0.11ML Covered Co (111) surface

Table 4.3 Adsorption Energies and sites for 0.25 ML and

0.11 ML bare and sulfur covered Co(111) surface

Species (Adsorption Site)		Adsorption Energy [kJ/mol]	
		0.25 ML	*0.11 ML*
CO*	Bare	-124 *(fcc)*	-125.4*(fcc)*
		-124.3 *(top)*	-125.3 *(top)*
	With S	-64	*Far from Sulfur*
			-122
			Close to Sulfur
			-115*(top)*
OH (hcp)	Bare	-318	-317
	With S	-209	*Far from Sulfur*
			-311
			Close to Sulfur
			-297
H_2O (top)	Bare	-24	-17
	With S	-11.13	*Far from Sulfur*
			-3
HCO (bridge)	Bare	-228 (-217) [60]	-218
	With S	-130	*Far from Sulfur*
			-198
COH (hcp)	Bare	-382 (-435) [60]	-378
	With S	-319	*Far from Sulfur*
			-360
			Close to Sulfur
			-362
HCOH (bridge)	Bare	-359 (-297) [60]	-362
	With S	-252	*Far from Sulfur*
			-320
			Close to Sulfur
			-323

Table 4.3 (cont.)

Species (Adsorption Site)		Adsorption Energy [kJ/mol]	
		0.25 ML	0.11 ML
H_2CO (bridge)	Bare	-67 (-82) [60]	-61
	With S	-36	Far from Sulfur
			-46
			Close to Sulfur
			-28
CH (hcp)	Bare	-611 (641.3,hcp) [61]	-596
	With S	-581	Far from Sulfur
			-591
			-597*
			Close to Sulfur
			-596
CH_2 (fcc)	Bare	-411 (410.2,hcp) [61]	-410 -402 (hcp)
	With S	-322	Far from Sulfur
			-391
			Close to Sulfur
			-384 (hcp)
CH_3 (fcc)	Bare	-230 (207, fcc) [61]	-232
	With S	-161	Far from Sulfur
			-224
			-235*
CH_4 (Not disstored)	Bare	-9 (6, not disstored) [61]	-3
	With S	-	Far from Sulfur
			-53
C_2H_2 (fcc)	Bare	-190 (fcc) (-212) [60]	-226
	With S	-	Far from Sulfur
			-197
C_2H_3 (fcc)	Bare	-239 (-246) [60]	-249 -248 (hcp)
	With S	-151	Far from Sulfur
			-227
			Close to Sulfur
			-222 (hcp)

Table 4.3 (cont.)

C$_2$H$_4$ (fcc)	Bare	-102 (-77) [60]	-95
	With S	-79	*Far from Sulfur*
			-78

*: sulfur shifted fcc to hcp site

Regions that are close or far from sulfur atoms affect the adsorption energies of species. For 0.11 ML sulfur covered Co(111) surface, these changes are not remarkable. For example, adsorption energy of CO changes 7 kJ/mol between close and far regions, and far region has high adsorption energy (122 kJ/mol) when compared to close region (115 kJ/mol). Additionally, 0.11 ML sulfur covered Co(111) surfaces give another information for the study. That is, low sulfur coverage (<0.25 ML) provides a positive effect on the adsorption energies of species.

4.3. Effect of Sulfur on the Elementary Reaction of Fischer Tropsch Synthesis

The other goal of study is to determine the effect of sulfur on the elementary reactions of FTS which are direct CO dissociation, removal surface free oxygen as H$_2$O and CO$_2$, carbon-carbon coupling reactions and hydrogenation/dehydrogenation of C$_1$H$_X$ and C$_y$H$_z$ species. [62]

4.3.1. Effect of Sulfur on CO dissociation

CO dissociation is an essential reaction for FTS. In this reaction, atomic carbon and oxygen, the dissociation products, are further hydrogenated to end products of paraffins/olefins and water/CO$_2$. The current consensus in literature is CO dissociation mainly takes place in two ways, the first is direct dissociation and the second is hydrogen-assisted dissociation.[63]

CO adsorbs on the top site with 124 kJ/mol adsorption energy for bare surface. However, in the presence of the sulfur, its adsorption site changes from top to fcc and its adsorption energy decreases from 124 kJ/mol to 64 kJ/mol. At the bare surface, oxygen

places on the hollow site, with co-adsorption with sulfur both place on the hollow sites. Sulfur adsorbs on fcc site on the bare Co(111) surface. But, between fcc and hcp sites' adsorption energies are relatively close to each other. These are -486 kJ/mol and -479 kJ/mol, respectively, where the difference is 7 kJ/mol. When S co-adsorb on the surface with CO, CO shifts from fcc to hcp site. At this situation, adsorption energy of CO becomes 64 kJ/mol. If sulfur comes to hcp site, CO shifts to fcc site and adsorption energy of CO becomes 67 kJ/mol. This shows that, both adsorption energy of sulfur at fcc and hcp site are close to each other and the adsorption energy of CO has no an essential difference (~4 kJ/mol) between these two situations.

Table 4.4 List of surface structures for initial, transition and final states for direct CO Dissociation Reaction

Direct CO Dissociation : $CO \leftrightarrow C + O$		
Initial State	*Transition State*	*Final State*
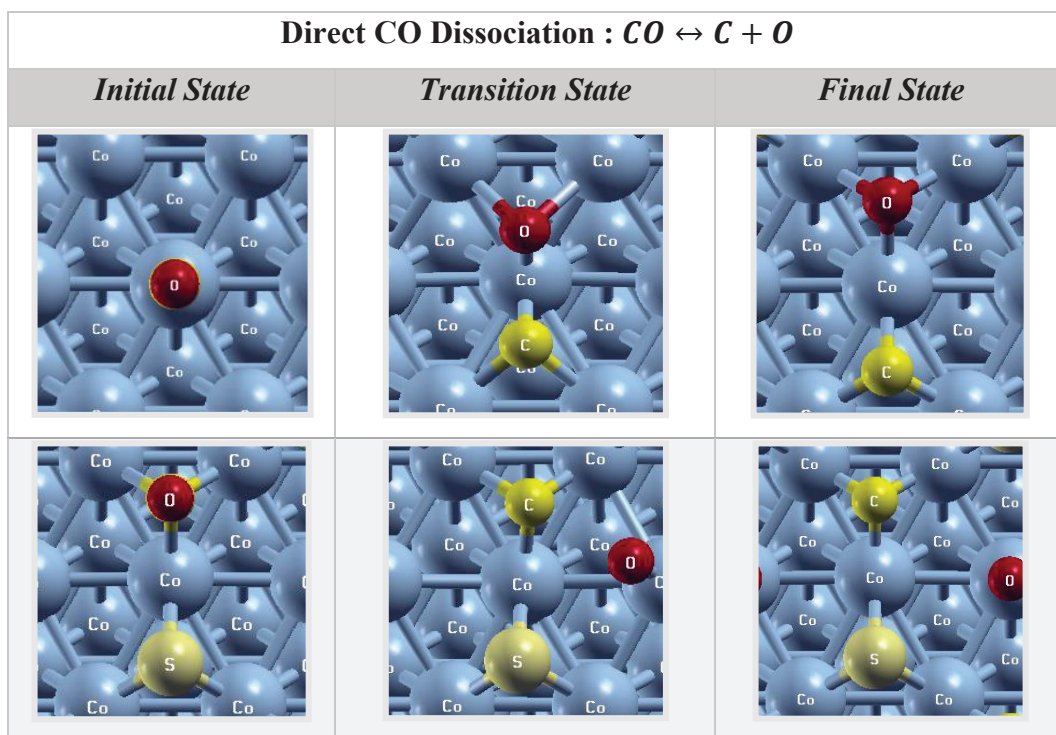
Based on Figure 4.6, activation barrier of sulfur covered surface is higher than the bare surface's activation barrier. These barriers are, 295 kJ/mol and 392 kJ/mol, respectively.

H-assisted CO dissociation takes place in two paths. Figure 4.7 is the schematic representation of the paths. According to the Figure 4.7, first path for H-assisted CO dissociation is more likely to occur, because it has low activation barrier compared to

second path. The barriers that are stated for sulfur covered surface are 119 kJ/mol and 183 kJ/mol for first and second path, respectively.
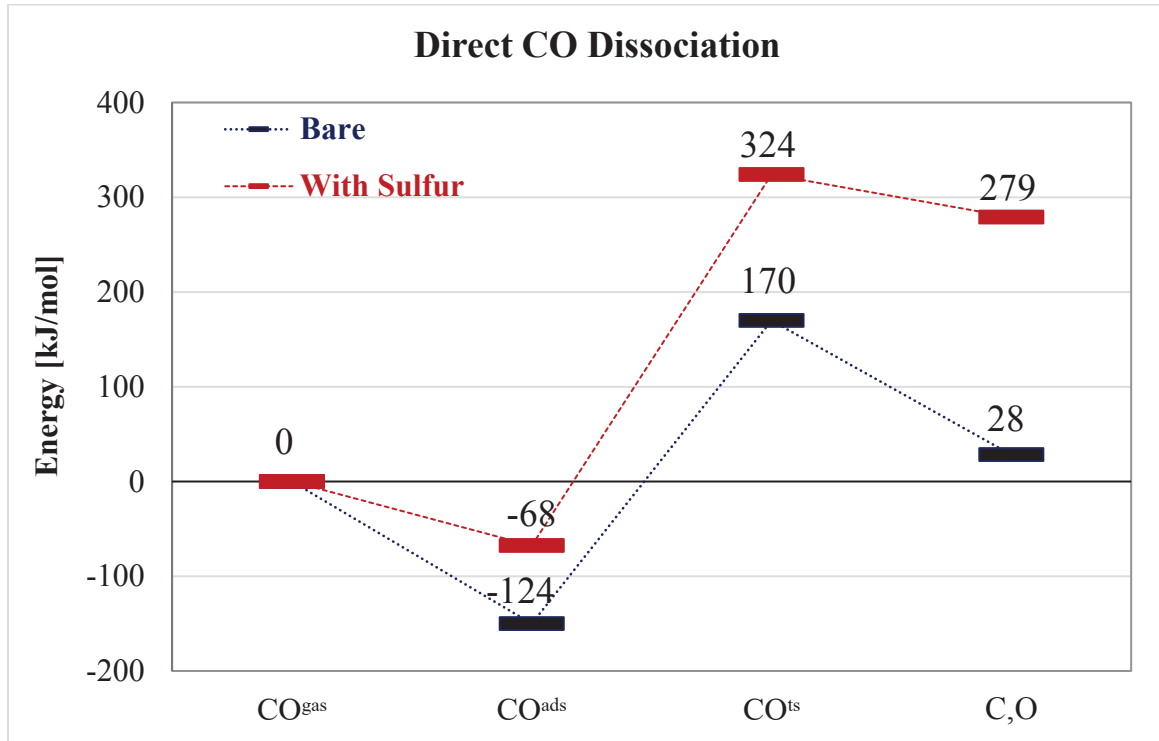
Figure 4.6 Potential Energy Diagram for direct CO dissociation for bare and 0.25 ML sulfur covered Co(111) surface

Table 4.5 CO Dissociation barriers and reaction enthalpies for forward and reverse reactions for 0.25 ML bare and sulfur covered Co(111) surface

Reaction		Forward Barrier (E^a_f) [kJ/mol]	Reverse Barrier (E^a_r) [kJ/mol]	Heat of Reaction (ΔH_{rxn}) [kJ/mol]
CO → C + O	bare	295 (220)[59]	142 (167)[59]	140 endothermic
	With S	392	45	347 endothermic

$$COH \longrightarrow C + OH$$

Second Path   +H

$E^a_{f,b}$: 230 $E^a_{r,b}$: 140
$E^a_{f,s}$: 183 $E^a_{r,s}$: 190

$$CO \longrightarrow C + O$$

+H   First Path

$E^a_{f,b}$: 136 $E^a_{r,b}$: 43
$E^a_{f,s}$: 119 $E^a_{r,s}$: 108

$$HCO \longrightarrow HC + O$$

$E^a_{f,b}$ = activation energy for forward reaction for bare surface [kJ/mol]

$E^a_{r,b}$ = activation energy for reverse reaction for bare surface [kJ/mol]

$E^a_{f,s}$ = activation energy for forward reaction for surface with Sulfur [kJ/mol]

$E^a_{r,s}$ = activation energy for reverse reaction for surface with Sulfur [kJ/mol]

Figure 4.7 H-assisted CO dissociation schema

Table 4.6 H-assisted CO Dissociation barriers and reaction enthalpies for forward and reverse reactions for 0.25 ML bare and sulfur covered Co(111) surface

Reaction		Forward Barrier (E^a_f) [kJ/mol]	Reverse Barrier (E^a_r) [kJ/mol]	Heat of Reaction (ΔH_{rxn}) [kJ/mol]
CO +H $\rightarrow$ COH	bare	230 (180^{60})	140	90 endothermic
	with S	183	190	-7 exothermic
CO +H $\rightarrow$ HCO	bare	136 $(146)^{59}$	43 $(29)^{59}$	93 endothermic
	with S	119	108	12 endothermic
HCO $\rightarrow$ HC + O	bare	94 $(90, 96)^{59}$	95 $(187, 74)^{59}$	-1 exothermic
	with S	149	72	78 endothermic

58

Table 4.6 (cont.)

Reaction		Forward Barrier (E^a_f) [kJ/mol]	Reverse Barrier (E^a_r) [kJ/mol]	Heat of Reaction (ΔH_{rxn}) [kJ/mol]
HCO + H →H₂CO	bare	40 (60, 53)[59]	39 (42, 36)[59]	1 endothermic
	with S	8	95	-87 exothermic
H₂CO → H₂C + O	bare	102 (68, 92)[59]	110 (151, 133)[59]	-8 exothermic
	with S	369	283	86 endothermic
HCO + H → HCOH	bare	59 (80)[60]	17	42 endothermic
	with S	90	68	21 endothermic
HCOH → HC + OH	bare	50 (73)[60]	96	-46 exothermic
	with S	90	26	64 endothermic

Table 4.7 List of surface structures for initial, transition and final states for H-assisted CO Dissociation Reactions

CO + H ↔ HCO		
Initial State	*Transition State*	*Final State*

Table 4.7 (cont.)

	$HCO \leftrightarrow CH + O$	
Initial State	*Transition State*	*Final State*

	$HCO + H \leftrightarrow H_2CO$	
Initial State	*Transition State*	*Final State*

Table 4.7 (cont.)

$H_2CO \leftrightarrow CH_2 + O$		
Initial State	*Transition State*	*Final State*

$HCO + H \leftrightarrow HCOH$		
Initial State	*Transition State*	*Final State*

$HCOH \leftrightarrow CH + OH$		
Initial State	*Transition State*	*Final State*
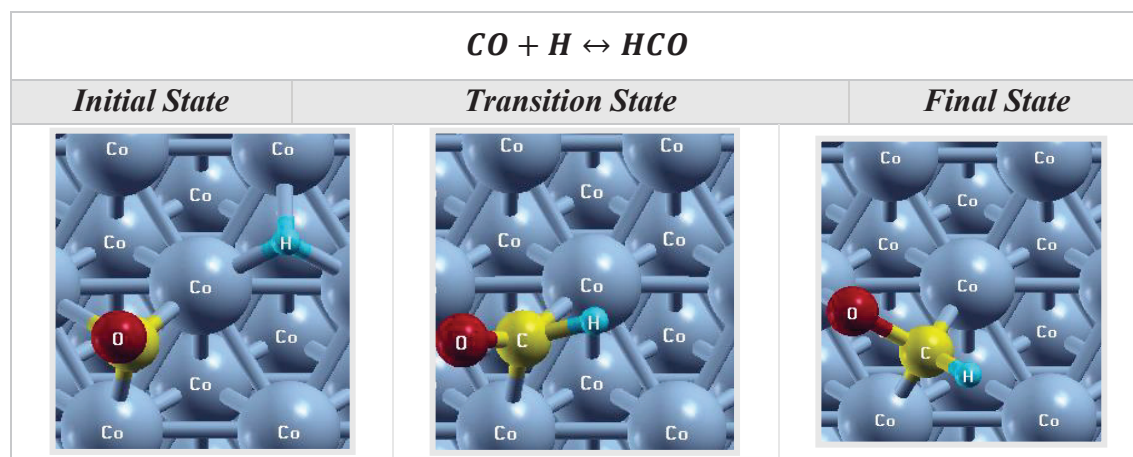
Table 4.7 (cont.)
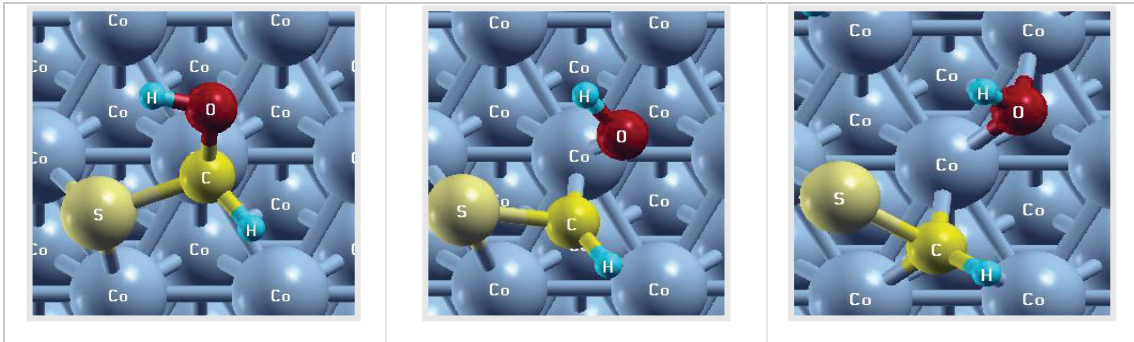
4.3.2. Effect of Sulfur on Removal of Surface Oxygen as H_2O or CO_2

Chemisorbed oxygen resulting from CO dissociation can leave cobalt surfaces as water as CO_2. In this section, CO_2 and water formation reactions are investigated.

Table 4.8 H_2O and CO_2 formation reactions barriers and reaction enthalpies for forward and reverse reactions for 0.25 ML bare and sulfur covered Co(111) surface

Reaction		Forward Barrier (E^a_f) [kJ/mol]	Reverse Barrier (E^a_r) [kJ/mol]	Heat of Reaction (ΔH_{rxn}) [kJ/mol]
$O + H \rightarrow OH$	bare	110	109	1 endothermic
	with S	162	221	-59 exothermic
$OH + OH \rightarrow H_2O + O$	bare	6	64	-58 exothermic
	with S	125	243	-117 exothermic
$CO + O \rightarrow CO_2$	bare	113	62	51 endothermic
	with S	179	289	-110 exothermic

Table 4.9 List of surface structures for initial, transition and final
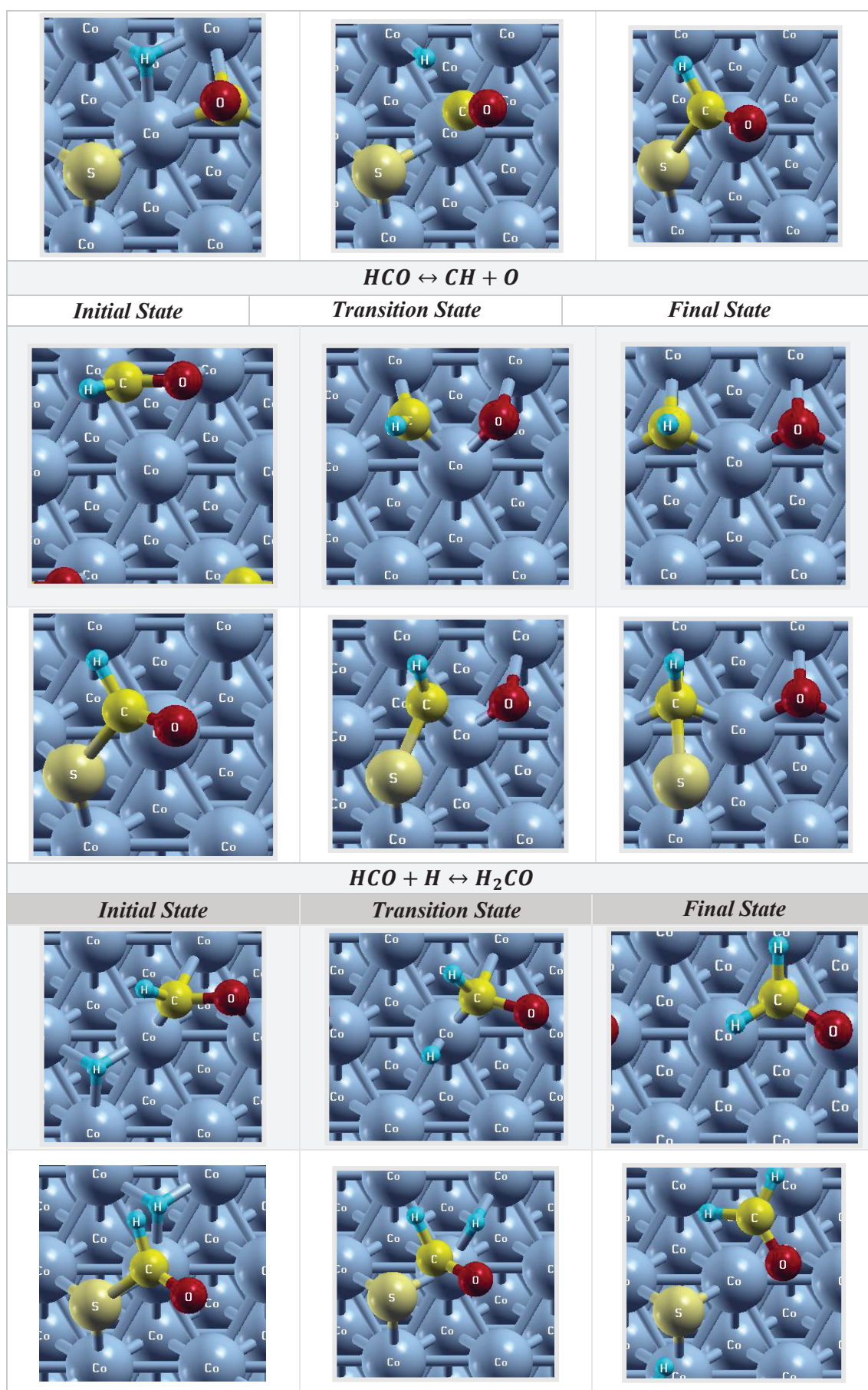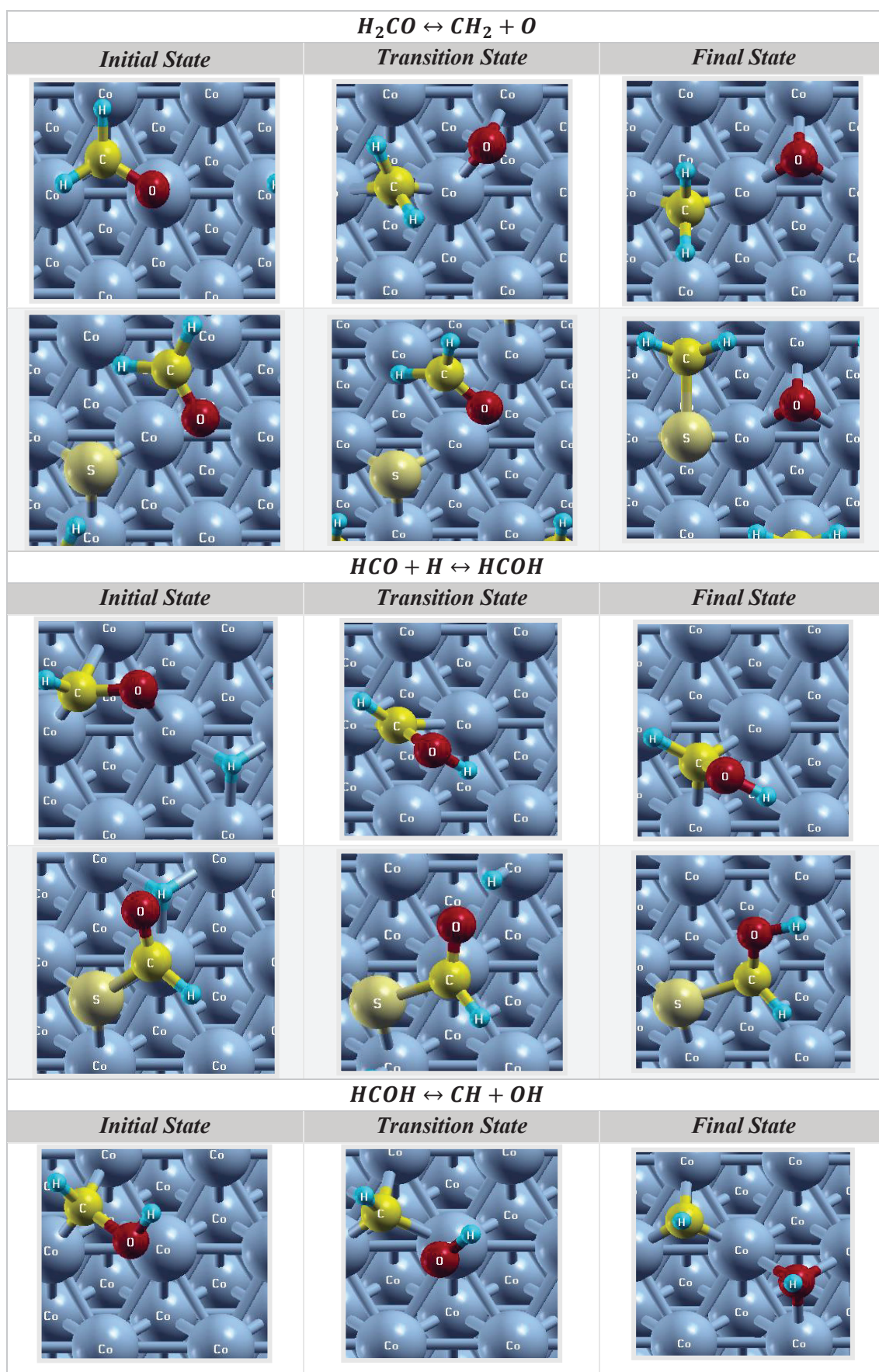states for H_2O and CO_2 formation reactions

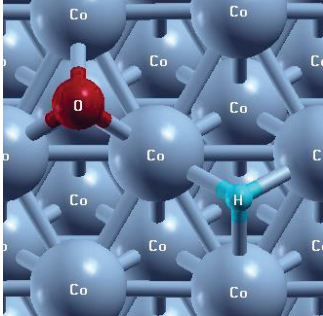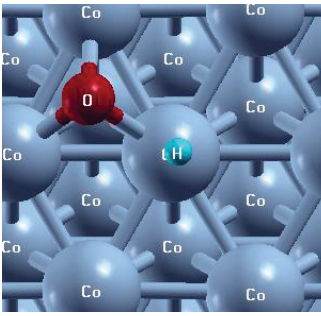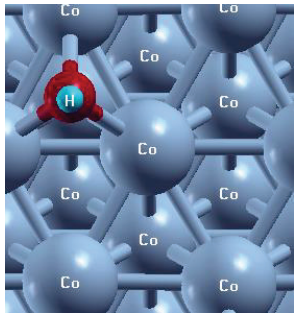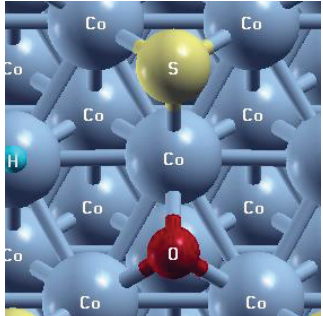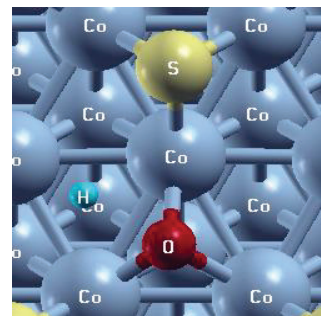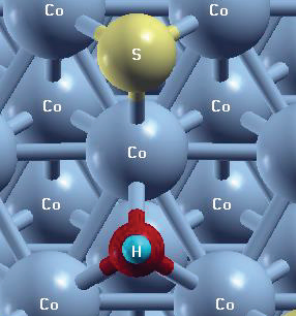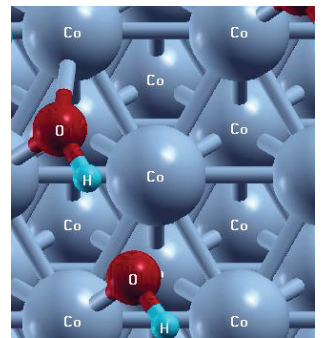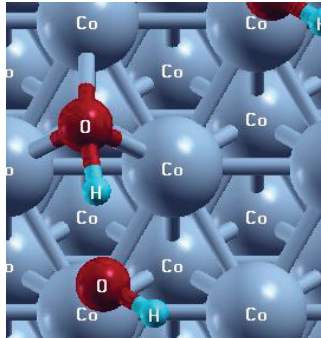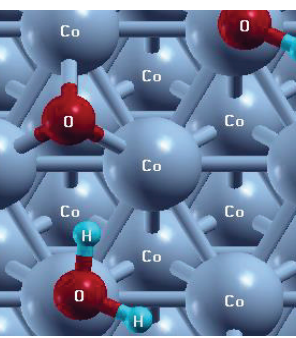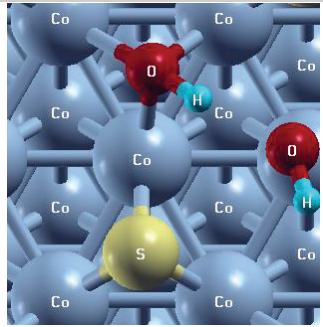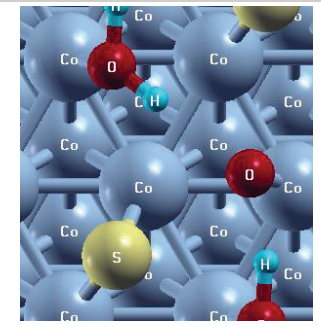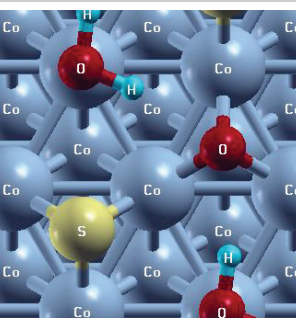| $O + H \rightarrow OH$		
Initial State	*Transition State*	*Final State*

$OH + OH \rightarrow H_2O + O$		
Initial State	*Transition State*	*Final State*

Table 4.9 (cont.)

CO + O → CO₂		
Initial State	*Transition State*	*Final State*
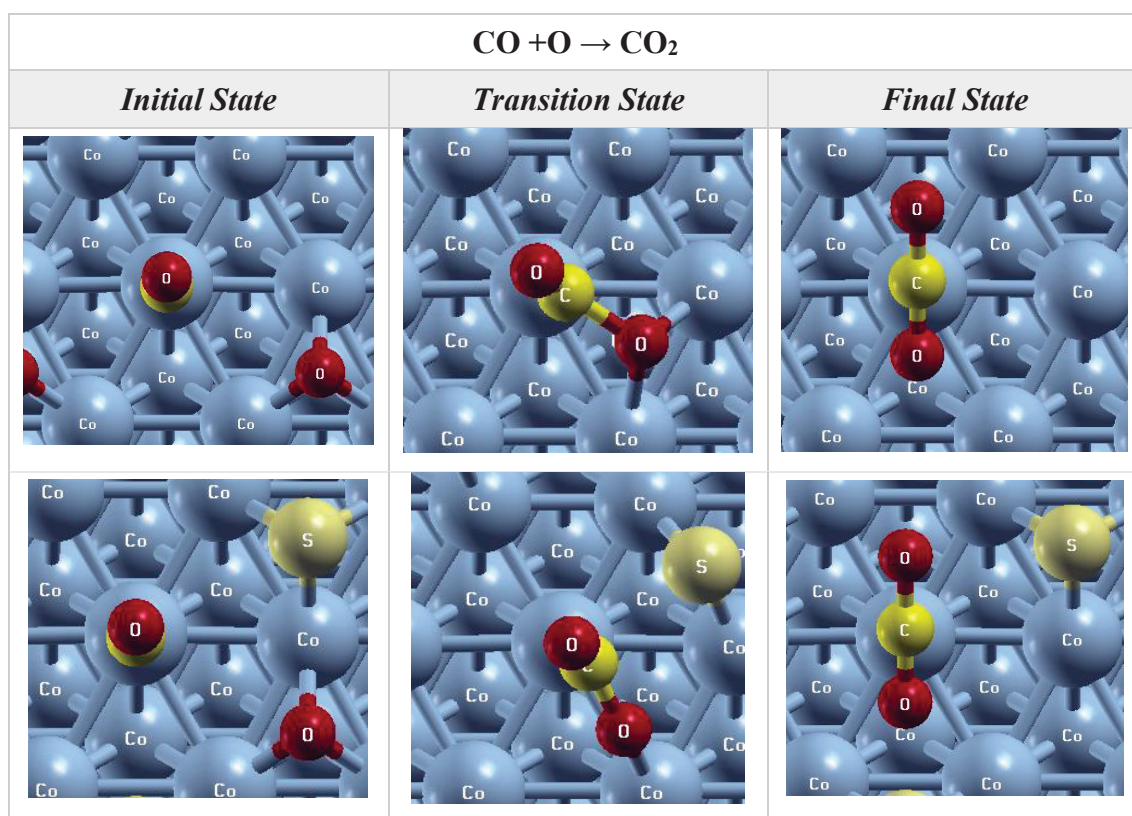
4.3.3. Effect of Sulfur on Carbon-Carbon Coupling

Fischer Tropsch synthesis aims to form long chain hydrocarbons. Long chain hydrocarbons are formed by carbon-carbon coupling reactions.

Table 4.10 Carbon – carbon coupling reaction barriers and reaction enthalpies for forward and reverse reactions for 0.25 ML bare and sulfur covered Co(111) surface

Reaction		Forward Barrier (E^a_f)	Reverse Barrier (E^a_r)	Heat of Reaction (ΔH_{rxn})
$CH + CH \rightarrow C_2H_2$	bare	53 (57)[60]	131	-78 exothermic
	with S	57	111	-56 exothermic

Table 4.11 List of surface structures for initial, transition and final states for Carbon – Carbon coupling reactions

CH +CH → C₂H₂		
Initial State	*Transition State*	*Final State*
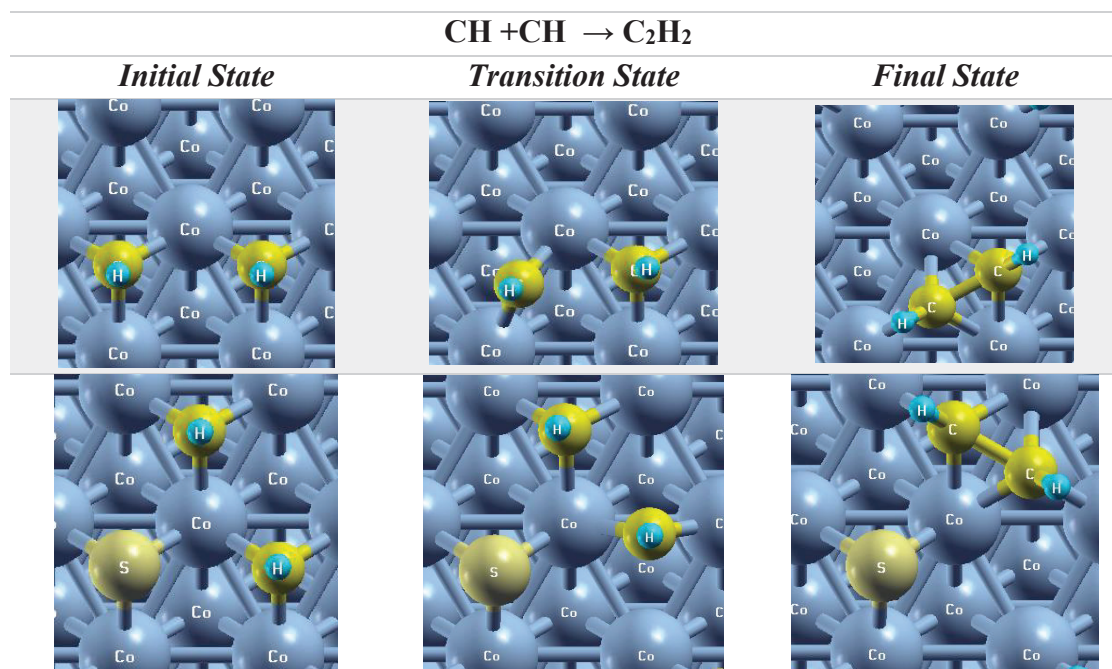
4.3.4. Effect of Sulfur on Hydrogenation/dehydrogenation of CH$_x$ and C$_Y$H$_Z$ species

In FTS, CH$_4$ is one of the undesired products. In this section, sulfur effect on CH$_4$ formation and C$_2$ hydrogenation reaction is investigated.

Table 4.12 CH$_4$ formation and C$_2$ hydrogenation reactions barriers and reaction enthalpies for forward and reverse reactions for 0.25 ML bare and sulfur covered Co(111) surface

Reaction		*Forward Barrier (E^a_f) [kJ/mol]*	*Reverse Barrier (E^a_r) [kJ/mol]*	*Heat of Reaction (ΔH_{rxn}) [kJ/mol]*
C + H → CH	**bare**	105 (53) [60]	159	-54 endothermic
	with S	24	246	-222 exothermic

Table 4.12 (cont.)

Reaction		Forward Barrier (E^a_f) [kJ/mol]	Reverse Barrier (E^a_r) [kJ/mol]	Heat of Reaction (ΔH_{rxn}) [kJ/mol]
$CH + H \rightarrow CH_2$	bare	55 (47) [60]	32	23 endothermic
	with S	18	44	-26 exothermic
$C_2H_2 + H \rightarrow C_2H_3$	bare	86 (49) [60]	70	16 endothermic
	with S	45	210	-165 exothermic

Table 4.13 List of surface structures for initial, transition and final states for CH_4 formation and C_2 hydrogenation reactions

Table 4.13 (cont.)

CH + H → CH₂		
Initial State	*Transition State*	*Final State*

C₂H₂ + H → C₂H₃		
Initial State	*Transition State*	*Final State*

67

Figure 4.8 Overall Schema for elementary reactions on
0.25 ML Sulfur Covered Co(111) Surface
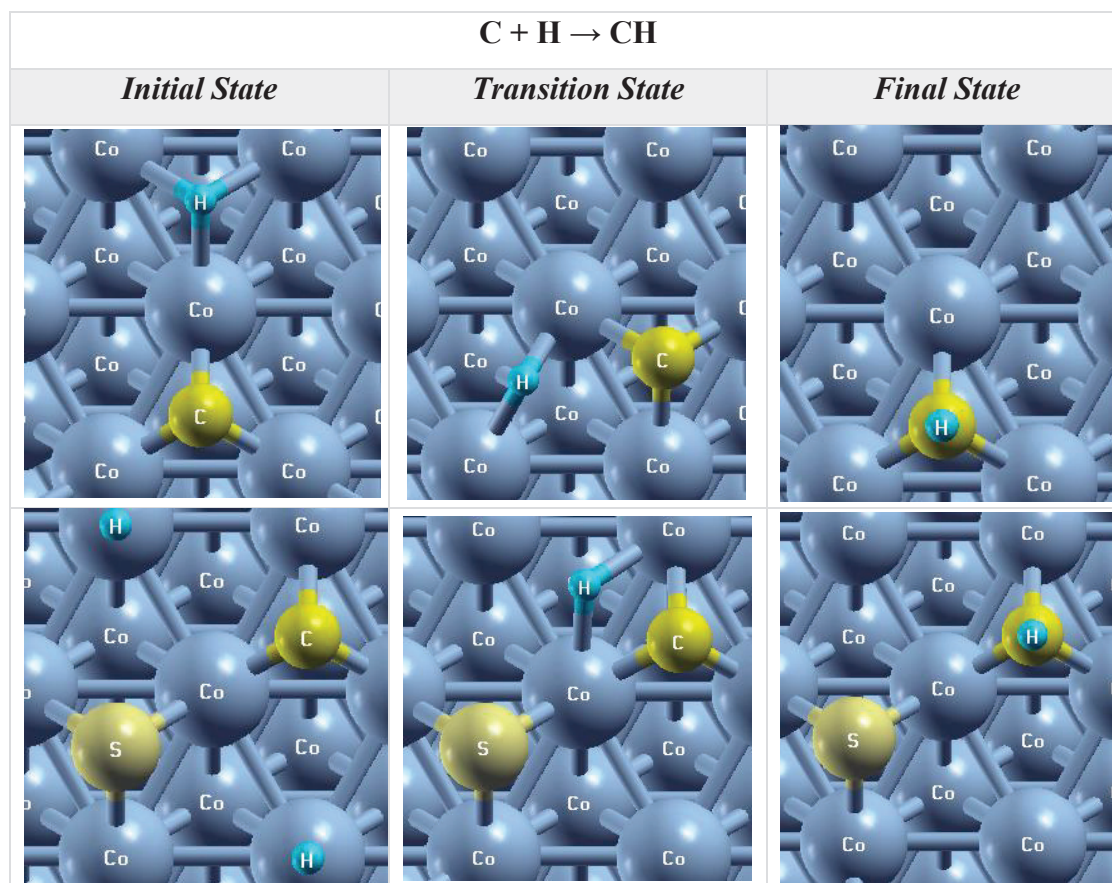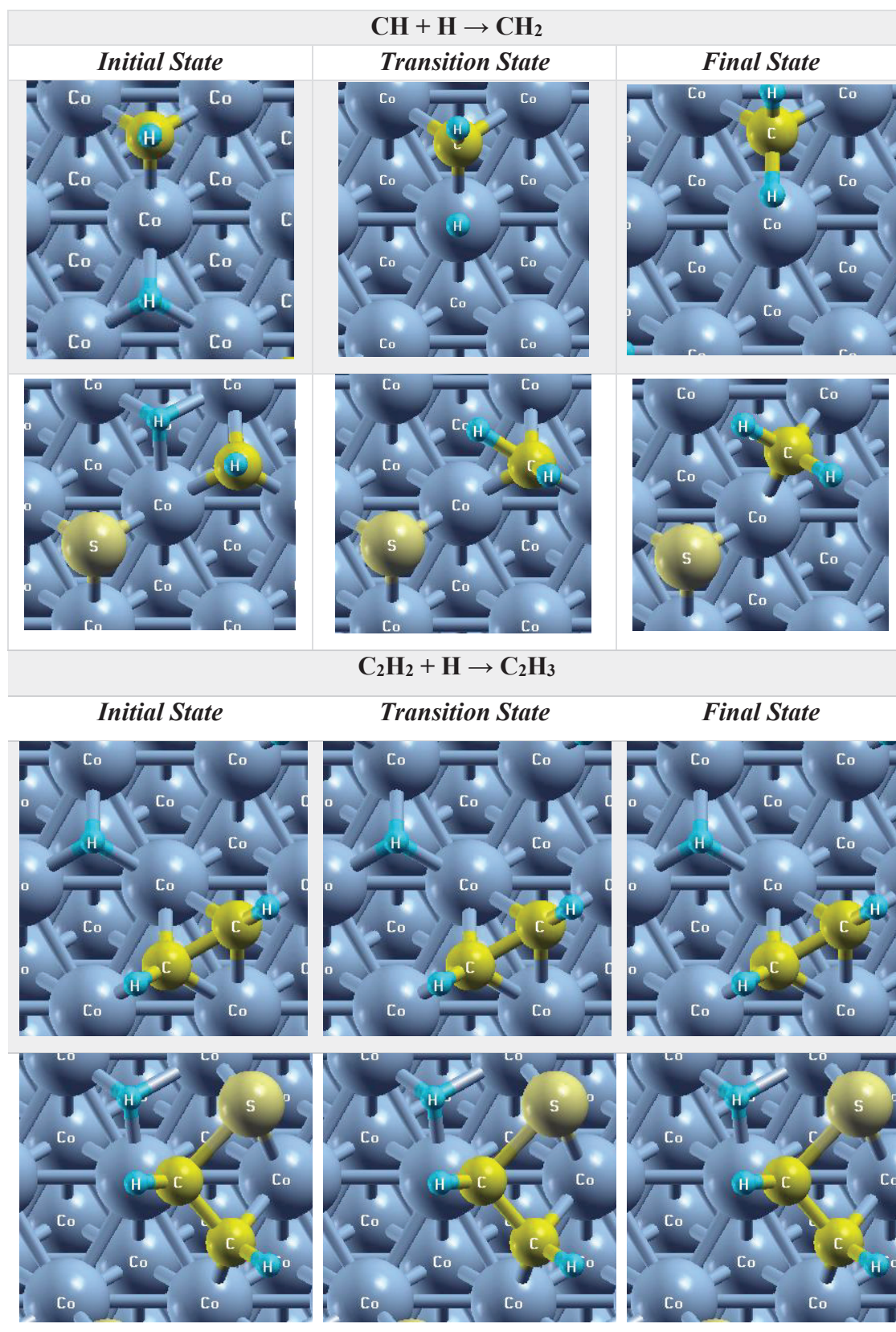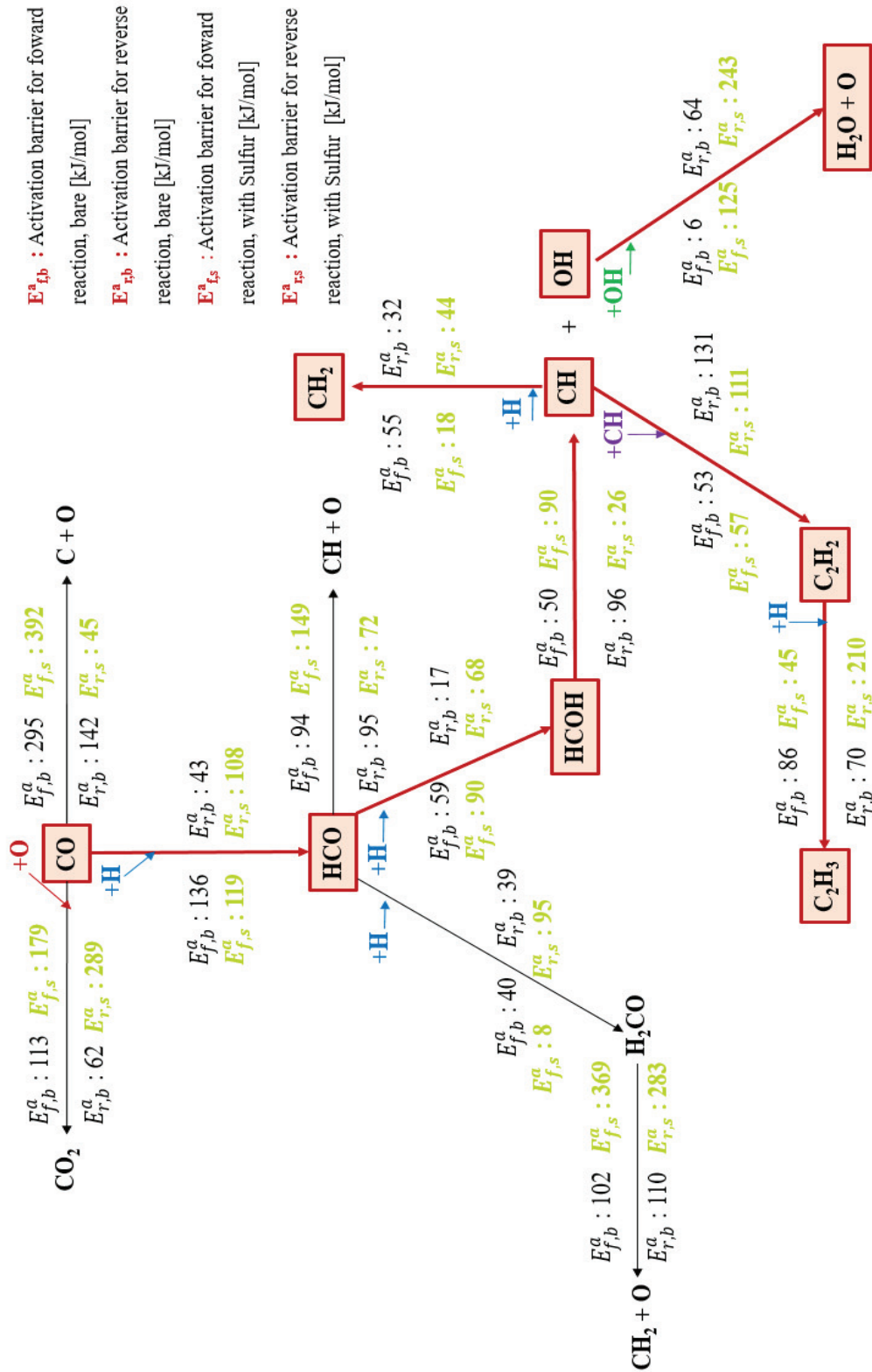
$\mathbf{E^a_{f,b}}$: Activation barrier for foward reaction, bare [kJ/mol]

$\mathbf{E^a_{r,b}}$: Activation barrier for reverse reaction, bare [kJ/mol]

$\mathbf{E^a_{f,s}}$: Activation barrier for foward reaction, with Sulfur [kJ/mol]

$\mathbf{E^a_{r,s}}$: Activation barrier for reverse reaction, with Sulfur [kJ/mol]

68

CHAPTER 5

DISCUSSION

This study aims to observe the effect of sulfur on activity and selectivity of Fischer-Tropsch synthesis, by investigating how sulfur effects the adsorption of reactants/intermediates and the activation barriers of main elementary reactions of FTS. Based on these goals, firstly main sulfur component which is likely to be present on the Co(111) surface, the most abundant surface on fcc cobalt nanoparticles, are determined. Secondly, the sulfur effect was observed on adsorption energy of species at various sulfur covered Co(111) surface as 0.25 ML and 0.11 ML. Finally sulfur effect was observed on the elementary reactions of FTS.

5.1. S/HS/H$_2$S Adsorption and H$_2$S Dissociation

The change of species' adsorption energies with the addition of additives may be an indication whether the additive is a promoter or a poison. For instance, if adsorption energy of CO increases with the additive, promoter effect is more likely dominant (the activity and selectivity of FTS to long chain hydrocarbons can be expected to increase [64]), but if adsorption energy of species decreases with the additive, poison effect is dominant, i.e. a decrease in activity/selectivity may be expected.

Firstly, main sulfur component that causes a positive/negative effect on the activity and selectivity of cobalt based FTS catalyst must be determined. H$_2$S is the main sulfur source that comes from the feedstock (biomass, natural gas or coal) into the reactor[13]. According to this, adsorption energies of S, HS and H$_2$S was calculated as -480 kJ/mol, -278 kJ/mol and -34 kJ/mol, respectively. Sulfur has highest adsorption energy compared to HS and H$_2$S. It strongly chemisorbs on the surface. However, H$_2$S has weak interaction with cobalt metal due its low adsorption energy. So, dissociation of H$_2$S is predicted to be easily on cobalt surface because of its low adsorption energy. These results are verified with the study of adsorption diffusion and dissociation on Fe(100) by Jiang et al. (2004) and first principle of H$_2$S dissociation on the metal surfaces by Alfonso et al. (2008). The numeric values are presented in Table 5.1 and Table 5.2.

Table 5.1 Adsorption energies of sulfur species for 0.25 ML covered Co(111) surface compared with literature

Species	The study [kJ/mol]	Literature [kJ/mol] (for Ni(111) surface) [47]
H	-281 (fcc)	-281 (fcc)
S	-480 (fcc)	-531 (fcc)
HS	-278 (bridge)	-322 (bridge)
H_2S	-34 (top)	-56 (top)

Table 5.2 Dissociation barriers of H_2S for 0.25 ML covered Co (111) surface compared with literature

Reactions	The study [kJ/mol]	Literature [kJ/mol] (for Ni(111) surface) [47]
$H_2S \rightarrow HS + H$	32	21
$HS \rightarrow S + H$	32	1

The investigation of H_2S dissociation on bare(clean), C and O covered Co(111) surfaces indicated that atomic sulfur is the main dissociation product of H_2S on cobalt surfaces , in line with the experimental results by Lahtinen et al. (2005) [65]. Nevertheless, the feasible barriers for hydrogenation of atomic S to HS indicate that HS may be also present on the catalyst surface, probably in much lower amounts. So, both S and HS effects on the adsorption energies of species were calculated, as discussed in next section. Furthermore, the low dissociation barriers for H_2S on the flat surface indicate that the dissociation would dissociate much easier on the stepped Co(211) surface, as stepped surfaces such as Co(211) are in general more active for decomposition reactions compared to flat surfaces such as Co(111) [66]. Therefore, only the diffusion barrier of S from Co(211) to Co(111) was investigated in this study. The low diffusion barrier of 62 kJ/mol indicates that the dissociation products formed on Co(211) will diffuse to the flat surface, conforming the validity of the investigation of S poisoning effect on the flat Co(111) surface.

5.2. Effect of S and HS on the Adsorption Energies of Reactants and Intermediates of FTS

For 0.25 ML coverage on Co(111) surface, sulfur and HS decrease adsorption energies of all species, the effect is most severe for CO and least for H (See in Figure 4.4). However, for 0.11 ML Co(111) surface, poison effect of sulfur decreases noticeably. These results indicate that at high coverage (0.25 ML), S results in an decreased H/CO coverage, while at low coverage S or HS may have a slight poison or even promoting effect, as observed experimentally [36].

For 0.25 ML sulfur covered Co(111) surface, sulfur decreases adsorption energies of all species. To clarify this, sulfur effect on the adsorption energies on CO and OH can be discussed. For example, both oxygen and sulfur are negatively charged, and they repel each other. OH is adsorbed on the cobalt surface from oxygen. This affect the strength of OH adsorption on the surface negatively and its adsorption energy decreases nearly 100 kJ/mol when compared with no sulfur covered surface. Because sulfur repels oxygen from the surface, and adsorption strength of oxygen or OH molecule decreases. Carbon is not much electronegative as oxygen, so this repulsion is not strong as oxygen sulfur interaction. The adsorption energy of CO decreases as 60 kJ/mol compared with the no sulfur covered situation. The sulfur effect the OH adsorption on surface can be explained with repulsive interaction. The effect of sulfur on CO adsorption may cause from the adsorption site shifting. Because, the favorable adsorption site of CO is the top site but CO adsorption site shifts from top to fcc site when it co-adsorbed with sulfur on the Co(111) surface. As a result, at high sulfur coverage the attraction forces increase, so that adsorption energies of species decrease, and the sulfur poisoning effect may originate from this situation.

For 0.11 ML sulfur covered Co(111) surface, poison effect of sulfur decreases noticeably when compared with the 0.25 ML sulfur covered surface (See in Figure 4.3). The reason is the increased opportunity of the adsorption sites on the surface with decreasing sulfur coverages. It means that, species can adsorb on the far adsorption sites from sulfur. Therefore, decreasing sulfur coverage removes negative sulfur effect. For example, CO adsorption energy changes only 3 kJ/mol between the far and close regions from the sulfur atom. Its adsorption energy was calculated as 120 kJ/mol at far region

from sulfur and 117 kJ/mol for close region to sulfur. When these energies are compared with the energy value of no sulfur coverage (125 kJ/mol), it can be said that sulfur lost its negative effect on the adsorption energy of CO. The same trend is valid for other species. The change of adsorption energies between two regions were shown in Table 4.3. These results indicate that, at low coverage S has a slight poison or even promoting effect, as observed experimentally. Adsorption energy of sulfur with different coverages was tabulated in Table 4.1.

As a result, at high coverage sulfur blocks the neighbor active sites and also decreases the adsorption energies of species while at low coverage, the effects are less severe, in line with the literature [23–27,36].

5.3. Effect of Sulfur on Elementary Reactions of Fischer-Tropsch Synthesis

For observing the sulfur effect on the activity and the selectivity of the FTS, elementary reactions of FTS must be investigated. There are four elementary reactions of FTS. These are, CO dissociation, removal surface oxygen as water or CO_2, carbon-carbon coupling and hydrogenation/dehydrogenation of C_1H_x and C_yH_z species [62].

5.3.1. Effect of Sulfur on CO dissociation

CO dissociaiton is one of the essential steps of FTS. CO adsorbs on the surface with -125 kJ/mol and it dissociates with -295 kJ/mol as carbon and oxygen. Under FTS reaction conditions, CO does not dissociate on the flat cobalt surfaces[such as hcp Co(0001) and fcc-Co(111)]. As an alternative way to this reaction is h-assisted CO dissociation, which was investigated in literature[63,67]. H-assisted CO dissociation leads to dissociation of CO linked with H atom. This reaction can take place in two forms. These are:

1st reaction: CO + H → COH → C + OH

2nd reaction: CO + H → HCO → CH + O

At the first reaction, C bonds on the cobalt surface and OH molecule bonds on the carbon atom. For the second reaction, C and O bond on neighbor cobalt atoms together

and H atom bonds to carbon atom. The formation barrier of COH and HCO were presented in Figure 4.6. COH formation is harder than HCO formation on 0.25 ML sulfur covered Co(111) surface with the activation barriers of 183 kJ/mol and 125 kJ/mol, respectively. Activation barriers is a tool to understand the reaction rate. Based on the Arrhenius Equation (see in Appendix C), as activation energy term (E_a) increases, the rate constant (k) decreases and therefore the rate of reaction decreases. For this reason, when the two reactions are compared, the reaction which has low activation barrier value takes place is faster than the other. According to this, HCO based CO dissociation pathway is calculated to be the preferred CO dissociation mechanism, on both bare and S covered Co(111) surfaces. Based on the Table 4.6, HCO dissociation and hydrogenation is the key element for the starting point of carbon coupling and CH hydrogenation reactions for this study. The reaction mechanism as stated for the study can be figured out as below. For related reactions, barriers were shown in Figure 5.4.
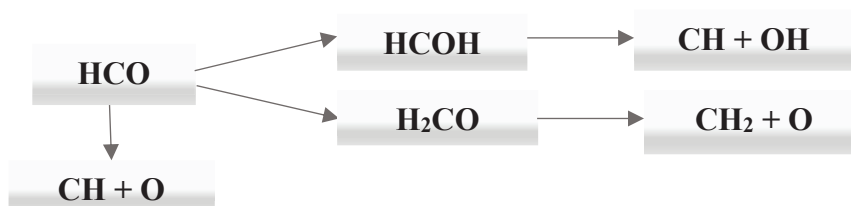
Figure 5.1 HCO dissociation and hydrogenation pathway

Based on the Table 4.6, H_2CO formation is easier than the HCOH formation according to the formation barriers as 8 kJ/mol and 90 kJ/mol, respectively for 0.25 ML sulfur covered Co(111) surface. The situation is inverse for dissociation barrier, which are 369 kJ/mol and 90 kJ/mol, respectively. The difference between formation barriers of HCOH and H_2CO can be explained as the effect of sulfur on adsorption energies. It can be said that, sulfur decreases the adsorption energy of H_2CO species as -29 kJ/mol.

Compared to this, the sulfur effect causes -203 kJ/mol decrease on adsorption energy of HCOH species. Dissociation barriers of these species are inversely proportional with their formation barriers. Because, C-O bond is weaker in HCOH as its vibrational frequency is decreased from 3575 cm^{-1} to 3463 cm^{-1}, but C-O bond is stronger in H_2CO. Vibrational frequency of HCOH is increased from 3008 cm^{-1} to 3109 cm^{-1} at 0.25 ML sulfur covered Co(111) surface. The adsorption energies of species and their literature values were given in Table 4.6.

The adsorption energies of species are close with the literature values. However, there are some differences might be caused from functional differences. Qi et al [60] used the PBE functional for their studies. However, PBE functional is not an accurate selection for the calculation of CO adsorption energy. In literature, CO adsorption energy was calculated in the range of -96 to -126 kJ/mol at top site [68]. However, its adsorption energy is calculated as ~180 kJ/mol at hollow site in the literature with PBE functional. Based on this, VDW Functional is used in this study, and CO adsorption energy was calculted as -124 kJ/mol at top site.
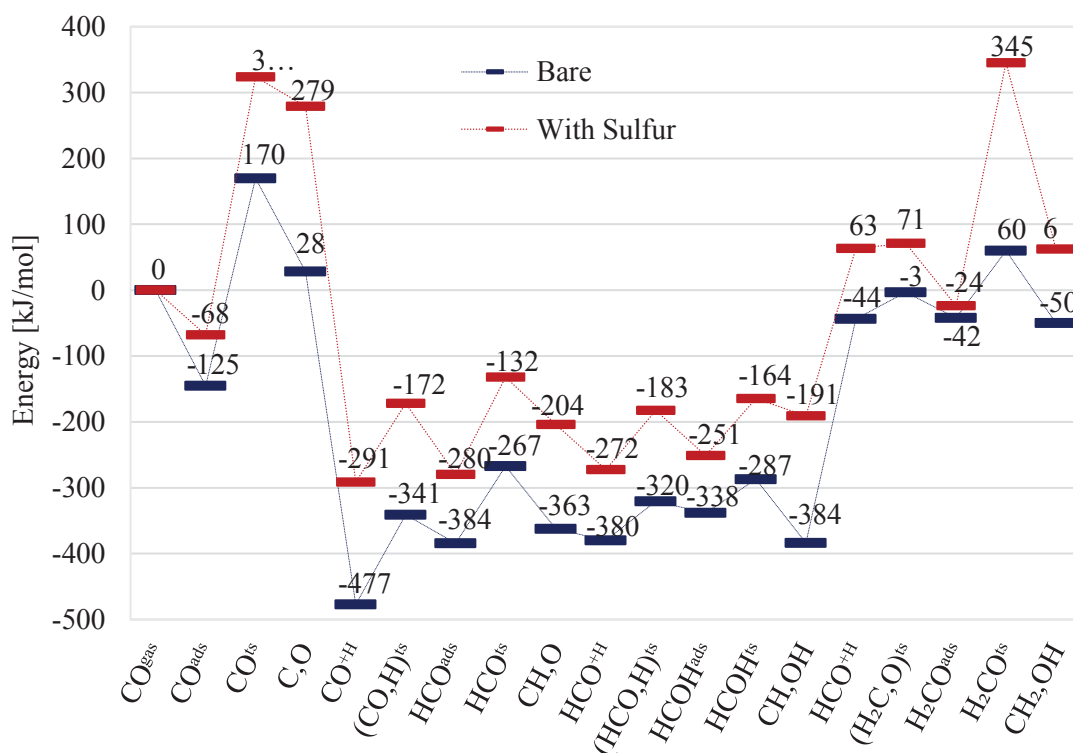
Figure 5.2 Potential Energy Diagram for H-assisted CO dissociation mechanism

In Figure 5.2, H-assisted CO dissociation mechanism is given. The graph shows the relation between the 0.25 ML sulfur covered Co(111) surface and bare Co(111) surface. As a result the calculations indicate that in the energetically favored mechanism for S covered Co(111) surface, CO undergoes through hydrogenation reaction to form HCOH. Then, HCOH is dissociated into CH and OH. CH further undergoes through stepwise hydrogenation to form CH_4, which is investigated in Section 5.3.3, or carbon coupling as it forms C_2H_2, which is investigated in Section 5.3.4. The OH might be gone through the stepwise hydrogenation to form H_2O, which was investigated in Section 5.3.2

5.3.2. Effect of Sulfur on H_2O/CO_2 Formation

In the FTS, the second main reaction is surface free oxygen which comes from the CO dissociation. Surface free oxygen is removed from the surface as CO_2 and H_2O. In the previous section, it was calculated that CO does not dissociate to C and O at 0.25 ML sulfur covered Co(111). Based on the calculations for H-assisted CO dissociation pathway, it is found that on the S-covered Co(111) surface, HCOH dissociation, which leads to hydrogenation of HCO is faster than the HCO dissociation. Because, its dissociation barrier is 90 kJ/mol. The products of HCOH dissociation is OH and CH. Based on this reaction, water formation can progress mainly in the form of OH recombination, namely OH + OH $\rightarrow$ H_2O + O. This is because the presence of sulfur hinders the formation of atomic O on the surface, as it increases the activation barriers above 130 kJ/mol (the max. approximate activation barrier that can be overcome based on the operating temperature of 250°C, 523 K for low-temperature FTS) for both CO dissociation and OH decomposition to O and H . This pathway for water formation on S-covered Co(111), i.e. OH + OH $\rightarrow$ H_2O + O, has an activation barrier of 6 kJ/mol at bare Co(111) surface, while . The barrier increases to 125 kJ/mol at 0.25 ML sulfur covered Co(111) surface. One OH molecule is stable at hcp site and the other OH molecule prefers to adsorb on fcc site for bare surface. This co-adsorption situation is the most stable combination for OH-OH co-adsorption. However, adsorption sites of OH molecules shift to fcc and top site for the co-adsorption due to sulfur atom. The stable configuration of OH-OH coadsorption changes because of sulfur atom. According to this, reaction pathway follows a longer way, which leads to this barrier getting higher than the bare condition. For the other oxygen removal pathway, CO_2 formation, the barrier also increases from 113 to 179 kJ/mol. Therefore, the results indicate that a coverage of 0.25 ML sulfur on the Co(111) surface mainly inhibits the oxygen removal reaction. This finding indicates that other than decreasing adsorption energies and adsorbate coverages, the presence of sulfur also acts a poison for FTS because it inhibits oxygen removal.

5.3.3. Effect of Sulfur on CH_x Formation

According to the literature research, sulfur atom increases the selectivity towards methane [36]. Based on this, this study aims to observe methane formation reaction on 0.25 ML sulfur covered Co(111) surface.
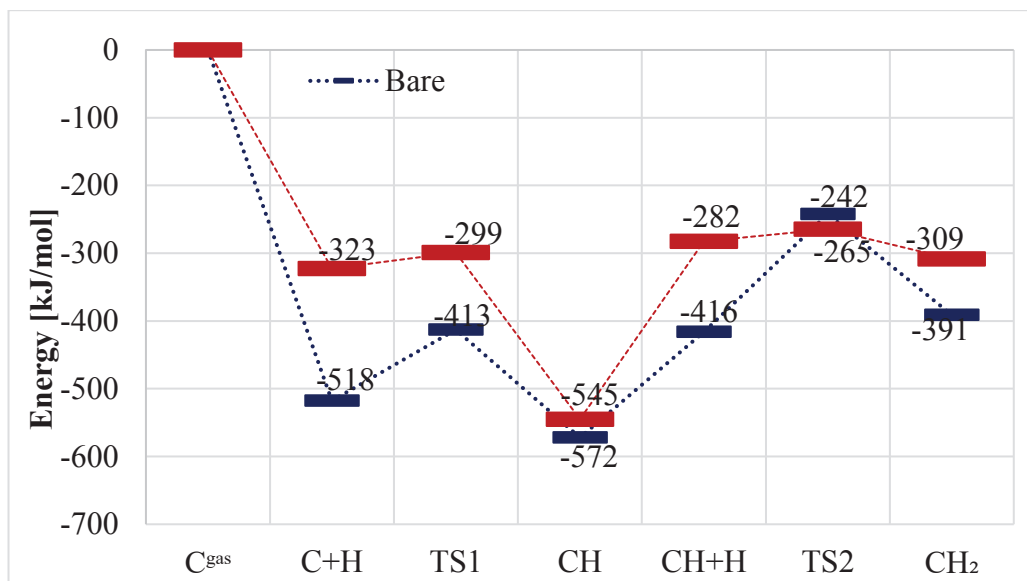
Figure 5.3 Potential Energy Diagram for CH hydrogenation reactions

Based on the Figure 5.3, hydrogenation of C and CH on sulfur covered Co(111) have the low formation barriers as 23 and 17 kJ/mol when compared with the activation barriers of bare Co(111) surface, which was 87 and 55 kJ/mol, respectively. Therefore, it can be said that high sulfur coverage (0.25 ML) leads to reduce activation barriers of reaction. The results are parallel with the literature values and our study predicts direct computational evidence that the high sulfur coverage increses the selectivity towards methane because it decreases the activation barriers for carbon hydrogenation [36,61].

5.3.4. Effect of Sulfur on Carbon Coupling

FTS aims to form long chain hydrocarbons. Based on this, observing carbon chain is the key element to obtain sulfur effect on the selectivity on long chain hydrocarbons.

Sulfur shows no effect on the activation barrier of CH-CH reaction, i.e. the CH coupling barrier stays at 57 kJ/mol, so C_2H_2 species can be formed at the 0.25 ML sulfur covered Co(111) surface. However, compared with CH hydrogenation barrier of 18 kJ/mol in the presence of sulfur, the results indicate that sulfur would increase the rate of carbon hydrogenation more than the rate of C-C coupling, therefore decreasing the selectivity to long chain hydrocarbons. . These results are parallel with the literature which state high sulfur coverage decreases the selectivity towards long chain hydrocarbons [35,36].
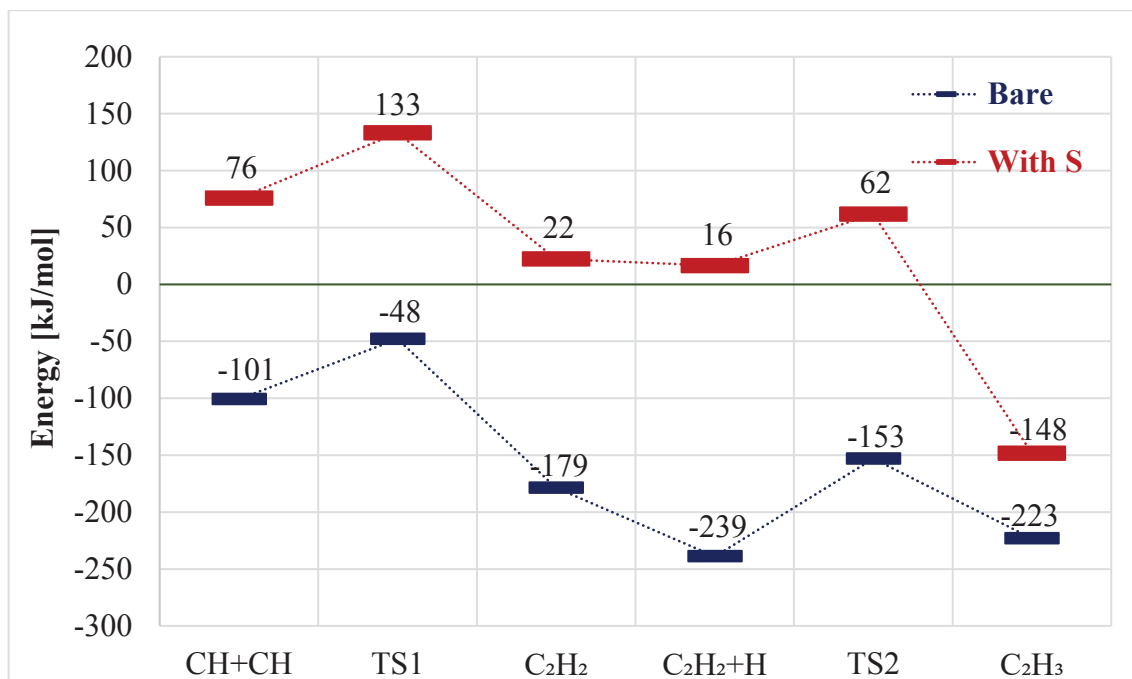
Figure 5.4 Potential Energy Diagram for Carbon

coupling and C_2 hydrogenation reaction

CHAPTER 6

CONCLUSIONS

Fisher-Tropsch Synthesis (FTS) consists of the exothermic reaction between CO and H_2, which produces long chain hydrocarbons as the main product and water as the main by-product. Industrial observations indicated that sulfur, one of the impurities in the syngas feed, acts as a poison for FTS and surface science studies showed that sulfur blocks the adsorption sites for CO and H_2 on cobalt surfaces. However, various experimental studies have shown contradictory results, i.e. that ppm amounts of sulfur result in the increase/decrease of catalytic activity or selectivity increases towards olefins or methane. Our study aims to clarify the effect of sulfur on cobalt FTS catalysts by molecular (computational) modelling of the adsorption of the reactants CO and H, and the elementary reactions of FTS on surfaces that are present on fcc-cobalt nanoparticles, using periodic plane-wave Density Functional Theory (DFT) calculations utilizing Vienna ab-Initio Simulation Package (VASP).

To determine the S-based surface species, that are responsible for the poison/promoter effect, the dissociation of H_2S, which is the main sulfur source at the reactants, was investigated on the Co(111) surface. H_2S dissociation was investigated on carbon and oxygen covered Co(111) surfaces and it was found that H_2S can completely dissociate into S. The activation barriers for $H_2S \rightarrow HS+S$ and $HS \rightarrow H+S$ were calculated as 32 kJ/mol on bare Co(111), 102 and 72 kJ/mol on C covered and 74 and 83 kJ/mol on O covered surfaces. These findings show that, while S is the main S-compound which is most likely responsible for the poison effects in cobalt based FTS, HS can also exits although probably in low concentrations. The results indicate that, for 0.25 ML coverage, adsorption on an S/HS pre-covered Co(111), resulted in a 60/58 kJ/mol decrease of CO and 24/22 kJ/mol decrease in H adsorption energies, respectively. Interestingly, for 0.11 ML coverage on Co(111) surface, CO/H adsorption energies decreased 3/1 kJ/mol for co-adsorption with S, while they increased 3/27 kJ/mol for co-adsorption with HS. Based on the investigation of elementary reactions of FTS on sulfur covered Co(111), the following conclusions can be drawn:

- Sulfur does not decrease, but significantly (around 100 kJ/mol) increases the activation barrier for direct CO dissociation. This indicates that CO does not dissociate directly on Co(111) surfaces, similar to the case on clean(bare) Co(111) Based on this result, h-assisted CO dissociation reactions are also The preferred pathway is found to be CO +H → HCO +H →HCOH →HC + OH, as sulfur decreases or slightly increases the barriers in this pathway.

  Sulfur increased the OH coupling and CO_2 formation reactions above 130 kJ/mol, therefore it can be said that sulfur inhibits the oxygen removal reaction.

- Sulfur decreases most of the hydrogenation reactions in particular carbon hydrogenation to CH_x species. However, S does not induce a change on the carbon coupling reaction investigate, namely CH + CH → C_2H_2. These results indicate that sulfur poisoning can be expected to increase the selectivity to methane, while decreasing the selectivity to long chain hydrocarbons.

REFERENCES

(1) Sieminski, Adam. "International Energy Outlook" *Energy Information Administration (EIA)* 18, (2014) (Accessed Jan 14, 2020)

(2) Guettel, Robert, Ulrich Kunz, and Thomas Turek. "Reactors for Fischer-Tropsch Synthesis." *Chemical Engineering and Technology* 31, no. 5 (2008): 746–54. https://doi.org/10.1002/ceat.200800023.

(3) Tsakoumis, Nikolaos E., Magnus Rønning, Øyvind Borg, Erling Rytter, and Anders Holmen. "Deactivation of Cobalt Based Fischer-Tropsch Catalysts: A Review." *Catalysis Today 154*, no.3-4 (2010):162-82. https://doi.org/10.1016/j.cattod.2010.02.077.

(4) Habermehl-Ćwirzeń, Karin, and Jouko Lahtinen. "Sulfur Poisoning of the CO Adsorption on Co(0001). "*Surface Science* 573, no.2 (2004):183–90. https://doi.org/10.1016/j.susc.2004.09.024.

(5) McCue, Alan J., and James A. Anderson. "Sulfur as a Catalyst Promoter or Selectivity Modifier in Heterogeneous Catalysis." *Catalysis Science and Technology* 4, no. 2 (2014): 272–94. https://doi.org/10.1039/c3cy00754e.

(6) Baron, Kenneth. "Carbon monoxide oxidation on platinum-lead films." *Thin Solid Films* 55.3 (1978): 449-462. https://doi.org/10.1016/0040-6090(78)90162-1

(7) Barrientos, Javier. "Deactivation of cobalt and nickel catalysts in Fischer-Tropsch synthesis and methanation." *PhD Thesis. US-AB*. (2016): 9-13.

(8) Barbato, Maurizio, and Bruno Claudio. "Heterogeneous catalysis: theory, models and applications." *Molecular Physics and Hypersonic Flows*. Springer, Dordrecht, (1996): 139-160.

(9) Chorkendorff, Ib and Johannes W. Hans Niemantsverdriet. "Concepts of modern catalysis and kinetics". *John Wiley & Sons*, (2017) : 79-119.

(10) Bond, Geoffrey. "Heteregenous Catalysis: Princples and Applications" *Clarendon Press,* (1974): 65-72

(11) Maier, F. Wilhelm, Hee-Chan Ko. "Poison resistant catalysis with microporous catalyst Membranes." *Catalysis Today*, 25 no.12 (1995): 429-440.

(12)   Argyle, Morris, and Calvin Bartholomew. "Heterogeneous Catalyst Deactivation and Regeneration: A Review." *Catalysts* 5, no. 1 (2015): 145–269. https://doi.org/10.3390/catal5010145.

(13)   Mahmoudi, Hamid, Maedeh Mahmoudi, Omid Doustdar, Hessam Jahangiri, Athanasios Tsolakis, Sai Gu, and Miroslaw LechWyszynski. "A Review of Fischer Tropsch Synthesis Process, Mechanism, Surface Chemistry and Catalyst Formulation." *Biofuels Engineering* 2, no.1 (2018): 11-31 https://doi.org/10.1515/bfuel-2017-0002.

(14)   Davis, Burtron H. "Fischer−Tropsch Synthesis: Comparison of Performances of Iron and Cobalt Catalysts." *Industrial & Engineering Chemistry Research* 46, no. 26 (2007): 8938–45. https://doi.org/10.1021/ie0712434.

(15)   Ma, Wenping, Gary Jacobs, Wilson D. Shafer, Venkat Ramana Rao Pendyala, Qunfeng Xiao, Yongfeng Hu, and Burtron H. Davis. "Effect of H_2S in Syngas on the Fischer–Tropsch Synthesis Performance of a $0.5\%Pt–25\%Co–Al_2O_3$ Catalyst." *Catalysis Letters* 146, no.7 (2016): 1204–12. https://doi.org/10.1007/s10562-016-1747-0.

(16)   Wiberg, Kenneth B. "Ab Initio Molecular Orbital Theory." *Journal of Computational Chemistry* 7 no.3 (1986): 379 https://doi.org/10.1002/jcc.5400703 14.

(17)   Nørskov, Jens K, Frank Abild-Pedersen, Felix Studt, and Thomas Bligaard "Density Functional Theory in Surface Chemistry and Catalysis". *Proceedings of the National Academy of Sciences of the United States of America*. (2011) : 937–943. https://doi.org/10.1073/pnas.1006652108.

(18)   Sham, Lu Jeu, and Walter Kohn. "One-particle Properties of an in Homogeneous Interacting Electron Gas." *Physical Review* 145.2 (1966): 561.

(19)   Perdew, John P., and Yue Wang. "Accurate and Simple Analytic Representation of the Electron-Gas Correlation Energy." *Physical Review B* 45, no. 23 (1992): 13244–49. https://doi.org/10.1103/PhysRevB.45.13244.

(20)   Haynes, Anthony. "Concepts of Modern Catalysis and Kinetics." *Synthesis* 2005.05 (2005): 851-851.

(21)   Nørskov, Jens K., Frank Abild-Pedersen, Felix Studt, and Thomas Bligaard. "Density Functional Theory in Surface Chemistry and Catalysis." *Proceedings of the National Academy of Sciences of the United States of America* (2011): 937–943. https://doi.org/10.1073/pnas.1006652108.

(22)   Bartholomew, Calvin H., "Mechanisms of Catalyst Deactivation." *Applied Catalysis A: General* 212, no. 1–2 (2001): 17–60. https://doi.org/10.1016/S0926-860X(00)00843-7.

(23)   Trenary, Micheal, Kevin Uram, and John T.Y. Yates "An Infrared Reflection-Absorption Study of Co Chemisorbed on Clean and Sulfided Ni (111)—Evidence for local surface interactions." *Surface Science* 157.2-3 (1985): 512-538.

(24)   Hardegree, Eric L., Pin Ho, John Micheal White "Sulfur Adsorption on Ni(100) and Its Effect on CO Chemisorption. I. TDS, AES and Work Function Results." *Surface Science* (1986)*, 165* (2–3), 488–506. https://doi.org/10.1016/0039-6028(86) 90822-8.

(25)   Kiskinova, Maya, and D. Wayne Goodman. "Modification of Chemisorption Properties by Electronegative Adatoms: H_2 and CO on Chlorided, Sulfided, and Phosphided Ni(100)." *Surface Science* 108, no. 1 (1981): 64–76. https://doi.org/10.1016/0039-6028(81)90358-7.

(26)   Yamada, Taro, Takaharu Onishi, and Kenzi Tamaru. "Adsorption-Desorption Kinetics of Carbon Monoxide on Palladium Polycrystalline Surfaces. *Surface Science* 133, no. 2–3 (1983): 533–46. https://doi.org/10.1016/0039-6028(83)90018-3.

(27)   Jorgensen, W. Scott, Robert J. Madix."Steric and Electronic Effects of Sulfur on CO Adsorbed on Pd(100)." *Surface Science 163* no.1 (1985):19–38. https://doi.org /10.1016/0039-6028(85)90845-3.

(28)   Barrientos, Javier, Vicente Montes, Magali Boutonnet, Sven Järås, "Further insights into the effect of sulfur on the activity and selectivity of cobalt-based Fischer–Tropsch catalysts." *Catalysis Today, 275* no.29 (2016):119-126.

(29)   Madon, Rostam J., and Harris Seaw. (1977). Effect of sulfur on the Fischer-Tropsch synthesis. Catalysis Reviews Science and Engineering, 15(1), 69-106.

(30)   Dry, Mark E. , "Catalytic Aspects of Industrial Fischer-Tropsch Synthesis". *Journal of Molecular Catalysis* 17, no. 2–3 (1982): 133–44. https://doi.org/10.1016/0304-5102(82)85025-6.

(31)   Dry, Mark E., "The Fischer-Tropsch Process: 1950-2000." *Catalysis Today* 71, no. 3–4 (2002): 227–41. https://doi.org/10.1016/S0920-5861(01)00453-9.

(32)   Bartholomew, H. Calvin, Richard M. Bowman, "Sulfur poisoning of cobalt and

iron Fischer-Tropsch Catalysts." *Applied Catalysis*, 15 no.1 (1985): 59-67. https://doi.org/10.1016/S0166-9834(00)81487-6

(33)   Borg, Øyvind, Nina Hammer, Bjørn Christian Enger, Rune Myrstad, Odd Asbjørn Lindvg, Sigrid Eri, Torild Hulsund Skagseth, and Erling Rytter. "Effect of Biomass-Derived Synthesis Gas Impurity Elements on Cobalt Fischer-Tropsch Catalyst Performance Including in Situ Sulphur and Nitrogen Addition." *Journal of Catalysis* 279, no. 1 (2011): 163–73. https://doi.org/10.1016/j.jcat.2011.01.015.

(34)   Pansare, Sourabh S., and Joe D. Allison. "An Investigation of the Effect of Ultra-Low Concentrations of Sulfur on a Co/γ-Al2O3 Fischer-Tropsch Synthesis Catalyst." *Applied Catalysis A: General* 387, no. 1–2 (2010): 224–30. https://doi.org/10.1016/j.apcata.2010.08.031.

(35)   Visconti, Carlo Giorgio, Luca Lietti, Pio Forzatti, and Roberto Zennaro. "Fischer-Tropsch Synthesis on Sulphur Poisoned Co/Al$_2$O$_3$ Catalyst." *Applied Catalysis A: General* 330, no. 1–2 (2007): 49–56. https://doi.org/10.1016/j.apcata.2007.07.009.

(36)   Curtis, Vickie; Christakis P. Nicolaides, Neil Coville, Diane Hildebrandt, David G. Glasser. "The Effect of Sulfur on Supported Cobalt Fischer-Tropsch Catalysts." *Catalysis Today*, *49* no. 1–3, (1999): 33–40. https://doi.org/10.1016/S0920-5861(98)00405-2.

(37)   Li, Jinlin, and Neil J. Coville. "Effect of Boron on the Sulfur Poisoning of Co/TiO2 Fischer-Tropsch Catalysts." *Applied Catalysis A: General* 208, no. 1–2 (2001): 177–84. https://doi.org/10.1016/S0926-860X(00)00705-5.

(38)   Bromfield, C. Tray, and Neil J. Coville. "Surface Characterization of Sulfided Precipitated-Iron Fischer-Tropsch Catalysts by X-Ray Photoelectron Spectroscopy." *Applied Surface Science* 119, no. 1–2 (1997): 19–24. https://doi.org/10.1016/S0169-4332(97)00186-4.

(39)   Madikizela-Mnqanqeni, N. Nobuntu, and Neil J. Coville. "The Effect of Sulfur Addition during the Preparation of Co/Zn/TiO$_2$ Fischer-Tropsch Catalysts." *Applied Catalysis A: General* 340, no. 1 (2008): 7–15. https://doi.org/10.1016/j.apcata.2008.01.028.

(40)   Bambal, Ashish S., Vidya S. Guggilla, Edwin L. Kugler, Todd H. Gardner, and Dady B. Dadyburjor. "Poisoning of a Silica-Supported Cobalt Catalyst Due to Presence of Sulfur Impurities in Syngas during Fischer-Tropsch Synthesis: Effects of Chelating Agent." *Industrial and Engineering Chemistry Research* 53, no. 14 (2014): 5846–57. https://doi.org/10.1021/ie500243h.

(41)   Ma, Wenping, Gary Jacobs, Dennis E.Sparks, Wilson D.Shafer, Hussein H.Hamdeh, Shelley D.Hopps, Venkat Raman, Rao Pendyala, Yongfeng Hu, Qunfeng Xiao, Burtron H.Davis, "Effect of H_2S in Syngas on the Fischer–Tropsch Synthesis Performance of a 0.5% Pt–25% Co–Al_2O_3 Catalyst." *Catalysis Letters*, 146(7), (2016): 1204-1212.

(42)   Stenger Jr, Harvey G., and Charles N. Satterfield. "Effects of Sulfur Poisoning of a Reduced Fused Magnetite Catalyst in The Fischer-Tropsch Synthesis. " *Industrial & Engineering Chemistry Process Design and Development* 24.2 (1985): 415-420.

(43)   Kim, Myungsoo, Nelly M. Rodriguez and Terry Baker, "The Interplay between Sulfur Adsorption and Carbon Deposition on Cobalt Catalysts." *Journal of Catalysis* 143, no. 2 (1993): 449–63. https://doi.org/10.1006/jcat.1993.1289.

(44)   Habermehl-Cwirzen, Karin, Kalle Kauraala, and Jouko Lahtinen. "Hydrogen on cobalt: the effects of carbon monoxide and sulphur additives on the D_2/Co (0001) system." Physica Scripta 2004.T108 (2004): 28.

(45)   Lahtinen, Jouka, Pekka Kantola, Salla Jaatinen, Karin Habermehl-Cwirzen, Petri Salo, Johannes Vuorinen, Matti Lindroos, Katariina Pussi, and Ari P. Seitsonen. "LEED and DFT Investigation on the (2 × 2)-S Overlayer on Co(0 0 0 1)." *Surface Science* 599, no. 1–3 (2005): 113–21. https://doi.org/10.1016 /j.susc. 2005.09.042.

(46)   McAllister, Blake, and Ai-Ping Hu. "A Density Functional Theory Study of Sulfur Poisoning." *Journal of Chemical Physics* 122, no. 8 (2005). https://doi.org/10. 1063/1.1854125.

(47)   Alfonso, Dominic R. "First-Principles Studies of H_2S Adsorption and Dissociation on Metal Surfaces." Surface Science 602, no. 16 (2008): 2758–68. https://doi.org/10.1016/j.susc.2008.07.001.

(48)   Zhang, Chong Jing, and Peijun Hu. "Methane Transformation to Carbon and Hydrogen on Pd(100): Pathways and Energetics from Density Functional Theory Calculations." Journal of Chemical Physics 116, no. 1 (2002): 322–27. https:// doi.org/10.1063/1.1423663.

(49)   Michaelides, Angelos, and Peijun Hu. "Catalytic Water Formation on Platinum: A First- Principles Study." *Journal of the American Chemical Society* 123, no. 18 (2001):4235–42.https://doi.org/10.1021/ja003576x.

(50)   Tang, Qian Lin, Si Rui Zhang, and Yan Ping Liang. "Influence of Step Defects on the H_2S Splitting on Copper Surfaces from First-Principles Microkinetic

Modeling." *Journal of Physical Chemistry C* 116, no. 38 (2012): 20321–31. https://doi.org/10.1021/jp304106f.

(51)   Jiang, De-en, and Emily A. Carter. "Adsorption, Diffusion, and Dissociation of H_2S on Fe(100) from First Principles." *The Journal of Physical Chemistry B* 108, no. 50 (2004): 19140–45. https://doi.org/10.1021/jp046475k.

(52)   Kresse, Georg, Martjin Masman and Jürgen Furtmüller. "The VASP Manual" *Vaspwiki, (2018)* https://www.vasp.at/wiki/index.php/The_VASP_Manual (Feb 5, 2020-Accessed)

(53)   Kresse, Georg, Martjin Marsman and Jürgen Furthmüller,"The VASP Manual INCAR" - *Vaspwiki*, (2018) https://www.vasp.at/wiki/index.php/Category: INCAR (Feb 5, 2020- Accessed).

(54)   Henkelman, Graeme, and Hannes Jónsson. "A Dimer Method for Finding Saddle Points on High Dimensional Potential Surfaces Using Only First Derivatives." *Journal of Chemical Physics* 111, no. 15 (1999): 7010–22. https://doi.org/10.1063/1.480097.

(55)   Shan, Nannan, Mingxia Zhou, Mary K. Hanchett, Josephine Chen, and Bin Liu. "Practical Principles of Density Functional Theory for Catalytic Reaction Simulations on Metal Surfaces–from Theory to Applications." *Molecular Simulation* 43, no.10–11 (2017): 861–85. https://doi.org/10.1080/08927022.2017. 1303687.

(56)   Halgren, Thomas A., and William N. Lipscomb. "The Synchronous-Transit Method for Determining Reaction Pathways and Locating Molecular Transition States." *Chemical Physics Letters* 49, no.2 (1977): 225–32. https://doi.org /10.1 016/00092614(77)80574-5.

(57)   Fischer, Stefan, and Martin Karplus. "Conjugate Peak Refinement : An Algorithm for Finding Reaction Paths and Accurate Transition States in Systems with Many Degrees of Freedom." *Chemical Physics Letters*. Vol. 194, (1992):252-261.

(58)   Ionova, Irina V., and Emily A. Carter. "Ridge Method for Finding Saddle Points on Potential Energy Surfaces." *The Journal of Chemical Physics* 98, no. 8 (1993): 6377–86. https://doi.org/10.1063/1.465100.

(59)   Henkelman, Graeme, Gísli Jóhannesson, and Hannes Jónsson."Methods for finding saddle points and minimum energy paths." *Springer, Dordrecht* (2002), 269-302.

(60)   Qi, Yanying, Jia Yang, Xuezhi Duan, Yi An Zhu, De Chen, and Anders Holmen. "Discrimination of the Mechanism of CH_4 Formation in Fischer-Tropsch Synthesis on Co Catalysts: A Combined Approach of DFT, Kinetic Isotope Effects and Kinetic Analysis." *Catalysis Science and Technology* 4, no. 10 (2014): 3534–43. https://doi.org/10.1039/c4cy00566j.

(61)   Hao, Xiaobin, Qiang Wang, Debao Li, and Baojun Wang. "RSC Advances The Adsorption and Dissociation of Methane on Cobalt Surfaces : Thermochemistry and Reaction." *RSC Advances* 4, no. 111 (2014): 43004–11. https://doi.org/10.1039/C4RA04050C.

(62)   Weststrate, Kees-Jan, Pieter V. Helden, and Johannes W. Hans Niemantsverdriet. "Reflections on the Fischer-Tropsch Synthesis: Mechanistic Issues from a Surface Science Perspective." *Catalysis Today* 275 (2016): 100–110. https://doi.org/10.1016/j.cattod.2016.04.004.

(63)   Zhuo, Mingkun, Kong Fei Tan, Armando Borgna, and Mark Saeys. "Density Functional Theory Study of the CO Insertion Mechanism for Fischer - Tropsch Synthesis over Co Catalysts," The Journal of Physical Chemistry C, 113(19), (2009): 8357–8365.

(64)   Johnson, Gregory R., and Alexis T. Bell. "Role of ZrO_2 in Promoting the Activity and Selectivity of Co-Based Fischer-Tropsch Synthesis Catalysts." *ACS Catalysis* 6, no. 1 (2016): 100–114. https://doi.org/10.1021/acscatal.5b02205.

(65)   Kizilkaya, Ali Can, Johannes W. Hans Niemantsverdriet, and Kees- Jan Weststrate. "Effect of Ammonia on Cobalt Fischer-Tropsch Synthesis Catalysts: A Surface Science Approach." *Catalysis Science and Technology* 9, no. 3 (2019): 702–10. https://doi.org/10.1039/c8cy01723a.

(66)   Yang, Kuiwei, Minhua Zhang, and Yingzhe Yu. "Direct versus Hydrogen-Assisted CO Dissociation over Stepped Ni and Ni3Fe Surfaces: A Computational Investigation." *Physical Chemistry Chemical Physics* 17, no. 44 (2015): 29616–27. https://doi.org/10.1039/c5cp04335b.

(67)   Weststrate, Kees-Jan, Pieter V. Helden, Jan Van De Loosdrecht, and Johannes W. Hans Niemantsverdriet. "Elementary Steps in Fischer-Tropsch Synthesis: CO Bond Scission, CO Oxidation and Surface Carbiding on Co(0001)." *Surface Science* 648 (2016): 60–66. https://doi.org/10.1016/j.susc.2015.10.050.

APPENDICES

APPENDIX A

Adsorption Energy of Atoms for 0.25 ML and 0.11 ML Sulfur Coverages

Species / (adsorption site)		0.25 ML Adsorption Energy [kJ/mol]	0.11 ML Adsorption Energy [kJ/mol]
C (HCP)	Bare	-637	-644
	With S	-547	*Far from Sulfur*
			-617
O (HCP)	Bare	-599	-567
	With S	-521	*Far from Sulfur*
			-531
H (FCC)	Bare	-277	-281
	With S	-253	*Far from Sulfur*
			-281
			Close to Sulfur
			-269

APPENDIX B

INCAR File For NEB Calculation

```
SYSTEM = CO diss with S
ISTART = 0
!PREC = HIGH
ENCUT = 600
ISMEAR = 1 ; SIGMA = 0.2;
EDIFFG = -0.015
NSW = 100
POTIM = 0.5
IBRION = 1
ISPIN = 2
MAGMOM = 20*3 1*0 1*0
LREAL = AUTO
NFREE = 20
LDIPOL = .TRUE.
IDIPOL = 3
ALGO = Fast
IMAGES = 8
SPRING = -5
ICHAIN = 0
LCLIMB = .TRUE.
LTANGENTOLD = .FALSE.
LDNEB = .FALSE.
GGA = RE
LUSE_VDW = .TRUE.
AGGAC = 0.0000
LASPH = .TRUE.
```

APPENDIX C

Related Equations

Redhead Equation:

$$E_{des} = RT_{max}\left[In\left(\frac{vT_{max}}{\beta}\right) - 3.46\right]$$

Where;

E_{des} : activation energy of desorption

R : gas constant

T_{max} : peak maximum temperature

v : pre-exponential factor

β : heating rate, dT/dt

Arrhenius Equation:

$$k = Ae^{-\frac{E_a}{RT}}$$

Where;

k : Reaction rate constant

A : The pre-exponential factor

R : The gas constant

T : The temperature

E_a : The activation Energy